Fractal and Multifractal Analysis of Runoff Time Series and Stream Networks in Agricultural Watersheds

By

Xiaobo Zhou

Dissertation submitted to the Faculty of the
Virginia Polytechnic Institute and State University
in partial fulfillment of the requirements for the degree of

DOCTOR OF PHILOSOPHY
IN
CROP AND SOIL ENVIRONMENTAL SCIENCES

APPROVED:

_____
N. Persaud, Chairman

_____	_____
M. M. Alley	R. B. Clark
_____	_____
C. D. Heatwole	Y. Pachepsky

October, 2004
Blacksburg, Virginia

Keywords: Runoff, Stream Network, Fractal, Multifractal, Scaling
Copyright 2004, Xiaobo Zhou

FRACTAL AND MULTIFRACTAL ANALYSIS OF RUNOFF TIME SERIES AND STREAM NETWORKS IN AGRICULTURAL WATERSHEDS

By

Xiaobo Zhou

Dr. Naraine Persaud

ABSTRACT

The usefulness of watershed hydrological process models is considerably increased when they can be extrapolated across spatial and temporal scales. This scale transfer problem, meaning the description and prediction of characteristics and processes at a scale different from the one at which observations and measurements are made, and has become the subject of much current research in hydrology and other areas. Quantitative description of fractal scaling behavior of runoff and stream network morphometry in agricultural watersheds has not been previously reported.

In the present study, fractal and multifractal scaling of daily runoff rate in four experimental agricultural watersheds and their associated sub-watersheds (32 in total) were investigated. The time series of daily runoff rate were obtained from the database (comprising about 16,600 station years of rainfall and runoff data for small agricultural watersheds across the U.S.) developed by the Hydrological and Remote Sensing Laboratory, Agricultural Research Service, US Department of Agriculture (HRSL/ARS/USDA). Fractal scaling patterns of the Digital Elevation Model (DEM)-extracted stream network morphometry for these four watersheds were also examined. The morphometry of stream networks of four watersheds were obtained by Geographic Information System (GIS) manipulation of digital elevation data downloaded from the most recent (July 2004) U.S. Geological Survey (USGS) National Elevation Dataset (NED). Several threshold values of contribution area for stream initiation were used to extract stream networks for each of the four watersheds.

The principal measures of fractal scaling determined for the runoff series were the Hurst exponent obtained by rescaled range (R/S) analysis, the fractal dimension estimated by the shifted box-counting method, and the multifractal scaling function parameters (α and C_1) of the Universal Multifractal Model (UMM). Corresponding measures for the DEM-extracted stream networks at each threshold value were the fractal dimension estimated using the box-counting technique and the Horton ratios of the network.

Daily runoff rate exhibited strong long-term dependence and scale invariance over certain time scales. The same fractal dimensions and Hurst exponents were obtained for the sub-watersheds within each watershed. Runoff exhibited multifractal behavior that was well described by UMM. The multifractal parameters α ($0 \leq \alpha \leq 2$, quantifies how far the process is from monofractality) and C_1 ($0 \leq C_1 \leq 1$, characterizes the sparseness or inhomogeneity of the mean of the process) were reasonably close to each other for sub-watersheds within a watershed and were generally similar among four watersheds.

For the DEM-extracted networks, the morphometric attributes and Horton ratios as well as their fractal dimensions were dependent on the threshold values of contribution area used in the extraction process. The fractal dimensions were almost identical for DEM-extracted stream networks of the four watersheds. The DEM-extracted stream network displayed a single scaling pattern, rather than multifractal behavior. Explanation of the physical significance of fractal characteristics of the stream network in relation to runoff time series would require more data than were available in this study.

DEDICATION

This dissertation is dedicated to my grandfather who provided much love and support until he passed away last year.

ACKNOWLEDGEMENTS

I would like to express my appreciation to Dr. Naraine Persaud, my advisor and mentor, for his assistance, patience, kindness, and invaluable guidance in my study and research. Without his support and encouragement, this research would not have been possible.

My graduate committee members Drs. Marcus M. Alley, Ralph B. Clark, Conrad D. Heatwole, and Yakov Pachepsky, provided much helpful support, encouragement, and advice for which I am very grateful.

I gratefully acknowledge the financial support provided through the collaborative research agreement between the USDA-ARS Appalachian Farming Systems Research Center, Beaver, West Virginia and Virginia Polytechnic Institute and State University. Also, I would like to thank Dr. Jane L. Thurman of the USDA-ARS Hydrological and Remote Sensing Laboratory, Beltsville, Maryland for kindly providing the CD-ROM with data on the agricultural watersheds used in this research.

I deeply thank my wife, Bing Liu, for her constant love, encouragement, and support and also my parents and my sister for their endless love.

TABLE OF CONTENTS

LIST OF TABLES……...viii

LIST OF FIGURES……....x

CHAPTER I - OVERVIEW 1

REFERENCES……....14

CHAPTER II - SCALE INVARIANCE IN DAILY RUNOFF TIME SERIES……...18

INTRODUCTION……...18

MATERIALS AND METHODS 22

Data……22

Shifted Box-Counting Analysis……..24

Rescaled Range (R/S) Analysis……..26

RESULTS AND DISCUSSION……..28

Estimated Fractal Dimension……..28

Estimated Hurst Exponent…... ……..……39

FINDINGS AND CONCLUSIONS……44

REFERENCES……45

CHAPTER III - MULTIFRACTAL SCALING OF DAILY RUNOFF TIME SERIES……....48

INTRODUCTION……...48

MATERIALS AND METHODS……....55

Trace Moment Method……...55

Estimation of the Universal Multifractal Model (UMM) Parameters by the Double Trace Moment (DTM)……...55

RESULTS AND DISCUSSION……58

Empirical Moment Scaling Function……58

Exceedance Probability Distribution.....59

Multifractal Parameters α and C_1……...65
FINDINGS AND CONCLUSIONS……74
REFERENCES……75
CHAPTER IV - FRACTAL CHARACTERISTICS OF STREAM NETWORKS EXTRACTED WITH THE DIGITAL ELEVATION MODEL……78
INTRODUCTION……....78
Estimating the Fratcal Dimension of Stream Networks…....79
Relationship between Network Fractal Dimension and Geomorphology…....83
Extraction Stream Network Using DEM……...84
MATERIALS AND METHODS……...88
DEM Data and Stream Network Extraction……..88
Modified Box-Counting Method……...89
Estimation of Horton Ratios of DEM Extracted Stream Networks……...89
Multifractal Analysis of DEM-Extracted Stream Networks……..91
RESULTS AND DISCUSSION……93
Fractal Dimension Estimated by Box-Counting Method……101
Fractal Dimension Estimated by Horton Ratios……...102
Cumulative Probability Distribution of Contribution Area……..104
Multifractal Analysis of Stream Networks……...107
FINDINGS AND CONCLUSIONS……..109
REFERENCES……..110
CHAPTER V - SUMMARY……116
REFERENCES……..122
VITA……...123

LIST OF TABLES

Table 1.1. Definitions for different fractal dimensions……5

Table 2.1. Properties of agricultural watersheds and sub-watersheds studied……....23

Table 2.2. Fractal dimensions of daily runoff rate for six sub-watersheds of the Little River watershed in Tifton, Georgia. Fractal dimensions corresponding to four threshold levels of the runoff rate (0, 0.5M, M, and 1.5M, where M is the daily mean runoff rate) were obtained as the absolute value of the slope of straight lines fitted to plots as shown in Figure 2.2…….. ……..……..33

Table 2.3. Fractal dimensions of daily runoff rate for seven sub-watersheds of the Little Mill Creek watershed in Coshocton, Ohio. Fractal dimensions corresponding to four threshold levels of the runoff rate (0, 0.5M, M, and 1.5M, where M is the daily mean runoff rate) were obtained as the absolute value of the slope of straight lines fitted to plots as shown in Figure 2.2. ……..……...34

Table 2.4. Fractal dimensions of daily runoff rate for ten sub-watersheds of the Reynolds Creek watershed in Boise, Idaho. Fractal dimensions corresponding to four threshold levels of the runoff rate (0, 0.5M, M, and 1.5M, where M is the daily mean runoff rate) were obtained as the absolute value of the slope of straight lines fitted to plots as shown in Figure 2.2……...35

Table 2.5. Fractal dimensions of daily runoff rate for nine sub-watersheds of the Sleepers Creek watershed in Vermont. Fractal dimensions corresponding to four threshold levels of the runoff rate (0, 0.5M, M, and 1.5M, where M is the daily mean runoff rate) were obtained as the absolute value of the slope of straight lines fitted to plots as shown in Figure 2.2……..……36

Table 2.6. Hurst exponent (H) of daily runoff time series estimated using the rescaled range analysis method. Scaling range 1 corresponds to the

lag time less than the break point of rescaled range plot, and range 2 corresponds to the lag time greater than the break point. H for each range was obtained as the slope of fitted straight lines to plots as shown in Figure 2.4……..……...…….41

Table 3.1. Estimates of parameters $q_{D,}$ α and C_1 of daily runoff time series. The critical moment q_D was estimated as the absolute value of the slope of the algebraic tail of the exceedance probability distribution plot as shown in Figure 3.2. The multifractal parameters α and C_1 were estimated from UMM……...……63

Table 4.1. Description of elevation data…….88

Table 4.2. Morphometric characteristics of DEM-extracted stream networks using different contributing threshold areas for four agricultural watersheds……..……98

Table 4.3. Fractal dimensions of stream network estimated as the absolute value of slope of linear fit to plots of N(r) versus r as shown in Figure 4.6 using the box-counting method for various threshold values……99

Table 4.4. Estimated fractal dimension of stream length (d) and stream network (D) using Horton's ratios for four agricultural watersheds, where d = max (1, 2 log R_L/log R_A), D_1 = log R_B/log R_L, and D_2 = 2*log R_B/log R_A……...……103

LIST OF FIGURES

Figure 2.1. Illustration of shifted box-counting method for estimating the fractal dimension of time series data……25

Figure 2.2. Log-log plots of number of boxes [N(ε)] versus box size (ε) for different threshold values (0, 1.76, 3.52, and 5.28 m^3/s) using the shifted box counting method to analyze the runoff rate series for sub-watershed W-TB of the Litter River watershed in Tifton, Georgia. In all cases, r^2 was > 0.990 for the straight lines fitted to the sections of the graph. Box sizes were exponentially doubled starting at ε = 1 day……...…….30

Figure 2.3. Shifted box counting graph as in Figure 2.2 but with one day increment of box size (ε) for sub-watershed W-TB of the Litter River watershed in Tifton, Georgia. The break point of the slope occurs at approximately ε = 365 days..……31

Figure 2.4. Hurst rescaled range analysis plot for sub-watershed W-TB of the Little River watershed in Tifton, Georgia. A scaling break point occurs at about 18 months. r^2 was > 0.99 for the straight lines fitted to each scaling range.…… ……..40

Figure 3.1. Log of the average q^{th} moment of the daily runoff rate $<R_\lambda^q>$ versus log λ (scale ratio) for sub-watershed W-TB of the Little River watershed in Tifton, Georgia. In all cases, r^2 for linear regression lines fitted for time scales from 1 day (λ = 11292) to 1024 days (λ = 11) were > 0.99…….60

Figure 3.2 Exceedance probability distribution of daily runoff rate (Q) for sub-watershed W-TB of the Little River watershed in Tifton, Georgia. The critical moment q_D was estimated as the absolute value of the slope of the algebraic tail of the probability distribution plot. The value of q_D was about 5.42 in this case..……..62

Figure 3.3 Empirical moment function K(q) describing the scaling of the

moment of daily runoff time series over different scales for sub-watershed W-TB of the Little River watershed in Tifton, Georgia. r^2 for the straight line fitted to the linear portion of the curve was 0.99……64

Figure 3.4. Log of the average trace moment (q = 2) of the daily runoff rate $<R_\lambda(q,\eta)>$ versus log λ (scale ratio) for sub-watershed W-TB of the Little River watershed in Tifton, Georgia for η = 0.5, 1.0, 1.5, 2.0, 2.5, 3.0, 3.5. In all cases, r^2 for linear regression lines fitted for time scales from 1 day (λ = 11242) to 1024 days (λ = 11) were > 0.99. ……..……..…66

Figure 3.5. Double trace moment log-log plot of the moment scaling function K(q,η) versus moment order η with q = 2 for daily runoff rate in sub-watershed W-TB of Little River watershed in Tifton, Georgia. r^2 for the straight line fitted to the linear part of the plot was 0.99……68

Figure 3.6. Moment scaling functions K(q) for sub-watershed W-TB of the Little River watershed in Tifton, Georgia. Dots are the empirical values and the solid line is the universal multifractal function using α = 0.93 and C_1 = 0.19……..……...69

Figure 3.7. Moment scaling functions K(q) for sub-watershed W-2 of the Sleepers River watershed in Danville, Vermont. Dots are the empirical values and the solid line is the universal multifractal function using α = 1.94 and C_1 = 0.10……...70

Figure 4.1. Scheme of a Horton-Strahler stream network ordering system of order 4……...…….90

Figure 4.2. The stream network of the Little River watershed extracted using DEM……...……94

Figure 4.3. The stream network of the Little Mill Creek watershed extracted Using DEM……...……..…...95

Figure 4.4. The stream network of the Reynolds Creek watershed extracted Using DEM……...…….....96

Figure 4.5. The stream network of the Sleepers River watershed extracted

Using DEM……..……...……97

Figure 4.6. Log-log box counting plot of number of covering boxes N(r) at box size (r) for stream network using threshold = 0.05 km^2 for the Little River watershed in Tifton, Georgia. Separate straight lines were fitted to the points on either side of the break point. r^2 for fits were > 0.99……....100

Figure 4.7. Cumulative probability distribution for contribution area (a in m^2) of the Little River watershed in Tifton, Georgia. The theoretical distributions were calculated from Eq.(4.13) for various threshold values……...105

Figure 4.8. Scaling of the partition function Zq for moment order q = 2 to 15 versus box size (δ) for the Little River watershed, in Tifton, Georgia.……108

CHAPTER I
OVERVIEW

Runoff from watersheds in the U.S. impacts the water quantity/quality of 3.5×10^6 miles of rivers and streams; 16.5×10^6 hectares of lakes, ponds, and reservoirs; 8.9×10^6 hectares of estuaries; 58,000 miles of ocean shorelines; 5,559 miles of the Great Lakes shoreline; and 112.1×10^6 hectares of wetlands of which 68.8×10^6 hectares are in Alaska (USEPA, 1994). Current public policies are strongly committed to the sustainable development and use of these watersheds, and protecting the quality of their associated water resources from impairment. This has resulted in federal and state legislative requirements to continuously monitor the impact of agricultural and urban activities on the hydrology of these watersheds and the quality of their associated surface waters. Research geared to a deeper understanding of watershed hydrology is essential to support decisions pertinent to these mandates.

Predicting runoff has always been of great interest to hydrologists and they have developed many mathematical models for this purpose. The development of most of these models has been based on observations taken over relatively small spatial and temporal scales. Since watersheds vary in their size, topography, land use pattern, hydrogeology, and drainage network morphology, the usefulness of these models depend on how well they can be extrapolated across spatial and temporal scales. This scale transfer problem, meaning the description and prediction of characteristics and processes at a scale different from the one at which observations and measurements are made, remains a pervasive problem in many areas of science and engineering.

Parameters in runoff hydrological models are usually determined from monitoring data. However, stream networks in many watersheds in the U.S. are not gauged (or are partially gauged) and do not have flow records, or the flow record is often too short to obtain the required hydrological parameters. It would be very useful to find possible analytical tools that would enable extrapolation of observations of runoff processes in

gauged watersheds or portions thereof, to predict such processes in larger portions of the same watershed or in non-gauged watersheds. Runoff processes and drainage network morphology are the direct result of the interaction of the spatial and temporal distribution of precipitation and watershed physical characteristics such as topography and geology. Therefore, extrapolation between scales of observations and between watersheds would require identifying and quantifying the scaling behavior of temporal and spatial watershed characteristics and processes. Such information could result in reducing the extent and degree of monitoring required by legislative mandates and lead to significant savings in cost and time.

The self-similarity of fractal forms and fractal scaling dimensions (Mandelbrot, 1983; Feder, 1988) has provided a theoretical framework essential to enable any prediction of hydrological processes in a watershed at temporal and spatial scales other than the scale of observation. A universally accepted definition of a fractal form does not exist. Mandelbrot (1983) gave a strict mathematical definition of a fractal as: "a set for which the Hausdorff-Besicovitch dimension strictly exceeds the topological dimension". The form may represent a geometrical object or the output of a process in time. But in real practical applications, most definitions are based on the properties used to characterize a fractal (Falconer, 1990) as a mathematical object that:

i) is too irregular or complex to be described using traditional Euclidean geometrical concepts;
ii) has fine structure: i.e., has infinite details on any scale;
iii) has self-similar pattern: i.e., parts of it resemble the whole;
iv) in most cases, can be defined in a simple way.

The purpose of this dissertation would be best served if further elaboration on these properties were achieved heuristically rather than in mathematical terms.

In classical geometry, length is an appropriate measure to describe a line, so is area for a surface and volume for a three-dimensional object. However, geometrical shapes can be

constructed from mathematical sets that cannot be well defined using Euclidean measures. These objects are generally irregular, meaning they not sufficiently smooth and are not differentiable. They were regarded as a "gallery of mathematical monsters" (Mandelbrot, 1983) when they were first created. For example, the perimeter of the fractal object termed as the "Koch's Snowflake" is infinite but its area is finite. Hence perimeter that is often used to describe a Euclidean shape is no longer an appropriate description for a Koch's Snowflake.

These mathematical objects turned out to be better models for many objects in nature that were too complicated and irregular to be described using classical Euclidean plane geometrical concepts such as straight lines and simple curves. As human beings, we instinctively tend to describe physical objects using idealized shapes or graphs (or a combination of these) such as a line for a road, a circle for the sun, rectangles for a house, etc. Benoit Mandelbrot, the pioneer who popularized applications of fractals to describe natural objects and forms and shapes, realized that these previously introduced bizarre mathematical forms were common patterns of nature. For example, coastlines may have infinite length and snowflakes could have an infinite surface area. To quote Mandelbrot, "Clouds are not spherical, mountains are not cones, coastlines are not circles, and bark is not smooth". These mathematical and natural objects and forms are now commonly referred to as fractals, a term coined by Mandelbrot (1983) from the Latin "fractus" to describe objects that are too irregular or complex to fit into a classical geometrical setting.

Fractals have special properties. One of the most important is that a fractal can be subdivided into parts, each of which is (at least approximately) a reduced-size copy of the whole. This property is termed as self-similarity and implies that properties are invariant across spatial and temporal scales. As already indicated, another property is their irregularity or complexity, which can be characterized by their Hausdorff-Besicovitch dimension commonly called the fractal dimension. The dimension of classical geometrical objects is defined by integer numbers (termed as the topological dimension) that describes how points within an object are connected to each other. For example, a

line is topologically one-dimensional, a plane is two-dimensional, and a cube three-dimensional. However, the dimension of a fractal object is non-integer and exceeds the topological dimension. For example, the dimension of an irregular coastline may be greater than one but less than two, indicating it is not like a simple line but has space-filling characteristics in the plane, although its topological dimension remains equal to 1. Likewise, the surface area of a snowflake may be greater than two but less than three. According to Barnsley (1993), the dimension of a fractal "attempts to quantify a subjective feeling we have about how densely the fractal occupies the metric space in which it lies".

Generally, fractal properties of natural objects are quantified using the fractal dimension. An object with a low fractal dimension is less irregular or complicated than an object with a higher fractal dimension. The fractal dimension also accounts for how the Euclidean measure of the object changes after a change of scale. Previous research showed that the fractal dimension is very useful in describing irregular and fragmented patterns found in many disciplines including hydrological science (Lam and De Cola, 1993; Barton and La Pointe, 1995; Rodriguez-Iturbe and Rinaldo, 1997).

There are different ways to determine the fractal dimension of real objects, each of which characterizes different fractal properties of the object. The simplest fractal dimension is the self-similarity dimension. The self-similarity dimension requires that each little object formed by dividing the line segments of the whole object into smaller pieces must be an exact copy of the whole object implying that the scaling is isotropic. Thus the self-similarity dimension can only be used to analyze objects that are geometrically self-similar. It is hard to apply the self-similarity dimension to describe natural objects. Such objects that show self-similarity over a range of spatio-temporal scale and anisotropic scaling are termed as self-affine. Various practical definitions of the fractal dimension are summarized in Table 1.1.

Table 1.1. Definitions for different fractal dimensions

Name	*Definition*
Fractal dimension	General terminology and often identified with Hausdorff dimension or capacity dimension
Similarity dimension	Defined for strictly self-similar objects
Hausdorff dimension	Defined by most efficient covering for objects
Capacity dimension	Defined by covering objects with identical spheres or cubes
Fourier dimension	Defined from the power spectrum

If the scaling behavior of a fractal object can be characterized by a single scaling exponent (fractal dimension), the object is said to possess a monofractal scaling pattern. If multiple fractal dimensions were needed to describe the scaling behavior of the fractal object, i.e., the value of the fractal dimension changes with scale instead of being constant over all scaling ranges, the object is said to possess a multifractal scaling pattern. Monofractal scaling is common for mathematically defined fractal objects, such as the Cantor set and Koch curve, while multifractal scaling is generally found in natural fractal objects or phenomena.

Over the last two decades fractal concepts have been extended to model dynamical processes in nature, such as precipitation or voltage changes across the cell membrane. In this case, the concepts of fractal scaling are extended to include self similarity or self-affinity of the statistical measures (probabilities and moments) on series of observations over different resolutions in space or time. When the data series are fractal, unique probability distributions and values of the moments characterizing the series do not exist, but depend on the time resolution of the data series. For statistical fractals the dependency of the moments on the resolution used to measure them, constitutes a scaling relationship characterized by the fractal dimension.

The temporal fractal characteristics of watershed hydrological processes can be identified by analysis of hydrological time series. A useful measure of the fractal characteristic of time series of data such as stream flows is the Hurst exponent, which was developed

empirically by Hurst from long series of flow observations in the Nile River (Hurst, 1951). This coefficient allows comparison of time series for periods of time that may be many years apart. Because Hurst's study was empirical and lacked a foundation and framework in theory, it remained largely ignored until the work of Mandelbrot (1983). The discovery of self-similarity and self-affinity of fractal forms and fractal scaling dimensions provided the needed theoretical framework for interpretation of the Hurst exponent.

There are many general approaches, methods, and techniques that can be used to analyze the fractal scaling characteristics of hydrological and other time series data. A brief overview of some of these methodologies follows.

Spectral Analysis

Spectral analysis uses a Fourier series transformation of the discrete hydrological time series $f(t_n)$ for n = 1,2,...n into a finite set of sine and cosine functions. After the transformation, the time series is represented as a sum of sine and cosine functions with various frequencies and amplitudes (Chatfield, 1996):

$$f(t_n) = \frac{1}{2}a_0 + \sum_{i=1}^{k} a_i \cos 2\pi i t + \sum_{i=1}^{k} b_i \sin 2\pi i t \qquad (1.1)$$

where a_i, b_i are Fourier coefficients for frequency $2\pi i$ where i = 1,2,...k and k = (n-1)/2 for odd n and n/2 for even n. The first term on the right hand side represents the arithmetic mean of the series of observations. The amplitude for each frequency is given by the square root of the sum of the squares of the Fourier coefficients. Plotting the square of the amplitude of the Fourier coefficients against the frequency generates the power spectrum for the series. The square of the amplitude termed as the "power" is a measure of the contributions of each frequency to the total variance of the series. A time series with several embedded periodicities will have several distinct peaks. However, since white noise has no embedded periods, its power spectrum will be a straight horizontal line.

Generally, the power of each frequency component is inversely proportional to the frequency (f) raised to an exponent β. This implies that power $\propto f^{-\beta}$ and therefore β represents the slope of a log-log plot of power versus 1/f. In this case, the power spectrum is termed as 1/f noise (Mandelbrot, 2002). The value of β can therefore be used to distinguish whether a time series is the result of a purely random process, and if not, to characterize the periodic nature of the series (Mandelbrot, 2002). In this analysis, the series is characterized as "noise" or "motion" depending on the value of β. For a purely random process (white noise) β is equal to 0. For fractional Brownian motions (fBm), $1 < \beta < 3$, one for fractional Gaussian noises (fGn), $-1 < \beta < 1$. When β is equal to 2 the series is said to be result of a Brownian motion process. Fractional Brownian motions have proven to be a very useful model for describing fractal processes and explaining the Hurst phenomenon (Hurst, 1951). The exponent β is related to fractal dimension of the series D according to:

$$\beta = 2D + 1 \qquad (1.2)$$

Log-log power spectral plots are often used as the first test for existence of scaling and the scaling range (Svensson et al., 1996; Menabde et al., 1997; Pandey et al., 1998). A good straight line fit over the entire range of the plot (or portions thereof) is an indication of scale invariance over the entire range (or portions thereof).

Rescaled Range (R/S) Analysis

Hurst (1951) studied the 847-year record of the overflows of the Nile River, and found that successive observations in the series above or below the mean value tended to persist. He termed this tendency “long-term persistence” or “long-term memory”. Hurst’s subsequent investigations showed that this phenomenon was characteristic of the overflow, water storage, and stream flow of many other rivers. Detecting such persistence phenomena in hydrological series is typically obtained by the adjusted rescaled range (R/S) analysis (Mandelbrot and Wallis, 1969). This analysis involves a statistical rescaling of the original series over lag times of varying widths n. The

rescaling over these ranges of lag times permits extraction of a parameter known as the Hurst exponent (H) that empirically characterizes how these hydrological processes are scaled in natural drainage networks. The Hurst exponent can range between 0 and 1. A value of H = 0.50 signifies a completely random process (i.e., ordinary Brownian motion) having no long-term memory (Hurst, 1951). For non-random processes, H ranges between 0.5 and 1.0 and indicates degrees of long-term persistence in the time series. A series with H < 0.5 signifies "anti-persistence". H-values indicating long-term persistence are most common for hydrological time series. For the hydrological sequences that Hurst examined (Hurst 1951), the exponent H varied from 0.46 to 0.96 with a mean of 0.73 and a standard deviation of 0.09. The empirically defined Hurst exponent is related to the theoretical fractal dimension D of the graph of a corresponding time series, as:

$$D = 2 - H \tag{1.3}$$

The rescaling procedure allows comparison of periods of time that may be many years apart. Rescaled range analysis is more direct and robust compared with other methods such as modeling the series as a fractional Gaussian noise (Rao and Bhattacharya, 1999). Strong periodicities in the series should be removed before applying R/S analysis to obtain the Hurst exponent (Mandelbrot and Wallis, 1969). In addition, too small or too large values of the lag time results in the undesirable so-called “initial transient” and “final tightening” phenomenon in the estimation of H. It was suggested that the R/S values for small lag times should be discarded (Mandelbrot and Wallis, 1969). Generally, the lag time n is greater than 2 in R/S analysis. Small values of n produce unstable estimates when sample sizes are small.

If the primary purpose of R/S analysis is to characterize long-term memory in the series, the corresponding modified rescaled range as developed by Lo (1991) can be used to filter out the short-term memory. The effect of short-term memory on the Hurst phenomenon was investigated by Lye and Lin (1994) and Rao and Bhattacharya (1999). They found that for hydrological processes the short term memory has little effect on the Hurst exponent. Lye and Lin (1994) tested whether the calculated Hurst exponent for

two different series were significantly different. They developed an empirical statistical table to test the significance of the calculated Hurst exponent between series with length of observations between 50 and 200.

Box-counting Analysis

Box-counting analysis was originally created to measure the dimension of geometrical fractal objects (Mandelbrot, 1983). The basic idea is to superimpose a uniformly spaced grid (boxes) onto the geometrical fractal, such as a curve, and count the number of grids containing at least a piece of the curve (Mandelbrot, 1983). The number of boxes covering at least a piece of the object increases as the box size decreases. The slope of a log-log plot of this number versus box size gives an estimate (termed as the box dimension) of the fractal dimension of the fractal object.

The box-counting method has been modified to estimate the fractal dimension of one-dimensional time series (Olsson et al., 1992, 1993; Radziejewski and Kundzewicz, 1997; Prokoph, 1999; Peters and Christensen, 2002). In this case, some arbitrary "event" definition is used to generate a one-dimensional sequence based on the original series. For example, given a daily rainfall series, different derived one-dimensional sequences can be obtained by defining events as greater than some specified value of daily rainfall. In this case, the event is used to transform the original series to a binary series which can be modeled as a random Cantor set. The box-counting method can then be used to develop log-log plots for these binary series. Generally, since different threshold values can be used to define an event, the fractal dimension of corresponding binary sequences would depend on the threshold values (Olsson et al., 1992; Radziejewski and Kundzewicz, 1997). According to Radziejewski and Kundzewicz (1997), a shifted-box-counting method yields a smoother form of data series, and is adequately sensitive to small differences in box sizes.

Cumulative Probability Distribution Analysis

In general a cumulative frequency probability distribution is a function relating the probability (P) that a measure (x) is greater than or equal to some specified value (X).

Mathematically it describes P(x ≥ X) for binary time series such as rainfall and earthquakes the length of the gap between occurrences of two events would vary. In this case, a cumulative distribution function P ($l \geq$ L) can be defined for the probability of a gap length l greater than or equal to length L. If this function satisfies the relationship:

$$P(l \geq L) \propto L^{-D} \qquad (1.4)$$

then D is considered as the fractal dimension of the random Cantor set approximation of the binary series. This relationship has been successfully applied in earth science by relating the probability of earthquake occurrences to the energy flow in the lithosphere, and is known as the Gutenberg-Richter law (Gutenberg and Richter, 1944). Recently Peters et al. (2002) and Peters and Christensen (2002) established that a relationship similar to the Gutenberg-Richter law was also applicable to rainfall series. The probability of occurrences of defined rain events decayed as a power law over several orders of magnitude in rainfall kinetic energy. In some recent studies, it was reported that the fractal dimension D is a function of the statistical moment of L, implying multiple scaling dimensions rather than a single dimension (Lovejoy and Schertzer, 1990).

Many studies have since indicated that spatial and temporal scale invariance may be widespread in natural forms and time series of data. Fractal concepts have been used to analyze the scaling behavior of drainage networks and hydrological processes (Lovejoy and Schertzer, 1985; Tarboton et al., 1988; Rosso et al., 1991; Ijjasz-Vasquez et al., 1992). Several books and reviews have summarized applications of the scale invariance of fractal forms in the natural and earth sciences (Korvin, 1992; Turcotte, 1992; Barton and La Pointe, 1995). Results of very recent applications of fractal analysis to river networks have indicated that they may be fractal structures, presenting self-similar (or self-affine) properties over a significant range of scales. The emergence of these ideas has far-reaching and significant implications in studies on basin evolution, and on determination of the channel network response to rainstorms. A recent and extensive

review on the fractal nature of river basins has been compiled by Rodriguez-Iturbe and Rinaldo (1997).

Since the morphometric features of drainage networks and their hydrological processes both appear to have the characteristics of fractal scaling, it is reasonable to explore relationships between them. For example, runoff phenomena reflect the interaction of the local watershed characteristics and the precipitation processes. In other words, the gauged stream runoff reflects the overall behavior of the complex interactions of the precipitation inputs and the basin factors that modify it. However, the scaling behavior of these interactions has not been quantified. In this regard, an interesting question is: If the shape of a basin were known, can the main characteristics of its hydrologic response be forecast in a rational manner? Some research has shown that hydrological processes and time series of observations in drainage networks are closely related to their geometric form.

During short and intensive rainfall storms, most of the stream flow is generally contributed by either overland flow or by direct precipitation into the channel. Rosso (1984) showed that Horton's and Strahler's ordering system (Horton, 1945; Strahler, 1952, 1957), which is usually used in characterizing a stream network, could be used to obtain parameters of the Geomorphological Instantaneous Unit Hydrograph (GIUH). However, there is a continuing need for a comprehensive quantitative theory of channel networks as well as climatic, hydrologic, and geological control of network forms (Mesa and Gupta, 1987). It seems clear that the measurement and quantitative description of fractal scaling in drainage network morphology and hydrology is critical to a better understanding of watershed hydrology. An important aspect of this problem is investigation of the fractal properties of the watershed drainage networks. Few studies are available that quantify the scaling relationships that may exist between the geometry of the drainage network and the hydrological data of the same drainage network. Such studies are essential to developing models for prediction and extrapolation of the hydrological response of small watersheds.

Because of legislatively-mandated monitoring of watersheds in the U.S., some reasonably large data sets on the morphology and hydrology of drainage networks of watersheds spanning a wide range of scales exist and are accessible. These data sets were objectively collected and quality-assured, and were of acceptable precision. They permit investigations on the scale invariance of the characteristics of drainage networks and runoff processes in these watersheds.

One such database specifically targeting small agricultural watersheds was developed by the Hydrological and Remote Sensing Laboratory of the Agricultural Research Service of the US Department of Agriculture (USDA/ARS/HRSL). It consists primarily of rainfall/runoff data from the ARS monitored experimental agricultural watersheds nationwide. These watersheds represent numerous land uses and agricultural practices and cover a diverse range of climatic conditions across the U.S. About 16,600 station years of rainfall and runoff are available in the database. This database was chosen since there was little or no previous analysis undertaken on fractal scaling of agricultural watersheds. The metadata and auxiliary information such as map and land-use information can be accessed either by downloading from ARS website or on the CD-ROM distributed by ARS. This database provided the hydrological data analyzed in this study.

Digital Elevation Models (DEM) have been extensively used in hydrological modeling, and also used to extract the morphometry of stream networks from digital elevation data for watersheds. The availability of high resolution digital elevation data and GIS techniques permitted efficient extraction and examination of morphometry.

The primary objective of this research was to quantify fractal scaling in agricultural watersheds of different sizes and characteristics. Fractal and multifractal analytical methods were used to investigate time series of runoff data measured for these watersheds and the geometrical characteristics of their drainage networks extracted using DEM. The specific objectives were as follows:

1. To investigate temporal and spatial fractal scaling properties of daily runoff rates in these watersheds;

2. To examine the multifractal characteristics of daily runoff rates in these watersheds using multifractal techniques;

3. To determine the fractal characteristics of DEM-extracted stream networks in these watersheds.

REFERENCES

Barnsley, M. F. 1993. Fractals Everywhere. 2nd edition. Academic Press, Boston.

Barton, C.C., and P. R. La Pointe. 1995. Fractals in the earth sciences. Plenum Press, New York.

Chatfield, C. 1996. The Analysis of Time Series. Chapman and Hall, New York.

Falconer, K. J. 1990. Fractal geometry: Mathematical foundations and applications. John Wiley & Sons, New York.

Feder, J. 1988. Fractal. Plenum, New York.

Gutenberg, B., and Richter, C. F. 1944. Frequency of earthquakes in California. Bulletin Seismological Society of America 34: 185-188.

Horton, R. E. 1945. Erosional development of streams and their basins – hydrophysical approach to quantitative geomorphology. Geological Society of America Bulletin 56:275-370.

Hurst, H. E. 1951. The long term storage capacity of reservoirs. Transactions of the American Society of Civil Engineers 116: 770-808.

Ijjasz-Vasquez, E. J., I. Rodriguez-Iturbe, and R. L. Bras. 1992. On the multifractal characterization of river basins. Geomorphology 5: 297-310.

Korvin, G. 1992. Fractal models in the earth sciences. Elsevier, New York.

Lam, N. S., and L. De Cola. 1993. Fractals in geography. Prentice-Hall, New Jersey.

Lo, A. L. 1991. Long-term memory in stock market prices. Econometrica 59: 1279-1313.

Lovejoy, S., and D. Schertzer. 1985. Generalized scale invariance and fractal models of rain. Water Resources Research 21: 1233-1250.

Lovejoy, S. and D. Schertzer. 1990. Multifractal, universality classes and satellite and radar measurements of cloud and rain fields. Journal of Geophysical Research 95: 2021-2034.

Lye, L. M. and Y. Lin. 1994. Long-term dependence in annual peak flows of Canadian rivers. Journal of Hydrology 160: 89-103.

Mandelbrot, B. B. and J. R. Wallis. 1969. Some long-run properties of geophysical records. Water Resources Research 5: 321-340.

Mandelbrot, B. B. 1983. The fractal geometry of nature. W.H. Freeman, New York.

Mandelbrot, B. B. 2002. Gaussian self-affinity and fractals: Globality, the earth, 1/f noise, and R/S. Springer, New York.

Menabde, M., D. Harris, A. Seed, G. Austin, and D. Stow. 1997. Multiscaling properties of rainfall and bounded random cascade. Water Resources Research 33: 2823-2830.

Mesa, O. J., and V. K. Gupta. 1987. On the main channel length-area relationships for channel networks. Water Resources Research 23: 2119-2122.

Olsson, J., J. Niemczynowicz, R. Berndtsson, and M. Larson. 1992. An analysis of the rainfall time structure by box-counting—some practical implications. Journal of Hydrology 137: 261-277.

Olsson, J., J. Niemczynowicz, and R. Berndtsson. 1993. Fractal analysis of high-resolution rainfall time series. Journal of Geographic Research 98: 23265-23274.

Pandey, G., S. Lovejoy, and D. Schertzer. 1998. Multifractal analysis of daily river flows including extremes for basins of five to two million square kilometers, one day to 75 years. Journal of Hydrology 208: 62-81.

Peters, O. and K. Christensen. 2002. Rain: relaxation in the sky. Physical Review E 66:1-9.

Peters, O., C. Hertlein, and K. Christensen. 2002. A complexity view of rainfall. Physical Review Letter 88:1-4.

Prokoph, A. 1999. Fractal, multifractal and sliding window correlation dimension analysis of sedimentary time series. Computers & Geosciences 25: 1009-1021.

Radziejewski, M. and Z. W. Kundzewicz. 1997. Fractal analysis of flow of the river Warta. Journal of Hydrology 200: 280-294.

Rao, A. R. and D. Bhattacharya. 1999. Comparison of Hurst exponent estimates in hydrometeorological time series. Journal of Hydrologic Engineering 4: 225-231.

Rodriguez-Iturbe, I., and A. Rinaldo. 1997. Fractal river basins: Chance and self-organization. Cambridge University Press, New York.

Rosso, R. 1984. Nash model relation to Horton order ratios. Water Resources Research 20: 914-920.

Rosso, R., B. Bacchi, and P. La Barbera. 1991. Fractal relation of mainstream length to catchment area in river networks. Water Resources Research 27: 381-387.

Strahler, A. N. 1952. Hypsometric (area-altitude) analysis of erosional topography. Geological Society of America Bulletin, 63: 1117-1142.

Strahler, A. N. 1957. Quantitative geomorphology of drainage basins and channel networks. McGraw-Hill, New York.

Svensson, C., J. Olsson, and R. Berntsson. 1996. Multifractal properties of daily rainfall in two different climates. Water Resources Research 32: 2463-2472.

Tarboton, D. G., R. L. Bras, and I. Rodriguez-Iturbe. 1988. The fractal nature of river networks. Water Resources Research 24:1317–1322.

Turcotte, D.L. 1992. Fractal and chaos in geology and geophysics. Cambridge University Press, Cambridge, UK.

USEPA. 1994. The quality of our nation's water. Report 841-S-94-002. U.S. Environmental Protection Agency, Washington, DC.

CHAPTER II
SCALE INVARIANCE IN DAILY RUNOFF TIME SERIES

INTRODUCTION

Since the scale at which the available data are collected is usually different from the scale required by hydrological models, information transfer across scales is common to many hydrological investigations (Bloschl and Sivapalan, 1995). Moreover, different hydrological processes are dominant at different scales, therefore, the process descriptions or predictive model parameters derived at small laboratory or experimental plot scales would not necessarily hold true at the much larger scales of the sub-watershed or watershed. On the other hand, sometimes the available data, such as those obtained by remote sensing, are taken at a coarser spatial scale than that needed by the models. Thus, there is a continuing need to transfer information between different space-time scales.

Studies have shown that the scale invariance property is not only a feature of geometrical watershed characteristics, but may also be an inherent characteristic of hydrological processes (Schertzer and Lovejoy, 1987; Rodriguez-Iturbe and Rinaldo, 1997). Other reports indicate that some hydrological processes (e.g., rainfall), are spatially scale dependent processes (Gupta and Waymire, 1987). There is already a significant body of evidence indicating that hydrological scaling can be successfully applied in hydrological modeling (Bloschl and Sivapalan, 1995; Rodriguez-Iturbe and Rinaldo, 1997). Scale invariance implies an absence of characteristic scales and leads to relationships connecting statistical properties of the dynamic processes at different scales. Dynamic processes in watersheds are manifested as time series of observations or spatial distributions of observations. For example, records of stream stage, peak flows, sediment loads, pollutant concentrations, etc., observed periodically over time are the outputs of dynamic processes in a watershed.

Mathematically, statistical scale invariance manifests itself when the dependence of number of observations in the series greater than a specified value on the values themselves follows a power law. The existence of scale invariance would imply the theoretical possibility of making a scale shift from that defined by the specific time and space resolution of the collected data series (which is itself defined by the specific time and space resolution of the data collection system). For example, it would be possible to derive some information about the rainfall distribution during shorter time periods (< 1 day) from daily rainfall data. Similarly, it would be possible to derive some information about the rainfall distribution over an area smaller than that defined by the gauge network itself (Olsson et al., 1992). Scale invariant properties would be particularly useful in agricultural watersheds with sparse gauge networks, or where time series of rainfall and runoff records are relatively short.

Early research on the fractal nature of watershed hydrological characteristics and processes were mostly focused on time series of rainfall records (Lovejoy and Schertzer, 1985; Olsson et al., 1992, 1993; Schmitt et al., 1998). These studies have indicated that hydrological processes might be characterized by some time and/or space parameters, which are valid over all time and space scales. For example, models based on the assumption of a scale invariance property in the statistical distribution of time series of rainfall observations, have been used to describe space/time rainfall series over a range of scales (Schertzer and Lovejoy, 1987; Gupta and Waymire, 1993; Menabde et al., 1997). In contrast, stochastic models for rainfall processes are applicable only at scales similar to the scale used in the model calibration (Crane, 1990).

A so-called "doubling rule" has been observed for the intensity of rainfall with decreasing spatial scale. In this empirical rule, as the area is decreased by a factor of 10, the rainfall intensity roughly doubles, until very small scales are reached (Austin and Houze, 1972). Olsson et al. (1992) used the box-counting method to estimate the fractal dimension of several long, carefully-observed rainfall series of varying time resolution (minute, daily, and monthly data). The same estimated box dimension was obtained for

the three series within limited ranges in time depending on the rainfall intensity indicating that these rainfall series showed temporal scale invariance characteristics. Not surprisingly, the results of these early studies of rainfall series led naturally and logically to similar investigations of the fractal spatial and temporal scaling characteristics of other watershed hydrological processes such as runoff and stream flows. Reports of such investigations have increased in recent years (Radziejewski and Kundzewicz, 1997; Robinson and Sivapalan, 1997; Pandey et al., 1998). Since the demonstration of the validity of fractal concepts to describe natural objects by Mandelbrot (1983), the generality of the fractal nature of watershed hydrological characteristics and processes appears to be more and more widely acknowledged.

In many empirical studies of regional flood frequencies, a power law relationship has been observed to hold between mean annual peak discharge per unit area and drainage area (Robinson and Sivapalan, 1997). Gupta et al. (1996) argued that the hypothesis of self-similarity presented a powerful unifying theoretical framework, which can bridge statistical theory of regional flood frequency and important empirical features in watershed topographic, rainfall, and flood data sets. In making this argument, he used a random cascade type model of spatial rainfall intensities and a Peano space filling fractal curve as an idealized model of a river basin (Gupta et al., 1996). The simulated peak flows obeyed a simple statistical scaling with scaling exponent ($\alpha = \log 3/\log 2$). The scaling exponent of peak flows represented the box-counting dimension of the maximum contributing set for the Peano fractal, which was equivalent to the Hausdorff dimension of the simulated fractal network.

Radeziejewski and Kundzewicz (1997) analyzed a binary river flow time series derived by designating as 0 or 1 those time intervals in the original data series where the flow rate was below or above a predefined threshold. The fractal dimension of the binary flow series varied with the threshold value. However, the estimated fractal dimensions ranged from 0 to 1, but tended to remain at 0 or 1 over a range of threshold values (termed as aggregation). They also combined several normalized flow series and analyzed the resulting binary series to evaluate the impact of such combinations on the dimension of

the crossing over threshold (i.e., the range of threshold values for which the estimated dimension was >0 and <1). Their results indicated that such combination resulted in extending the crossing over threshold.

The objective in this chapter was to investigate the scale invariance behavior of daily runoff rate time series for four agricultural watersheds and their 32 sub-watersheds. The scaling property was examined by the fractal dimension estimated using the shifted box-counting method and long term dependence of the runoff time series evaluated from Hurst exponents estimated using R/S analysis.

MATERIALS AND METHODS

Data

The database developed by the Hydrological and Remote Sensing Laboratory of the Agricultural Research Service of the US Department of Agriculture (USDA/ARS/HRSL) was the source of the hydrological data analyzed in this study. It consisted primarily of rainfall/runoff data from the ARS monitored experimental agricultural watersheds nationwide. These watersheds represent numerous land uses and agricultural practices and cover a diverse range of climatic conditions across the U.S. About 16,600 station years of rainfall and runoff were available in the database. The metadata and auxiliary information such as map and land-use information were accessed either by downloading from the ARS /HRSL website (http://hydrolab.arsusda.gov/wdc/arswater.html) or from the CD-ROM distributed by HRSL.

Four agricultural watersheds were selected from the database: (1) the Little River watershed, Southeast Watershed Research Laboratory, Tifton, Georgia; (2) the Little Mill Creek watershed in the North Appalachian Experimental Watershed, Coshocton, Ohio; (3) the Reynolds Creek watershed, Northwest Watershed Research Center, Boise, Idaho; and (4) the Sleepers River watershed, Danville, Vermont. Several factors were taken into account in selecting watersheds for investigation, including length and completeness of the record, watershed and sub-watershed sizes, and availability of other ancillary information. Each watershed selected contained a number of sub-watersheds and their properties are summarized in Table 2.1.

Data from the 32 sub-watersheds listed in Table 2.1 were analyzed. These sub-watersheds covered a wide range of sizes from 0.01 km^2 (sub-watershed W-23 of the Reynolds Creek watershed) to 334 km^2 (sub-watershed W-TB of the Little River watershed). Surface runoff in these sub-watersheds was measured and recorded at various intervals, from a few minutes to several hours. In general, more frequent measurements were made during rain days. The runoff rate recorded was integrated to obtain daily runoff time series for further analysis.

Table 2.1 Properties of agricultural watersheds and sub-watersheds studied.

Watershed	Sub-watershed	Area (km^2)	Record Period	Daily Mean Runoff Rate (cubic meter per second)
Little River watershed	W-TB	333.8	11/1/1971 – 9/30/2002	3.52
	W-TF	114.8	1/1/1969 – 9/30/2002	1.33
	W-TI	49.9	1/1/1969 – 9/30/2002	0.67
	W-TJ	22.1	1/1/1969 – 9/30/2002	0.29
	W-TK	16.7	1/1/1969 – 9/30/2002	0.21
	W-TM	2.6	1/1/1969 – 12/31/1988	0.03
Little Mill Creek watershed	W-5	1.4	10/1/1938 – 10/1/1971	0.012
	W-10	0.5	10/5/1938 – 10/1/1971	0.004
	W-91	0.32	10/1/1938 – 10/1/1971	0.011
	W-92	3.7	10/1/1938 – 10/1/1971	0.035
	W-94	6.2	10/1/1938 – 10/1/1971	0.059
	W-95	11.1	10/1/1938 – 6/22/1972	0.098
	W-97	18.5	1/1/1937 – 10/1/1971	0.181
Reynolds Creek watershed	W-1	233.5	1/1/1963 – 9/30/1996	0.56
	W-2	36.4	1/29/1964 – 4/15/1994	0.082
	W-3	31.8	3/13/1964 – 12/31/1990	0.072
	W-4	54.4	3/29/1966 – 9/30/1996	0.42
	W-11	1.2	1/1/1967 – 12/31/1977	0.0075
	W-13	0.4	1/1/1963 – 9/30/1996	0.0067
	W-14	0.1	3/7/1996 – 4/17/1984	0.000041
	W-15	0.5	10/1/1964 – 12/31/1984	0.0069
	W-16	14.1	1/1/1973 – 12/20/1980	0.13
	W-23	0.01	1/15/1972 – 9/30/1996	0.00000057
Sleepers River watershed	W-1	42.9	1/23/1959 – 12/30/1973	0.67
	W-2	0.6	1/1/1961 – 11/29/1971	0.0073
	W-3	8.4	1/1/1960 – 1/2/1979	0.16
	W-4	43.5	1/1/1960 – 12/30/1973	0.72
	W-5	111.2	1/1/1960 – 12/30/1973	1.97
	W-7	21.8	1/1/1961 – 12/30/1972	0.34
	W-8	15.6	1/1/1961 – 5/15/1979	0.24
	W-9	0.5	9/15/1961 – 7/10/1973	0.0076
	W-11	2.3	5/1/1964 – 11/23/1972	0.026

Shifted Box-Counting Analysis

The records of a runoff time series can be regarded as a binary set of points, which is defined on some threshold value. Zero is generally used as a default threshold value, though other values >0 can be also used. In this case, only the observations with the value greater than the threshold are considered as points of the derived set. In this study, four threshold levels of the runoff rate (0, 0.5M, M, and 1.5M, where M is the average daily runoff rate) were used to define the sets. The scaling property of the runoff data series was measured by the shifted box-counting method on the resulting sets, which is an improvement of the conventional box-counting method (Radziejewski and Kundzewicz, 1997).

In this method, a uniform one-dimensional grid of box size ε was superimposed onto the time domain on which the series is defined. The number of non-overlapping grid segments (boxes) needed to cover the whole series to be analyzed was counted. Only those boxes that contained at least one element that was above the threshold value were counted. The grid position was then shifted in time different units, from 1 to ε - 1. The number of boxes, N(ε), containing elements of the set of interest for all possible shifts were counted, and finally the counts were averaged.

This procedure is illustrated for a data series of 20 values in Figure 2.2. The darkened rectangles represent values above the specified critical value. As shown, if the threshold value is set to 3, for ε = 4, N(ε) = 5; for ε = 2, N(ε) = 8 because two boxes do not contain darkened rectangles. Different box sizes were used to cover the sets. The minimum box size (ε) used was one day, and then the size was doubled (i.e., 2, 4, 8, . . .), until the maximum size (1/5 of the data length) was reached. For sufficiently small ε, $N(\varepsilon) \propto (1/\varepsilon)$. The relationship of N(ε) versus ε was fitted to a power law function:

$$N(\varepsilon) = c(1/\varepsilon)^{D} \qquad (2.1)$$

where c and D are constant values.

The fractal dimension, (D), was calculated as:

$$D = \lim_{\varepsilon \to 0} (\log N(\varepsilon) - \log c) / (\log(1/\varepsilon)) \qquad (2.2)$$

In applying this method log N(ε) was plotted versus log (1/ε), and D was estimated from the graph as the slope of the straight line best fitted to the points.

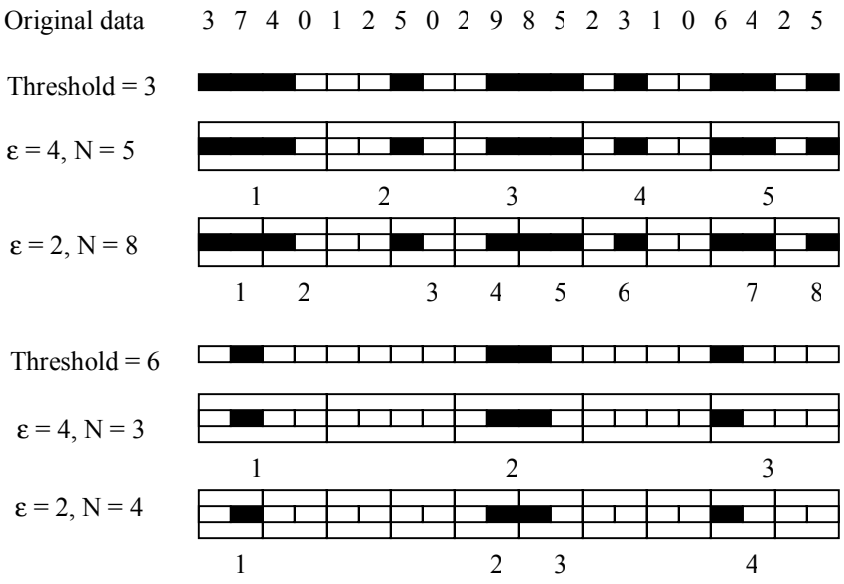

Figure 2.1 Illustration of shifted box-counting method for estimating the fractal dimension of time series data

Rescaled Range (R/S) Analysis

R/S analysis and the Hurst exponent (H) have been used to evaluate the long-term dependence of geophysical, economic, and biological time series (Hurst, 1951; Maldelbrot and Wallis, 1969; Peters, 1994). The procedures of R/S analysis used are described in detail as follows:

Let X(t) be a time series of recorded runoff containing N readings from t = 1 to t = N. Let $X^*(t) = X_{t+1}, \ldots, X_{t+n}$, represent consecutive observation values within a subset of the record from t+1 to time t+n. The lag time n denotes the interval of the subset, and t denotes the starting point for the subset. The mean value, X_m, of the time series X*(t) is defined as:

$$X_m = \left(\sum_{i=t+1}^{i=t+n} X_i\right)/n \qquad (2.3)$$

The standard deviation of the subset from t+1 to time t+n, S_n, is estimated as:

$$S_n = n^{-1/2} * \sqrt{\sum_{r=t+1}^{t+n} (X_r - X_m)^2} \qquad (2.4)$$

The rescaled range is calculated by first rescaling the subset data by subtracting the sample mean of X*(t) as:

$$Z_r = (X_r - X_m) \qquad r = t+1, \ldots, t+n \qquad (2.5)$$

And the cumulative time series, Y, is created by:

$$Y_{r+1} = Z_{t+1} \qquad r = t+1 \qquad (2.6)$$

$$Y_r = (Y_{r-1} + Z_r) \qquad r = t+2, \ldots, t+n \qquad (2.7)$$

The adjusted range, R_n, is the accumulative departure from the mean, i.e. the maximum minus the minimum value of Y_r:

$$R_n = Max(Y_{t+1},...,Y_{t+n}) - Min(Y_{t+1},...,Y_{t+n}) \qquad (2.8)$$

For the interval starting at time t, of width n, R and S are computed. This is repeated for each successive t, until t reaches N - n + 1. The procedures are repeated for the next lag time n, until all selected lags have been tested. A general form of the relationship of R/S to n (Hurst, 1951):

$$(R/S)_n = c * n^H \qquad (2.9)$$

A log transformation of (2.9) gives

$$\log(R/S) = H \log n + \log c \qquad (2.10)$$

Exponent H is estimated from the graph as the slope of the straight line best fitted to the points.

RESULTS AND DISCUSSION

Estimated Fractal Dimension

An example of the shifted box-counting graph log N(ε) versus log ε for the runoff time series in sub-watershed W-TB of the Little River watershed is displayed in Figure 2.2. The daily mean runoff rate (M) in this example was 3.52 m^3 s^{-1} (Table 2.1). Four intensity thresholds (0, 0.5M, M, and 1.5M, where M is the average daily runoff intensity) were used to define the sets. Since log N(ε) versus log ε was plotted instead of log N(ε) versus log (1/ε), the value of the negative slope represents the estimated fractal dimension of the sets. The box sizes (time scales) were between one day and 1/5 of the length of the records. If the runoff time series possessed a scale-invariance property, a straight line could be fitted to the box-counting graph or part of it, according to the Eq.(2.2). Figure 2.2 shows that for each threshold, two distinct scaling ranges are apparent, each of which can be fitted with a straight-line section by least square regression, instead of a single linear relationship over the entire range of time scales.

The negative slope of each regression line represents the fractal dimension within that scaling range. The existence of linear relationship over certain time scales indicates that there is a scale invariant distribution of runoff in time, which is valid within the defined linear scaling range. In fluid mechanics, dimensionless similarity parameters such as Reynolds number are used to bridge across scales in hydraulic design. However, it was not feasible to extend this principle of similarity using dimensional parameters to watershed hydrological processes across different scales (Dooge, 1986). By using fractal concepts, temporal scale invariance of runoff might be characterized by a single parameter, fractal dimension (D). Since two D values were obtained from the box-counting analysis for the time series in this example over the time period under consideration, it implies that its scaling properties vary with the time scales.

Likewise, the runoff time series of other five sub-watersheds in the Little River watershed as well as all the sub-watersheds in the other watersheds studied (Little Mill Creek watershed, Reynolds Creek watershed, and Sleepers River watershed) all displayed two

scaling ranges for each threshold in their box-counting graphs. The break point (intersection of the two straight line sections in the log N(ε) versus log ε plots) for all thresholds corresponded to the same box size, which indicates the same scaling ranges are valid no matter what runoff intensity threshold was used to define the set.

To further precisely locate the break point, the box-counting technique was applied with one-day increment of box size (Figure 2.3) instead of the exponential doubling increments used for Figure 2.2. In Figure 2.3, the break point was found to correspond to a box size of approximately 365 days. This may be explained by the obvious annual cycle of all the runoff time series. The fact that two scaling ranges were apparent would indicate that the scaling characteristics of the short-term process (< 1 year) and long-term process (> 1 year) for watershed runoff were different. Breakpoints in scaling ranges for watershed runoff were also found in other studies using the shifted box-counting analysis. In their investigation of daily flows of the river Warta in Poland, Radziejewski and Kundzewicz (1997) reported a distinct break point in the scaling ranges at approximately 2-4 years. They also detected another less distinct break point located at 10-15 days.

The pattern of multiple scaling segments in box-counting plot has been also observed in rainfall time series (Olsson et al., 1992, 1993). The box sizes corresponding to the break points on the plot were related to the average duration of rainfall events and the average duration of dry periods between rainfall events (Olsson et al., 1992). In another study of rainfall, Peters and Christensen (2002) detected a break point of scaling near 3-4 days. They concluded that parameters estimated from the rainfall series could not be used to characterize the frontal system if the estimates are based on observations that are temporally separated by significantly more than 3 days. Multiple scaling ranges seem to be a common phenomenon of natural hydrological series.

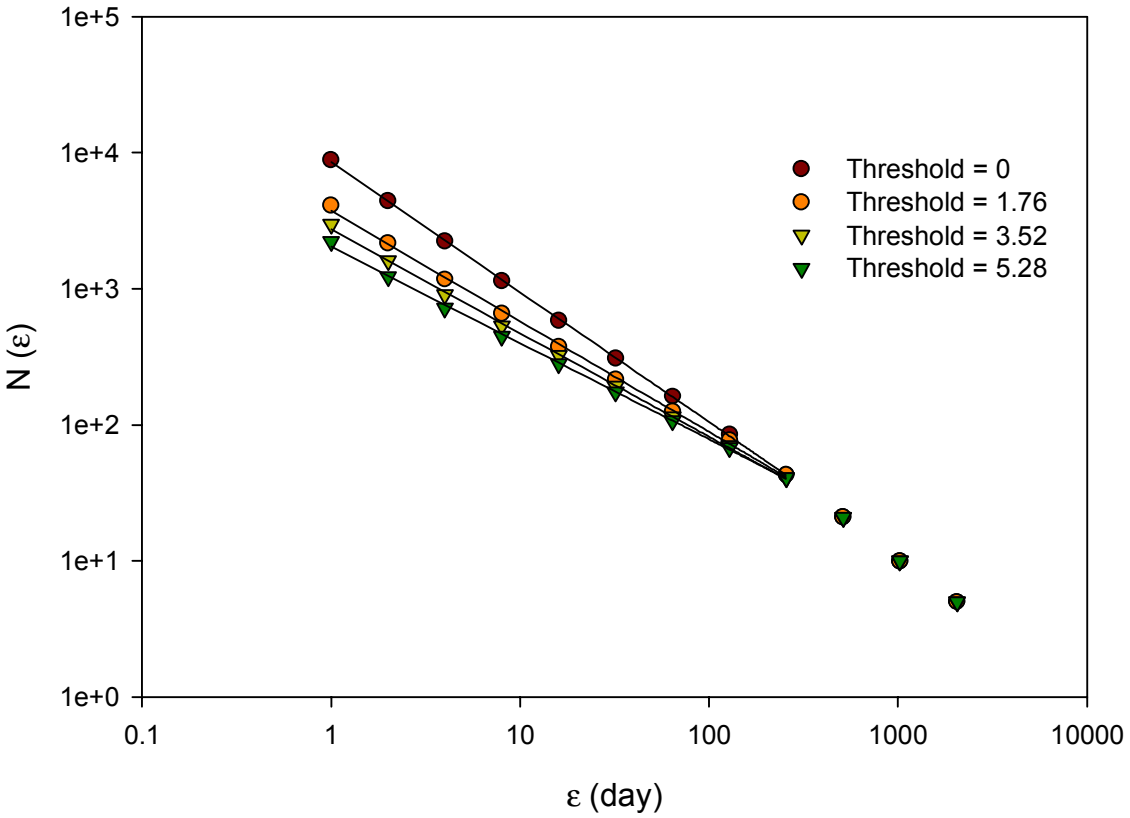

Figure 2.2. Log-log plots of number of boxes [N(ε)] versus box size (ε) for different threshold values (0, 1.76, 3.52, and 5.28 m^3/s) using the shifted box counting method to analyze the runoff rate series for sub-watershed W-TB of the Litter River watershed in Tifton, Georgia. In all cases, r^2 was > 0.990 for the straight lines fitted to the sections of the graph. Box sizes were exponentially doubled starting at $\varepsilon = 1$ day.

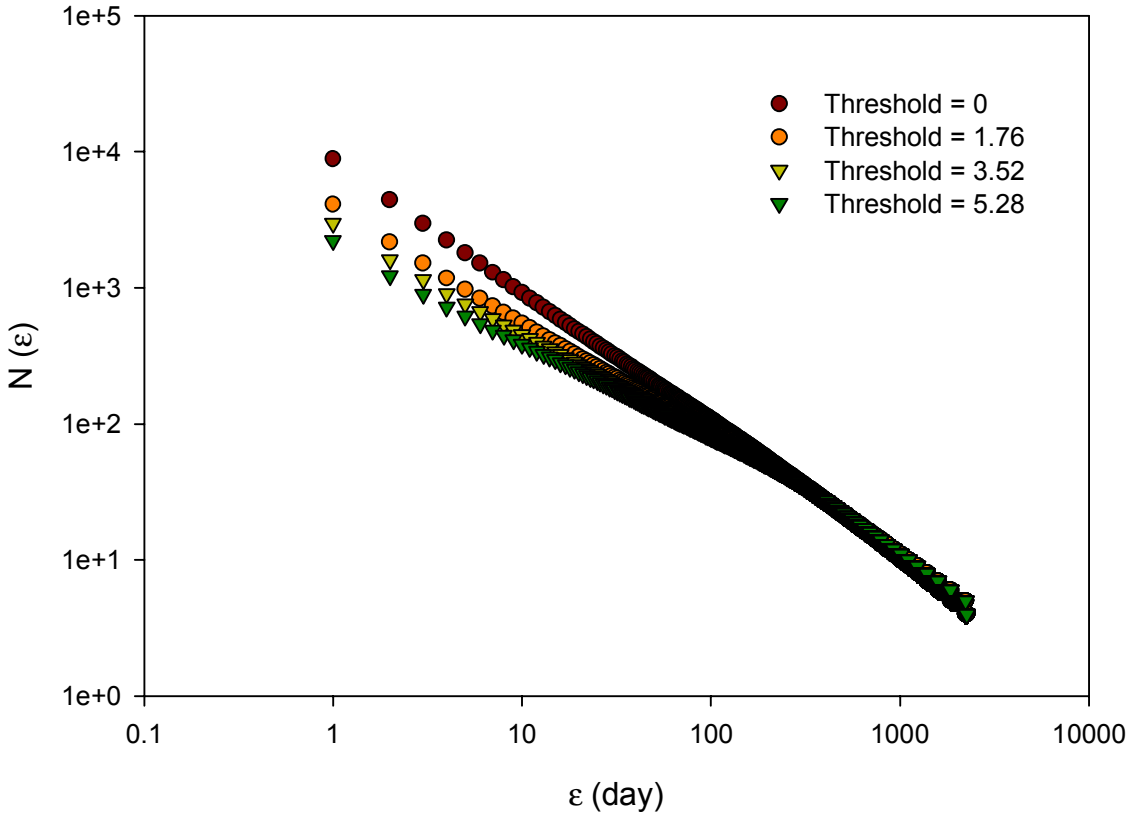

Figure 2.3. Shifted box counting graph as in Figure 2.2 but with one day increment of box size (ε) for sub-watershed W-TB of the Litter River watershed in Tifton, Georgia. The break point of the slope occurs at approximately ε = 365 days.

Estimated fractal dimensions of the runoff time series are summarized in Table 2.2 through 2.5 for each of the four watersheds. If we term the scaling range of box size less than 1 year as range 1, and as 2 otherwise, the fractal dimension in range 1 decreases as the threshold increases. In range 1, for example, D decreases from 0.96 at 0 $m^3 s^{-1}$ to 0.71 at 5.28 $m^3 s^{-1}$ for the runoff time series of sub-watershed W-TB (Table 2.2). However, the fractal dimensions at range 2 show almost no change for various thresholds with D = 1.0 (Figure 2.2). The dependence of the estimated fractal dimension on the defined threshold value was also observed in previous studies (Olsson et al., 1992, 1993; Radziejewski and Kundzewicz, 1997). In all of these studies, a fractal dimension of 1.0 was obtained when the time scale exceeded a certain value, which was about 365 days in this study.

Naturally, a runoff series of observations has an intermittent pattern. Especially in a dry area, runoff occurs over relatively short durations separated by much longer time intervals of various lengths with no measurable runoff. Therefore, the runoff can be best modeled as a random Cantor set (or Cantor dust), which is a strictly self-similar fractal geometrical object. It is constructed by iteratively removing portions from a line segment of unit length. The size of the portions and their location on the line segment on as well as on the remaining sub-segments are randomly selected. The simplest form of a Cantor set (a non-random set) is created by iteratively removing the central one-third portion of a unit line segment. As the process is repeated to infinity, the sub-segments become shorter and shorter, and form a set of points with different intervals (gaps) between them. If only the days when daily runoff intensity exceeds a selected threshold value are marked, and other days are considered as gaps, then the time structure of a runoff time series would closely resemble a Cantor dust, and their degree of clustering of runoff events can be estimated using the using a random Cantor dust model.

For the runoff series in this study, for the 0 $m^3 s^{-1}$ threshold, D appropriates or equals to 1.0 for all the runoff series (Table 2.2 ~ 2.5). This might be because the observations of daily runoff intensity are nearly all greater than 0, therefore, the generated set is almost continuous with few gaps (no runoff) between them. As the threshold increases, the

Table 2.2. Fractal dimensions of daily runoff rate for six sub-watersheds of the Little River watershed in Tifton, Georgia. Fractal dimensions corresponding to four threshold levels of the runoff rate (0, 0.5M, M, and 1.5M, where M is the daily mean runoff rate) were obtained as the absolute value of the slope of straight lines fitted to plots as shown in Figure 2.2.

Sub-watershed	Threshold ($m^3 s^{-1}$)	Fractal Dimension (D)	r^2
W-TB	0	0.96	0.999
	1.76	0.81	0.998
	3.52	0.76	0.997
	5.28	0.71	0.994
W-TF	0	0.94	0.999
	0.66	0.83	0.998
	1.33	0.77	0.995
	2.00	0.71	0.991
W-TI	0	0.93	0.999
	0.33	0.83	0.997
	0.67	0.77	0.995
	1.00	0.70	0.991
W-TJ	0	0.92	0.999
	0.15	0.81	0.996
	0.30	0.74	0.994
	0.45	0.68	0.990
W-TK	0	0.92	0.999
	0.10	0.84	0.997
	0.20	0.79	0.996
	0.30	0.73	0.994
W-TM	0	0.96	0.999
	0.015	0.83	0.998
	0.03	0.76	0.996
	0.045	0.69	0.991

Table 2.3. Fractal dimensions of daily runoff rate for seven sub-watersheds of the Little Mill Creek watershed in Coshocton, Ohio. Fractal dimensions corresponding to four threshold levels of the runoff rate (0, 0.5M, M, and 1.5M, where M is the daily mean runoff rate) were obtained as the absolute value of the slope of straight lines fitted to plots as shown in Figure 2.2.

Sub-watershed	Threshold ($m^3 s^{-1}$)	Fractal Dimension (D)	r^2
W-5	0	1.00	0.999
	0.006	0.83	0.995
	0.012	0.75	0.991
	0.018	0.69	0.986
W-10	0	0.99	0.999
	0.002	0.79	0.995
	0.004	0.71	0.990
	0.006	0.63	0.983
W-91	0	1.01	0.999
	0.0057	0.82	0.996
	0.011	0.75	0.991
	0.172	0.67	0.985
W-92	0	0.99	0.999
	0.018	0.82	0.999
	0.036	0.74	0.999
	0.054	0.66	0.998
W-94	0	1.00	0.999
	0.03	0.82	0.996
	0.06	0.73	0.991
	0.09	0.66	0.985
W-95	0	0.99	0.999
	0.049	0.82	0.997
	0.098	0.73	0.993
	0.147	0.67	0.989
W-97	0	1.00	0.999
	0.09	0.82	0.997
	0.18	0.73	0.993
	0.27	0.64	0.987

Table 2.4. Fractal dimensions of daily runoff rate for ten sub-watersheds of the Reynolds Creek watershed in Boise, Idaho. Fractal dimensions corresponding to four threshold levels of the runoff rate (0, 0.5M, M, and 1.5M, where M is the daily mean runoff rate) were obtained as the absolute value of the slope of straight lines fitted to plots as shown in Figure 2.2.

Sub-watershed	Threshold ($m^3 s^{-1}$)	Fractal Dimension (D)	r^2
W-1	0	1.00	0.999
	0.28	0.82	0.997
	056	0.77	0.996
	0.84	0.72	0.994
W-2	0	1.00	0.999
	0.041	0.85	0.998
	0.082	0.76	0.996
	0.123	0.70	0.994
W-3	0	1.00	0.999
	0.036	0.81	0.998
	0.072	0.74	0.996
	0.108	0.68	0.995
W-4	0	1.00	0.999
	0.21	0.82	0.997
	0.42	0.75	0.996
	0.63	0.72	0.994
W-11	0	0.98	0.999
	0.0038	0.84	0.998
	0.0075	0.77	0.998
	0.0113	0.72	0.997
W-13	0	1.00	0.999
	0.0034	0.76	0.993
	0.0067	0.80	0.990
	0.01	0.79	0.989
W-14	0	0.72	0.994
	0.00002	0.67	0.995
	0.00004	0.65	0.995
	0.00006	0.63	0.993
W-15	0	0.99	0.999
	0.0035	0.77	0.995
	0.0070	0.73	0.992
	0.0105	0.70	0.991
W-16	0	1.00	0.999
	0.065	0.84	0.999
	0.13	0.77	0.998
	0.195	0.74	0.996
W-23	0	0.41	0.976
	0.00000028	0.41	0.976
	0.00000057	0.41	0.976
	0.00000084	0.41	0.977

Table 2.5. Fractal dimensions of daily runoff rate for nine sub-watersheds of the Sleepers Creek watershed in Vermont. Fractal dimensions corresponding to four threshold levels of the runoff rate (0, 0.5M, M, and 1.5M, where M is the daily mean runoff rate) were obtained as the absolute value of the slope of straight lines fitted to plots as shown in Figure 2.2.

Sub-watershed	Threshold ($m^3 s^{-1}$)	Fractal Dimension (D)	r^2
W-1	0	1.00	0.999
	0.34	0.86	0.997
	0.67	0.73	0.991
	1.00	0.67	0.987
W-2	0	1.00	0.999
	0.0036	0.88	0.997
	0.0072	0.76	0.995
	0.0108	0.65	0.986
W-3	0	1.00	0.999
	0.08	0.88	0.998
	0.16	0.74	0.992
	0.24	0.65	0.987
W-4	0	1.00	0.999
	0.36	0.87	0.997
	0.72	0.74	0.992
	1.08	0.67	0.991
W-5	0	1.00	0.999
	0.98	0.87	0.997
	1.97	0.75	0.992
	2.95	0.67	0.989
W-7	0	1.00	0.999
	0.17	0.86	0.997
	0.34	0.73	0.994
	0.51	0.67	0.989
W-8	0	1.00	0.999
	0.12	0.84	0.999
	0.24	0.73	0.994
	0.36	0.66	0.989
W-9	0	0.98	0.999
	0.0038	0.83	0.998
	0.0076	0.73	0.995
	0.0114	0.66	0.994
W-11	0	0.99	0.999
	0.013	0.85	0.999
	0.026	0.77	0.995
	0.039	0.69	0.992

records that are not greater than the threshold are filtered out, and hence more gaps would appear in the newly defined set, and the corresponding Cantor set is sparser. As a result, a smaller dimension was obtained from the box-counting plot. In scaling range 2 where the box sizes are greater than one year the fractal dimension is equal to 1.0 at all the threshold levels (Figure 2.2). This might be because there would always have at least one day of a year that the runoff rate exceeded the threshold value. The regression coefficients of regression lines in the log $N(\varepsilon)$ versus log ε plots were high for all the runoff time series with values greater than or close to 0.990, which indicates a strong linear relation. These consistently high values are considered requisite to provide confidence in any inference that the runoff series under investigation demonstrate scale invariant characteristics.

Table 2.2 indicates that the fractal dimensions for all the 6 sub-watersheds of the Little River watershed at each level of the threshold were almost the same, although the contribution areas of these sub-watersheds are different (2.6 ~ 333.8 km^2 for sub-watersheds of the Little River watershed as listed in Table 2.1). For the sub-watersheds of the Little River watershed, the D-value ranged from 0.92 to 0.96 for threshold level 1, 0.81 to 0.83 for level 2, 0.74 to 0.79 for level 3, and 0.68 to 0.71 for level 4 (Table 2.2). The same pattern was found in all the other three watersheds (Tables 2.3 through 2.5).

The fractal dimension reflects the degree of irregularity by which the occurrence of an event, such as rainfall, is distributed within a time series (Olsson et al., 1992). Therefore, the estimated dimension of runoff time series might be interpreted as the reflection of the degree of irregularity by which the occurrence of runoff (based on the threshold defined) is distributed. The almost identical fractal dimension of different sub-watersheds at a given threshold level suggests that the irregularity of the runoff distribution in these sub-watersheds has the same pattern, and that the generation of the runoff might follow the same process for those sub-watersheds within a watershed.

The results presented in Tables 2.2 through 2.5, and the log $N(\varepsilon)$ versus log ε box-counting plots for the runoff time series were quite consistent across the sub-watersheds

of the four watersheds. With the exception of the two smallest sub-watersheds (W-14 and W-23 of the Reynolds Creek watershed), the same fractal dimension (estimated using the shifted box-counting method) was obtained for the runoff series at each threshold level although these watersheds varied markedly in climate, topography, and size (Table 2.1). For example, for a given threshold level, say level 2, the fractal dimension is about 0.85 for practically all the runoff time series in four watersheds (Tables 2.2 to 2.5). In other words, runoff time series in these watersheds and their sub-watersheds have similar distribution of occurrence of runoff, and exhibit the same pattern of scaling, although they have different climates, geography, soil type, land management, etc.

It should be pointed out that the threshold values used to define the sets were different for each runoff time series because the mean daily runoff rates of the sub-watersheds were different (Table 2.1). Selecting threshold values based on mean daily runoff rates allows comparison of the fractal dimensions estimated from different runoff time series. The results indicated that although the daily runoff rates were different by orders of magnitude (Table 2.1), the occurrence of runoff had the same distribution.

At threshold level 4, the fractal dimensions of runoff time series for the Little Mill Creek and Sleepers River watersheds were slightly less than that for the Little River and Reynolds Creek watersheds. A lower dimension means that more points are clustered in groups over time scales. Thus it indicated that high runoff occurrences are more clustered in the Little Mill Creek and Sleepers River watersheds than the other two watersheds.

As discussed above, the occurrence of runoff in agricultural sub-watersheds of various sizes had similar distribution, making it possible to extrapolate runoff behavior over a fairly large range of spatial scales within a watershed. However, this scaling property may not be valid when the sub-watersheds are small. The box dimension of the runoff series for the two smallest sub-watersheds (W-14 = 0.01 km^2 and W-23 =0.1 km^2) of the Reynolds Creek watershed, were much lower and did not change at different threshold levels (Table 2.4). It indicated that the distribution of runoff occurrence in very small

sub-watersheds might be different from larger watersheds, and extrapolation might not be feasible at relatively small scales. One possible explanation might be that the volume of surface runoff from a very small sub-watershed is limited, and measured runoff tends to be almost zero most of the time depending on the sensitivity and resolution of the measuring instruments. On the other hand, for the runoff series investigated in this study, no upper restriction of sub-watershed size was detected.

Estimated Hurst Exponent

The Hurst exponent (H) as a useful parameter to describe long-term persistence of observations in hydrological time series was initially applied in an empirical manner to water reservoir design (Hurst, 1951). It was later established that the Hurst exponent was theoretically related to the fractal dimension via Eq. (2.2) for idealized time series that can be modeled as fractional Brownian motions. Figure 2.4 shows an example of the rescaled range plot used to obtain the Hurst exponent of the runoff time series for sub-watershed W-TB in the Little River watershed. In the plot, two distinct scaling ranges (denoted as range 1 and range 2) are clearly displayed with a break point at a lag time of about 18 month. A straight line was fitted to each scaling range by least square regression. The regression coefficient of determination (r^2) was used to evaluate the goodness of the linear fit. The high value of r^2 for range 1 (>0.99) indicated a valid scaling range.

The rescaled range plots of all runoff time series had two obvious scaling ranges as shown in the example of Figure 2.4. The lag time corresponding to the break point of the two scaling ranges was about 15 ~ 18 months, which is consistently greater than the value of about 1 year obtained from box-counting plots (Figure 2.2).

The H values of each runoff time series are presented in Table 2.6. In general, the H values in scaling range 1 (lag time less than the break point) is greater than 0.5 with typical value being above 0.8 (Table 2.6). An H value greater than 0.5 indicates a persistent process or positive long-term dependence (Mandelbrot and Wallis, 1969). It implies that a greater than average runoff is more likely followed by another greater

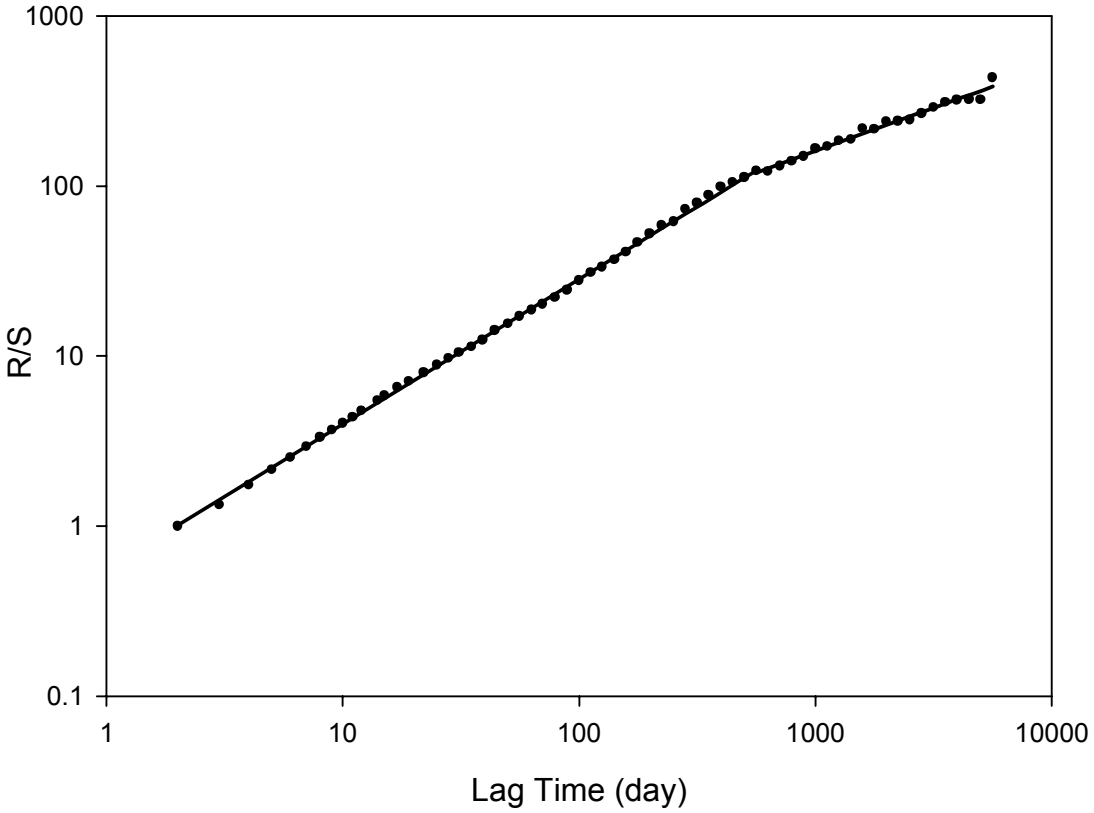

Figure 2.4. Hurst rescaled range analysis plot for subwatershed W-TB of the Little River watershed in Tifton, Georgia. A scaling break point occurs at about 18 months. r^2 was > 0.99 for the straight lines fitted to each scaling range.

Table 2.6. Hurst exponent (H) of daily runoff time series estimated using the rescaled range analysis method. Scaling range 1 corresponds to the lag time less than the break point of rescaled range plot, and range 2 corresponds to the lag time greater than the break point. H for each range was obtained as the slope of fitted straight lines to plots as shown in Figure 2.4.

Watershed	Sub-watershed	Range 1		Range 2	
		H	r^2	H	r^2
Little River Watershed	W-TB	0.85	0.999	0.50	0.992
	W-TF	0.85	0.998	0.49	0.983
	W-TI	0.82	0.999	0.48	0.988
	W-TJ	0.82	0.998	0.51	0.989
	W-TK	0.83	0.997	0.51	0.986
	W-TM	0.81	0.997	0.46	0.981
	Average	0.83		0.49	
Little Mill Creek watershed	W-5	0.83	0.999	0.52	0.988
	W-10	0.80	0.999	0.51	0.989
	W-91	0.85	0.999	0.46	0.991
	W-92	0.83	0.999	0.46	0.993
	W-94	0.82	0.999	0.47	0.992
	W-95	0.83	0.999	0.46	0.991
	W-97	0.80	0.999	0.53	0.990
	Average	0.82		0.49	
Reynolds Creek watershed	W-1	0.92	0.999	0.60	0.973
	W-2	0.92	0.999	0.54	0.983
	W-3	0.89	0.999	0.60	0.991
	W-4	0.95	0.999	0.59	0.978
	W-11	0.92	0.999	0.53	0.972
	W-13	0.93	0.999	0.43	0.971
	W-14	0.73	0.999	0.60	0.985
	W-15	0.92	0.999	0.35	0.988
	W-16	0.96	0.999	0.27	0.970
	W-23	0.60	0.996	0.37	0.984
	Average	0.87		0.49	
Sleepers River watershed	W-1	0.88	0.998	0.45	0.795
	W-2	0.87	0.998	0.30	0.892
	W-3	0.90	0.998	0.41	0.952
	W-4	0.91	0.997	0.32	0.888
	W-5	0.90	0.997	0.29	0.810
	W-7	0.87	0.998	0.39	0.958
	W-8	0.91	0.998	0.35	0.947
	W-9	0.91	0.999	0.42	0.709
	W-11	0.92	0.997	0.63	0.758
	Average	0.90		0.40	

than average runoff rather than by chance. In other words, the occurrences of the runoff have the tendency to appear in clusters, and the tendency is rather strong as indicated by the high values of H.

Similar H values were obtained for almost all of the runoff time series of sub-watersheds within each watershed (Table 2.6), which implies that these runoff time series might have similar long-term memory, though their contribution areas are much different. The two smallest sub-watersheds, namely W-14 and W-23 in the Reynolds Creek watershed, had a much smaller H value than the other relatively bigger sub-watersheds. The H value for W-14 is 0.73 and 0.60 for W-23, but about 0.90 for other sub-watersheds in the Reynolds Creek watershed (Table 2.6). Because the Hurst exponent captures the long-term persistence in the data series, similar values might be interpreted as a reflection of similarities in stable sub-watershed characteristics such as topography, meteorology, and soil type. However, this interpretation may not be applicable at very small scales.

The sub-watersheds of the Reynolds Creek and Sleepers River watershed had higher H values than those of the Little River and Little Mill Creek watersheds (Table 2.6), although H values were high for all four agricultural watersheds. The H values for the Reynolds Creek and Sleepers River sub-watersheds were about 0.9, and the H values of the other two sub-watershed groupings were about 0.8. As discussed above, the Hurst exponent reflects the long-term dependence of the time series. A higher H value indicates that the previous runoff record will positively affect the future runoff intensity, thus an extreme event would have higher probability of being followed by other extreme events.

In comparison with scaling range 1, the H-values for scaling range 2 above the break point were smaller and more variable among the sub-watersheds than for range 1. Also, the linear fits had smaller r^2 values, indicating that the scaling property in range 2 was not as persistent as in range 1. The smaller H values in range 2 imply that the strong long-term persistence dissipates beyond the lag time of about 15 ~ 18 months. In other words, observations in the runoff record separated by 15 months or more have little or no impact on each other. For the Little River and Little Mill Creek sub-watershed groups, H

values ranged from 0.46 to 0.53 (Table 2.6) for scaling range 2, indicating a random process (Mandelbrot and Wallis, 1969). This implies that the impact of past events on future runoff basically disappeared after 15 ~ 18 months. For the Sleepers River sub-watershed group, the H values were even smaller, much less than 0.50 (Table 2.6) indicating anti-persistence.

As previously indicated, the W-14 and W-23 sub-watersheds of the Reynolds Creek watershed have much different fractal dimension and Hurst exponent in comparison with other sub-watersheds, which might be explained by their relatively small size (0.1 km^2 and 0.01 km^2). Watershed hydrological response (e.g. surface runoff), is a function of the size of the area being considered. The effect of underlying heterogeneity on such response is somewhat random at smaller scales, but becomes more systematic at larger scales (DeCoursey, 1996). General terms such as local scale, hillslope scale, and catchment scale are often used to distinguish different spatial scales in hydrology (Kirkby, 1988). It is generally recognized that the dominance of various watershed features changes as scale changes. For example, soil properties dominate at local and hillslope scale, while the topography and basin morphology are important at the larger scale. However, the watershed size ranges that validly define these scales is hard to determine, since it would depend on the topography, soils, climate and other factors of the watershed. For example, it could be a square kilometer or larger in dry climates with gentle slope and sandy soils, but a hectare or less in humid areas with loam soils (DeCoursey, 1996). The analyses by Wood et al. (1988) showed plotted runoff and infiltration volume against catchment area showed a convergence of mean runoff and infiltration volumes at about 1.0 km^2. This area was described as a Representative Elementary Area (REA), which is a function of the particular catchment and climatic characterization and general topography. The REA's of two catchments (4.4 and 631 ha) were found to be 0.02-0.03 and 2.5-3.5 km^2 for the small and large areas, respectively (Goodrich et al., 1993). When the catchments are greater than the REA, the hydrological response of individual catchments becomes alike even though the patterns of properties within each catchment may be different (DeCoursey, 1996).

FINDINGS AND CONCLUSIONS

The scaling property of daily runoff for 32 sub-watersheds covering a wide range of sizes in four agricultural watersheds of different climate and topography was examined using the shifted box-counting method and Hurst rescaled range analysis. The results showed that long-term records of daily runoff rate exhibited scale invariance over certain time scales. Two scaling ranges were identified in the shifted box-counting plots with a break point at about 12 months. The Hurst analysis showed that the runoff time series also displayed a rather strong long-term persistence which dissipated after 15~18 months. The same fractal dimensions and Hurst exponents were obtained for the sub-watersheds within each watershed, indicating that the runoff of these sub-watersheds have similar distribution of occurrence and similar long-term memory.

These results indicated the existence of scale invariance in the runoff time series in agricultural watersheds over temporal and spatial scales. This finding would imply the theoretical possibility of deriving short-term estimates from longer-term measurements or vice versa, or to transfer information about runoff data and runoff processes from gauged to ungauged areas. Extrapolation between scales of observations and between watersheds would reduce the extent and degree of monitoring data required by legislative mandates or model simulation and lead to significant savings in cost and time.

REFERENCES

Austin, P. M. and R. A. Houze. 1972. Analysis of the structure of precipitation patterns in New England. Journal of Applied Meteorology 11: 926-935.

Bloschl, G. and M. Sivapalan, 1995. Scale issues in hydrological modeling: a review. Chapter 2 in: Scale Issues In Hydrological Modelling. John Wiley & Sons, New York.

Crane, R. K. 1990. Space-Time Structure of Rain Rate Fields. Journal of Geophysical Research D95: 2011-2020.

DeCoursey, D. G. 1996. Hydrological, climatological, and ecological systems scaling: A review of selected literature and comments. Interim Progress Report. USDA-ARS-NPA, GRSRU. Fort Collins, CO 80522.

Dooge, J. C. I. 1986. Looking for hydrologic laws. Water Resources Research 22: 46-58.

Goodrich, D. C., D. A. Woolhiser, and S. Sorooshian. 1993. A stabilization measure for stream network complexity and application of REA concepts to semi-arid watersheds. In Scale Issues in Hydrological/Enviormental Modeling (Kalma, J., M. Sivapalan, and E Wood, editors). CSIRO-UAW-ANU.

Gupta, V. K. and E. Waymire. 1987. On Taylor's hypothesis and dissipation in rainfall. Journal of Geophysical Research 92: 9657-9660.

Gupta, V. K. and E. Waymire. 1993. A statistical analysis of mesoscale rainfall as a random cascade. Journal of Applied Meteorology 32; 251-267.

Gupta, V. K., S. L. Castro, and T. M. Over. 1996. On scaling exponents of spatial peak flows from rainfall and river network geometry. Journal of Hydrology 187: 81-104.

Hurst, H. E. 1951. The long term storage capacity of reservoirs. Transactions of the American Society of Civil Engineers 116: 770-808.

Kirkby, M. J. 1988. Hillslope runoff processes and models. Journal of Hydrology 100: 315-339.

Lovejoy, S. and D. Schertzer. 1985. Generalized scale invariance and fractal models of rain. Water Resources Research 21: 1233-1250.

Mandelbrot, B. B. and J. R. Wallis. 1969. Some long-run properties of geophysical records. Water Resources Research 5: 321-340.

Mandelbrot, B. B. 1983. The fractal geometry of nature. W.H. Freeman, New York.

Menabde, M., D. Harris, A. Seed, G. Austin, and D. Stow. 1997. Multiscaling properties of rainfall and bounded random cascade. Water Resources Research 33: 2823-2830.

Olsson, J., J. Niemczynowicz, R. Berndtsson, and M. Larson. 1992. An analysis of the rainfall time structure by box-counting-some practical implications. Journal of Hydrology 137: 261-277.

Olsson, J., J. Niemczynowicz, and R. Berndtsson. 1993. Fractal analysis of high-resolution rainfall time series. Journal of Geographic Research 98: 23265-23274.

Pandey, G., S. Lovejoy, and D. Schertzer. 1998. Multifractal analysis of daily river flows including extremes for basins of five to two million square kilometers, one day to 75 years. Journal of Hydrology 208: 62-81.

Peters, E. E. 1994. Fractal market analysis: applying chaos theory to investment. John Wiley & Sons Inc., New York.

Peters, O. and K. Christensen. 2002. Rain: relaxation in the sky. Physical Review E 66:1-9.

Radziejewski, M. and Z. W. Kundzewicz. 1997. Fractal analysis of flow of the river Warta. Journal of Hydrology 200: 280-294.

Robinson, J. S. and M. Sivapalan. 1997. Temporal scales and hydrological regimes: Implications for flood frequency scaling. Water Resources Research 33: 2981-2999.

Rodriguez-Iturbe, I. and A. Rinaldo. 1997. Fractal river basins: chance and self-organization. Cambridge University Press, New York.

Schertzer, D. and S. Lovejoy. 1987. Physical modeling and analysis of rain and clouds by anisotropic scaling multiplicative processes. Journal of Geophysical Research 92: 9693-9714.

Schmitt, F., S. Vannitsem, and A. Barbosa. 1998. Modeling of rainfall time series using two-state renewal processes and multifractals. Journal of Geophysical Research 103: 23181-23193.

Wood, E. F., M. Sivapalan, K. Beven, and L. Band. 1988. Effects of spatial variability and scale with implications to hydrological modeling. Journal of Hydrology 102: 29-47.

CHAPTER III
MULTIFRACTAL SCALING OF DAILY RUNOFF TIME SERIES

INTRODUCTION

Fractals were regarded as bizarre mathematical objects when they were first discovered because their geometrical properties could not be interpreted using classical Euclidean concepts. The concepts of fractal geometry (Mandelbrot, 1983), were shown to provide more realistic descriptions of many natural shapes and forms such as clouds, trees, etc. (Barnsley, 1993). Since that time, fractal geometrical concepts have been extensively applied to diverse fields including physics, ecology, geology, medicine, etc. A key concept of fractal geometry is invariance of shape and form under affine scaling transformations. Scale invariance when the scaling factors of the transformation are different for different directions (anisotropic scaling) is termed as self-affinity. The case where they are the same in all directions (isotropic scaling) is termed as self-similarity. Strict self-similarity is only obtained for mathematical fractals. Most natural fractal objects and processes are self-affine.

The concepts of self-similarity and self-affinity proved to be useful tools to describe scale invariance in the statistical distribution of observations in space or time of some natural processes, such as rainfall (Lovejoy and Schertzer, 1985; Olsson et al., 1992) and sedimentary time series (Prokoph, 1999). In these early analyses, a single scaling exponent was used to describe the behavior of the moments of the statistical distribution at different time scales. This approach was in effect an extension of concepts associated with scaling of geometrical sets using single scaling exponents and can be regarded as the "monofractal" approach to describe fractal behavior. However, recent studies have indicated that multiple scaling exponents were needed to describe statistical scaling behavior in many natural time series. Analysis based on multiple scaling exponents can be regarded as the multifractal approach. Indeed it is now acknowledged that mutifractal

analyses provide more general description of natural series, and monofractals are indeed special cases (meaning that the scaling exponents are the same) for continuous or discrete multifractals (Lovejoy et al., 1987; Lovejoy and Schertzer, 1990). There is an increasing realization that multifractal approach might be more appropriate for analyzing and understanding the scaling behavior of natural time series. No extensive body of knowledge as yet exists on application of the multifractal approach to investigate scaling behavior in runoff time series. On the other hand, many reports exist on its application to rainfall time series. Since rainfall is the primary driver for most hydrological systems, valuable ideas and concepts may be obtained from these reports.

In monofractal analysis of the distributions of the occurrence or non-occurrence of events in rainfall time series, the fractal dimension is assumed to be independent of the intensity threshold (Lovejoy and Schertzer, 1985; Hubert et al., 1993). In reality, the occurrences of rainfall events is often defined in relation to rainfall intensity threshold. From analysis of rainfall data series using a multifractal approach, Lovejoy and Schertzer (1985) concluded that they exhibit a much more complex structure than was revealed assuming threshold independence. Based on analysis of the statistical scaling properties of rainfall in time or space, it became clear that precipitation was a strongly intermittent and nonlinear process, characterized by an infinite hierarchy of intensity-dependent dimension (Schertzer and Lovejoy, 1987; Lovejoy and Schertzer, 1990). They concluded that some complex phenomena and processes (e.g. cloud formation and rain generation) are the result of nonlinear dynamic processes, and that monofractal models were not the best way to generate synthetic space-time fields of precipitation because the scaling exponents depended on the statistical moments (Schertzer and Lovejoy, 1987). This problem can be overcome by using a multifractal approach.

In the multifractal approach, the scaling behavior of fields may be expressed using several scale-independent statistical relationships. Schertzer and Lovejoy (1987) related the probability distributions of rainfall intensities at different time scales via a scaling relationship:

$$\Pr(R_\lambda > \lambda^\gamma) = \lambda^{-c(\gamma)} \qquad (3.1)$$

Here λ is the scale ratio defined as T/τ where T is the total length of the discrete time series and τ is the elementary time-period; R_λ is the observed (or calculated by aggregation or averaging) intensity of the field at scale ratio λ, and $\Pr(R_\lambda > \lambda^\gamma)$ is the probability distribution (the frequency histogram) that the intensity (R_λ) at some scale ratio λ exceeds λ^γ. Here γ is a variable termed as "the order of singularity". For a given value of γ, Eq. (3.1) represents the exceedance probability for different values of λ, as a power function of λ raised to the exponent $c(\gamma)$. The scale-invariant exponent $c(\gamma)$ for different values of γ, is called the co-dimension function and is a nonlinear increasing and concave function of γ. The $c(\gamma)$ function diverges at high threshold values (λ^γ) due to the divergence of the statistical moments with increasing γ.

The multifractal analysis can be equivalently carried out using the trace-moment method. In this method, given the scale ratio λ and moment order q, the observed behavior of the statistical moments is given by:

$$< R_\lambda^q >= \lambda^{K(q)} \qquad \lambda > 1 \qquad (3.2)$$

where K(q) is the moment scaling function, and can be viewed as a characteristic function of the multifractal behavior of the series and $< >$ represents the ensemble average of independent realizations of R_λ at a given λ. Hence, $<R_\lambda^q>$ represents the ensemble average of the q^{th} moment of the series at a scale specified by λ.

The co-dimension function $c(\gamma)$, and the statistical moment scaling function K(q) are related to each other via a Legendre transform as:

$$c(\gamma) = \max(q\gamma - K(q)) \qquad (3.3)$$

$$K(q) = \max(q\gamma - c(\gamma)) \qquad (3.4)$$

A phenomenological model frequently used to mimic complex systems exhibiting multifractal behavior is the multiplicative cascade. It was initially used to describe observed turbulent fluid flows (Lovejoy et al., 1987). In this model, the total energy in the turbulent flow was redistributed from larger to smaller scales via an iterative splitting procedure involving random multiplicative factors known as cascade generators. As this process is repeated, the energy becomes concentrated into smaller and smaller fractions of the entire turbulent system resulting in a highly intermittent pattern, which is also a common characteristic of hydrological time series. Multiplicative random cascade models have become increasingly popular in modeling hydrological time series (e.g., rainfall) in recent years (Over and Gupta, 1996; Harris et al., 1996; Olsson and Niemczynowicz, 1996; Schmitt et al., 1998; De Lima and Grasman, 1999; Olsson et al., 1999). These models successfully reproduced the structures and patterns observed in real hydrological processes and their statistical properties. Examination of a long-term hydrological record over time would reveal fewer large events interspersed among abundant small events. Or spatially, clusters of high rainfall intensity occur in smaller areas that are embedded within clusters of lower intensity in a large mesoscale area (Gupta and Waymire, 1990).

The multiplicative cascade model generates fields with infinite hierarchies and associated dimensions, and therefore is naturally adapted to reproduce singularities (events or occurrences) of extreme orders, and generically exhibit asymptotic decays of such extreme events, which is very useful in rainstorm or flood analysis. Flood magnitude can be related to network size, or equivalently to drainage area, which serves as a fractal scaling variable. However, a critical drainage area exists at which the scaling behavior changes (Gupta et al., 1994).

The invariance of properties and multifractality of the hydrological process over a range of scales may lead to a better understanding of strongly irregular fluctuations of a process such as rainfall. Deidda et al. (1999) compared observed time series against synthetic rainfall data using statistical analyses of extreme events. They argued that multifractal

simulated rainfall data, in terms of a scale covariance field, is a good approximation to the statistical properties of observed rainfall time series.

Hubert et al. (1993) have shown that multifractal analysis can be used to characterize the observed maximum accumulated rainfall for events over a wide range of time scales. Based on the multiplicative cascade model, a statistically precise definition of possible maximum precipitation at a given scale was obtained. The two basic multifractal exponents (i.e., α and C_1) used to characterize the moment scaling function K(q), determined the maximum attainable singularities (γ_0 and γ_s) and hence the possible maximum precipitation at a given scale and on a given sample.

A major problem in rainfall studies especially for prediction purposes is its variability over different geographical and climatological regions. Multifractal methods have been applied to compare temporal or spatial distribution of rainfall fields corresponding to different climates (Olsson and Niemczyniwicz, 1996; Svensson et al., 1996; De Lima and Grasman, 1999). According to Olsson and Niemczynowicz (1996), the multifractal properties of daily rainfall displayed distinct differences for frontal and convective rainfall, which were regarded as being related to physical differences of the two rainfall generating mechanisms. They argued that the overall rainfall generating process might be viewed as a mixture of multifractal processes. The multifractal properties of daily rainfall were also investigated in two contrasting climates by Svensson et al. (1996). They observed differences in multifractal characteristics in the temporal data from the two climates. The monsoon area data exhibited statistical scaling for moments of orders up to 2.5 versus 4.0 for the temperate area data, and both sets showed clear multifractal properties. On the other hand, the spatial data exhibited scaling for moments of orders up to 4.0 for both rainfall mechanisms in the two climates over different scaling ranges. However, Svesson et al. (1996) found that a multifractal framework is well suited for description of convective rainfall but a monofractal approach is more appropriate for modeling frontal rainfall.

Multifractal analysis also can be used to optimize the frequency of observations in collection of hydrological data sets (de Lima and Grasman, 1999). For example, scale-invariant behavior of rainfall may give an indication of suitable temporal and spatial sampling resolution for data collection. de Lima and Grasman (1999) analyzed two time series of rainfall data collected at different resolutions (15-min and daily). They found that although the scale invariant ranges varied for the different resolutions, the same multifractal parameters can be used to characterize both rainfall series.

Generally, rainfall generation is regarded as a stochastic process and the random cascade approach is often used to model the process. However, Sivakumar (2001) used several methods to examine daily rainfall series for the Leaf River basin in Mississippi and observed the existence of both multifractal and chaotic behaviors. He argued that rainfall characterization could be viewed from a new perspective: the chaotic multifractal perspective. A chaotic process is determined by a few nonlinear variables and its output over time is sensitive to the initial conditions.

Since rainfall is the principal input for streamflow generation, it is not unreasonable to assume that time series of rainfall-generated runoff over a given area would inherit the multifractal nature of rainfall patterns over that area even though runoff is influenced by other geomorphological factors that tend to "smooth" the fluctuations of the input rain series (Tessier et al., 1996). Although there is little literature on multifractal analysis of river flow / runoff data compared to rainfall data, there are indications that increasing attention is being directed to investigation of the multifractal patterns of stream flow data (Gupta et al., 1994, Tessier et al., 1996, Pandey et al., 1998; Labat et al., 2002). Tessier et al. (1996) applied multifractal analysis to stream flow data from 30 small basins in France. Their results indicated that the time series of stream runoff were multifractal, with power law plots of $<R_\lambda^q>$ versus λ for the q^{th} moment of the series [Eq. (3.2)] showing two ranges separated at a 'synoptic maximum' at roughly two weeks. Other studies on river flows support this conclusion (Pandey et al., 1998).

Geophysical and geographical systems are considered to be non-linear dynamic systems characterized by extreme spatial and temporal variability spanning wide ranges of scales. An important property of multifractals is that their extremes are power-law functions of their space-time resolutions and therefore these functions can be readily used to disaggregate the properties of river runoff time series from coarser to finer time scales. It was found that runoff generated by different mechanisms had different scaling patterns. Floods mostly generated by snowmelt runoff manifest themselves as monofractal series, whereas floods mostly produced by rainfall are multifractal (Gupta and Dawdy, 1995). However, Labat et al.(2002) found that the basins of different internal structures had similar multifractal parameters α and C_1 used to characterize the moment scaling function K(q), when studying the scaling properties of karstic watersheds.

Multifractals were also applied to analyze river basin topography (Rodriguez-Iturbe and Rinaldo, 1997). Results indicated that in some cases, the modified box-counting dimensions at various altitude thresholds were not identical, which would violate a simple monofractal scaling assumption. According to a study by Ijjasz-Vasquez et al. (1992), four variables of river basins [contributing area, slope, flow energy dissipation per unit channel area (termed as energy expenditure), and channel initiation function] exhibited multifractal characteristics and had very similar multifractal spectra when analyzed for different basins.

Findings of the fractal analysis reported in Chapter II indicated that daily runoff time series in 30 sub-watersheds of four agricultural watersheds possess scale-invariance characteristics. However, two distinct scaling ranges were displayed in the shifted box-counting and R/S plots of those runoff time series. In addition, the estimated fractal dimensions depended on the threshold levels that define the derived set of runoff events. Since the runoff time series were characterized by a multi-scaling pattern and thus have multi-dimensions, multifractal analysis may be more appropriate to investigate the scaling property of the daily runoff time series. The objective of this investigation was to determine scaling characteristics of daily runoff of four agricultural watersheds as well as their sub-watersheds using trace moment multifractal techniques as described.

MATERIALS AND METHODS

Trace Moment Method

In this research, the multifractal fields of runoff rate time series of each sub-watershed were investigated using the trace moment method. Before performing the calculations, the measured runoff time series were normalized by dividing all values by the daily mean runoff rate of the total series to allow quantitative statistical comparisons of different watersheds (or sub-watersheds) of various sizes. The time intervals (box) started from one day, and were successively doubled to give box sizes of 2, 4, 8, . . . , but less than half of the total length of the series. For example, there were 11,292 total observations contained in runoff time series record for sub-watershed W-TB of the Little River watershed. Thus, the box size varied from 1 to 4,096 days. The scale ratio λ was computed as the total length of the runoff time series divided by the size of the box in each step. The values of the normalized runoff rate within each box were averaged to obtain the R_λ value for that box. Finally, the $<R_\lambda^q>$ of q^{th} moment was obtained by averaging R_λ^q over all boxes.

The $<R_\lambda^q>$ values were plotted as a function of λ in a log-log diagram for each power q. If Eq. (3.2) is valid, an appropriately linear relationships will be exhibited with an estimated K(q) value (corresponding to the moment q) equal to the slope of the line. By performing the procedure for different values of q, the empirical K(q) function was estimated. The appearance of the K(q) function specifies the type of scaling involved. A time series is a monofractal if K(q) is a linear function of q, and it is a multifractal if K(q) is a concave upward nonlinear function of q (Schertzer and Lovejoy, 1987).

Estimation of the Universal Multifractal Model (UMM) Parameters by the Double Trace Moment (DTM)

The UMM is based on random weights possessing log-Levy statistics and are believed to be the generic consequences of scaling non-linear dynamic processes with a large number of degrees of freedom. Schertzer and Lovejoy (1987) have argued that cascade processes

possess stable universal generators and hence are insensitive to the details of dynamics. In the universal class of multifractals for a conservative process, the scaling function K(q) is completely determined by two parameters α and C_1, for q greater than an arbitrary critical order q_D, which is based on the discontinuities of first order derivatives of the K(q) function:

$$K(q) = C_1 q \log(q) \quad \text{for} \alpha = 1 \tag{3.5}$$

$$K(q) = \frac{C_1 (q^{\alpha} - q)}{\alpha - 1} \quad \text{for} \alpha \neq 1 \tag{3.6}$$

where C_1 is the co-dimension of the set of events larger than the mean ($0 \leq C_1 \leq 1$ for time series), and hence characterizes the sparseness or inhomogeneity of the mean of the process. The parameter α is the Levy-stable index ($0 \leq \alpha \leq 2$), and also called the multifractal index. It quantifies how far the process is from monofractality: $\alpha = 0$ corresponds to a monofractal process, whereas $\alpha = 2$ corresponds to a lognormal multifractal process.

The DTM is the commonly used technique to determine the parameters for the UMM (Lavallee et al., 1993). In the trace moment method, the whole series was divided into subsets and the average intensity of the field for each subset was raised to a power q. In the DTM technique, values of the original series were raised to the power η before the series was analyzed following the same procedure as described in the trace moment method. Therefore, K(q) became a function of q and η, and was denoted as $K(q, \eta)$. For $\eta = 1$, $K(q,1) = K(q)$, which is the scaling exponent (characteristic function) for the moments of the multifractal cascade process. In other words, the trace moment method described above is a special case of the DTM technique.

$K(q, \eta)$ is related to K(q) as (Lavallee et al., 1993):

$$K(q,\eta) = K(q\eta) - qK(\eta) \tag{3.7}$$

In UMM, K(q, η) has a particular simple dependence on η:

$$K(q,\eta) = \eta^{\alpha} K(q) \tag{3.8}$$

For each fixed q, the scaling properties of the DTM for various values of η allows the determination of the scaling exponent K(q, η) as functions of η. The slope of (| K(q, η)|) as a function of η on a log-log graph, yields a value of the parameter α. The intercept of the regression (η = 1) gives the value of K(q, 1). From Eq. (3.5) or Eq. (3.6), the other parameter C_1 is expressed as:

$$C_1 = \frac{K(q,1)(\alpha - 1)}{(q^{\alpha} - q)} \tag{3.9}$$

RESULTS AND DISCUSSION

Empirical Moment Scaling Function

The characteristic statistical moment scaling function K(q) was obtained using the trace moment method. The value of K(q) is a function of the moments q, which were taken in the range of $0 \leq q \leq 4.0$ in this study due to divergence of K(q) for high order moments (Kumar et al., 1994). In addition, for high values of q, the contribution of the little higher intensity became dominant in the estimation of $\langle R_\lambda^q \rangle$. The value of K(q) corresponding to a moment q was estimated as the slope of the regression line fitted to the linear part of log $\langle R_\lambda^q \rangle$ versus log λ plot according to Eq. (3.2). Figure 3.1 shows an example of this plot for sub-watershed W-TB of the Little River watershed. For simplicity, only q = 0.5, 1.0, 1.5, 2.0, 2.5, 3.0, and 3.5 are shown in the plot. The double logarithmic plot exhibits linear relationships between the average q^{th} moment of daily runoff rate and the time scale, which are from 1 day (λ = 11292) to 1024 days (λ = 11) or about 3 year intervals. Such linear relationships were valid for the different moments (q).

The results indicated that the values of the function K(q) depended on the moment q. As q increased, the slope of the fitted regression line (value of K(q)) increased. The slopes were positive for q > 1, and negative for q < 1. For q = 1, the slope was close to 0 (= -0.0004 in Figure 3.1). Negative slopes can be explained as overestimation of the contribution of lower intensities and an underestimation of the higher intensities in the trace moment method (de Lima and Grasman, 1999). For q>1, the increasing contribution of the higher intensities resulted in positive slopes. The result that the value of K(q) depended on the moment q indicated that the scaling parameter of this daily runoff time series cannot be taken as a single value, but as a function of q.

All plots in Figure 3.1 showed that the last point (λ = 11,292 representing time interval = 1 day) showed some deviation from the regression line. This deviation increased with increasing values of q (Figure 3.1). A larger q highlighted strong singularities (extreme high valued events) of a series. That is, high values of the daily runoff rate would gain more weight in the new series when raised to a power q (q > 1). What indicated that it

would be more difficult to predict the higher runoff rate on a short term basis. de Lima and Grasman (1999) argued that the dominance of large observations in estimating the high-order moments would result in lowering the goodness of fit for the linear regression leading to uncertainty in the estimation of K(q). In a study of rainfall using the trace moment method, Svensson et al. (1996) found that the high order moments did not give good straight line fits, and attributed it to the influence of the extremely large rainfall events caused by typhoons (Svensson et al., 1996).

When box size was greater than 1024 days ($\lambda < 11$), the slopes of the regression lines were almost 0 regardless of the value of q was used (Figure 3.1). In other words, the statistical moment scaling function K(q) was independent of q for time interval greater than 1024 days. An identical K(q) value of various q indicates a monofractal object or process. Therefore, the daily runoff rates exhibited multifractal patterns in the short term (< 1024 days), but monofractal pattern in the long term (> 1024 days). It should be noted that since the box sizes were doubled in each step of the trace moment method, the time interval of 1024 days obtained from the trace moment plot (Figure 3.1) would not exactly correspond to the point on the time scale separating the multifractal and monofractal process.

Exceedance Probability Distribution

The statistics of a multifractal process (such as runoff in this study) at a larger scale can be obtained by averaging the statistics at the smaller scales and such empirical statistics are termed as "dress" quantities. These quantities are generally different from the statistics obtained based on some known or assumed factors contributing to the dynamics purely at the larger scale. Such theoretical statistics are termed as bare quantities (Tessier et al., 1996). Eq (3.2) is valid for arbitrary moment q for bare quantities but for dress quantities it is only valid when $q < q_D$, which is termed the critical moment. Divergence will occur in the K(q) function for dress quantities when $q \geq q_D$ because in this case, $\langle R_\lambda^q \rangle \rightarrow \infty$ as scale ratio $\lambda \rightarrow \infty$. The value of q_D can be estimated as the absolute value of the slope of the algebraic tail in the exceedance probability distribution

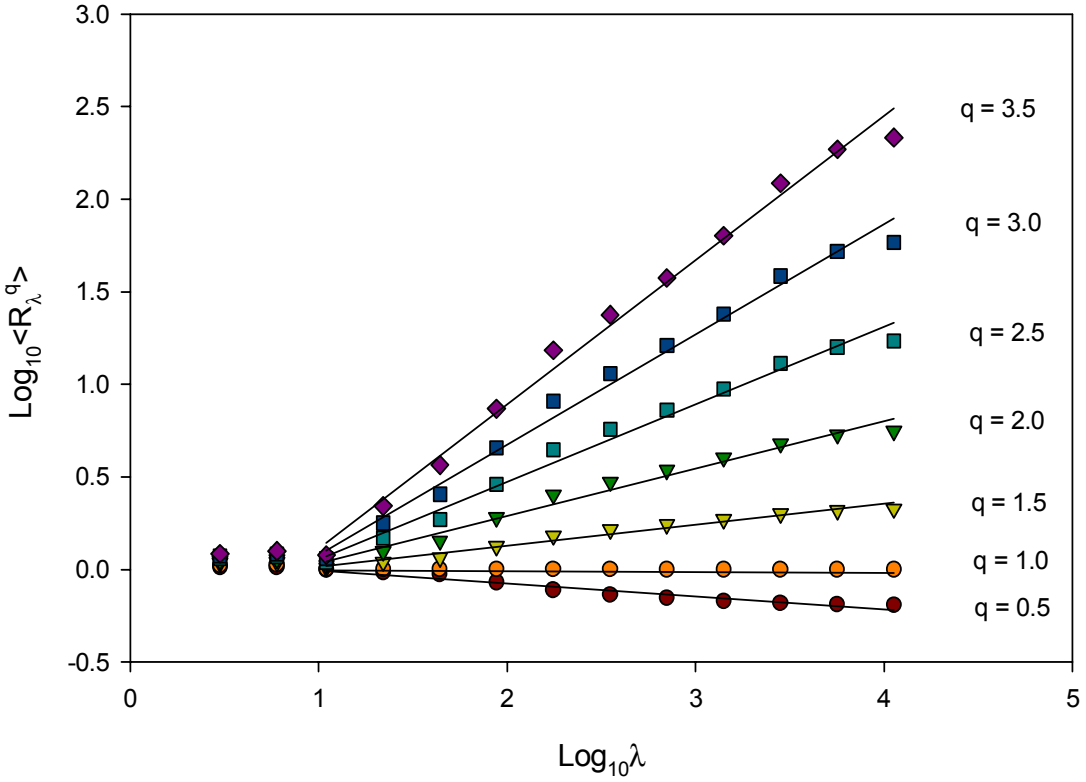

Figure 3.1. Log of the average q^{th} moment of the daily runoff rate $\langle R_\lambda^q \rangle$ versus log λ (scale ratio) for sub-watershed W-TB of the Little River watershed in Tifton, Georgia. In all cases, r^2 for linear regression lines fitted for time scales from 1 day (λ = 11292) to 1024 days (λ = 11) were > 0.99.

log-log plot. As an example, Figure 3.2 shows the exceedance probability distribution plot for sub-watershed W-TB of the Little River watershed and q_D was estimated to be about 5.4. Since the power law relationship between runoff rate (Q) and exceedance probability [Pr(Q > q)] were valid only when Q was greater than some threshold values, the probability distribution plot for small runoff rates was relatively flat (Figure 3.2).

Table 3.1 presents the values of q_D for all 32 sub-watersheds. The averaged q_D values of four watersheds were 3.64±1.02, 2.26±0.15, 3.66±1.30, and 4.44±0.60 (Table 3.1). The algebraic tails in the plots for sub-watersheds W-14 and W-23 of the Reynolds Creek watershed were poorly defined and it was not possible to obtain reasonable linear regression fits. Consequently no q_D values are reported in Table 3.1 for these sub-watersheds.

These q_D values in Table 3.1 were not much different with previous studies. Tessier et al. (1996) found the critical moment was about 3.2±1.5 for river flow, and 3.6±0.7 for rainfall. Pandey et al. (1998) analyzed 19 river flows and reported an average q_D value = 3.37±0.8. In another study, slightly higher q_D values were reported for karstic runoff and were explained by the higher variability of runoff in karst landforms (Labat et al., 2002). The results showed that the Little Mill Creek watershed had the smallest critical moment and the variation among the sub-watersheds was much smaller in comparison with the other three watersheds. A smaller value of q_D indicated that the fluctuations of the runoff series were larger and more irregular.

Figure 3.3 shows a plot of the empirical moment scaling function K(q) versus moment q for sub-watershed W-TB (the dots). The results showed that the function K(q) was a concave curve, which is characteristic of multifractal behavior. The portion of the curve for higher values of q was strongly linear and was fitted to a straight line by the least square regression (Figure 3.3). The best straight line was obtained by progressively decreasing the number of points in the portion of the K(q) curve used in the regression until the r^2 values reached a maximum. The portion of the K(q) curve for values of q

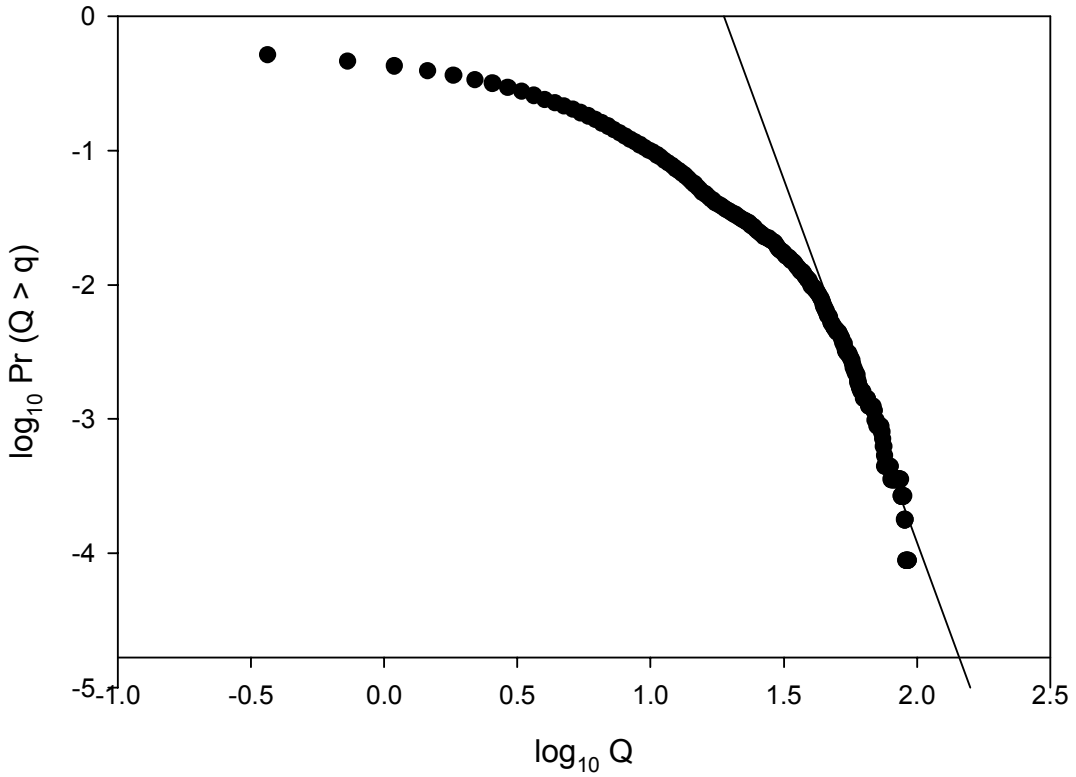

Figure 3.2 Exceedance probability distribution of daily runoff rate (Q) for sub-watershed W-TB of the Little River watershed in Tifton, Georgia. The critical moment q_D was estimated as the absolute value of the slope of the algebraic tail of the probability distribution plot. The value of q_D was about 5.42 in this case.

Table 3.1 Estimates of parameters q_D, α and C_1 of daily runoff time series. The critical moment q_D was estimated as the absolute value of the slope of the algebraic tail of the exceedance probability distribution plot as shown in Figure 3.2. The multifractal parameters α and C_1 were estimated from UMM.

Watershed	Sub-watershed	q_D	α	C_1
Little River Watershed	W-TB	5.42	0.93	0.19
	W-TF	3.31	1.19	0.18
	W-TI	3.14	1.13	0.19
	W-TJ	4.11	0.98	0.21
	W-TK	3.40	1.11	0.18
	W-TM	2.45	1.28	0.18
	Overall	3.64±1.02	1.10±0.13	0.19±0.01
Little Mill Creek watershed	W-5	2.23	1.58	0.18
	W-10	2.50	1.60	0.16
	W-91	2.30	1.57	0.16
	W-92	2.33	1.57	0.17
	W-94	2.11	1.65	0.17
	W-95	2.06	1.57	0.17
	W-97	2.28	1.73	0.17
	Overall	2.26±0.15	1.61±0.06	0.17±0.01
Reynolds Creek watershed	W-1	2.65	1.79	0.14
	W-2	2.15	1.62	0.14
	W-3	2.29	1.78	0.19
	W-4	4.92	1.60	0.15
	W-11	3.01	1.19	0.13
	W-13	4.13	1.80	0.22
	W-14	N/A	0.96	0.41
	W-15	5.58	1.32	0.23
	W-16	4.55	1.81	0.13
	W-23	N/A	0.77	0.67
	Overall	3.66±1.30	1.61±0.24	0.17±0.04
Sleepers River watershed	W-1	4.52	1.76	0.11
	W-2	3.34	1.94	0.10
	W-3	4.61	1.71	0.09
	W-4	4.59	1.72	0.10
	W-5	3.61	1.69	0.10
	W-7	4.54	1.51	0.14
	W-8	4.52	1.60	0.09
	W-9	5.14	1.36	0.16
	W-11	5.06	1.39	0.13
	Overall	4.44±0.60	1.63±0.19	0.11±0.02

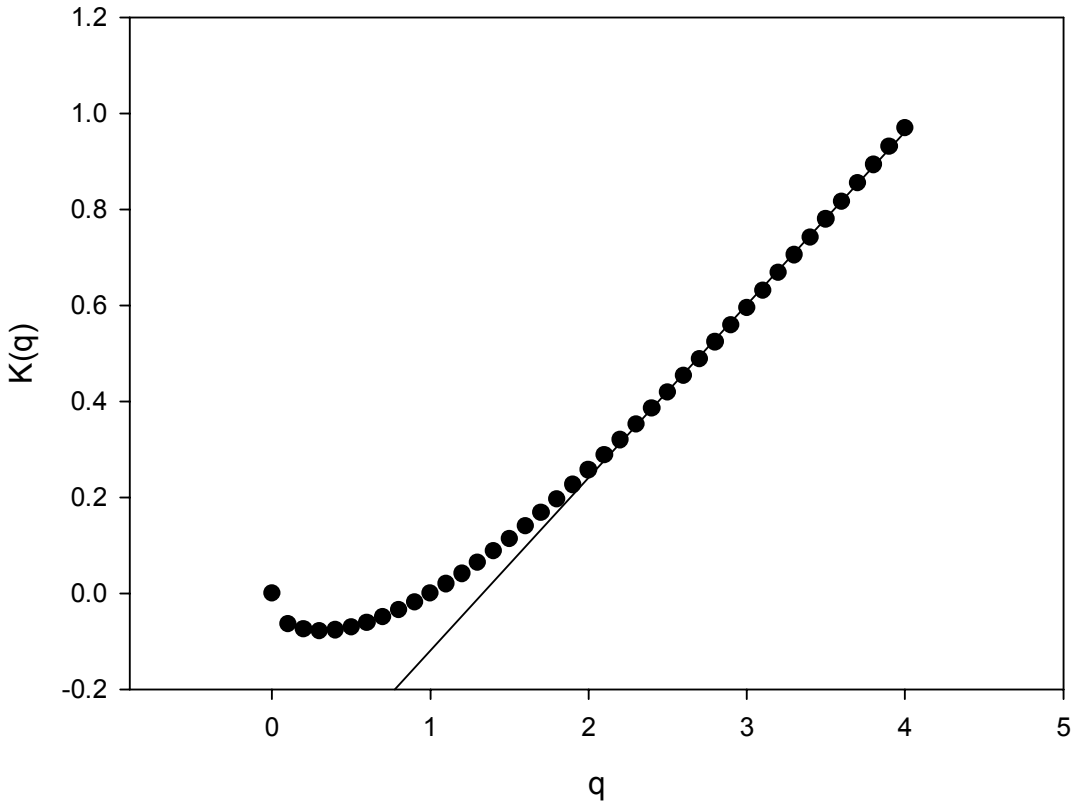

Figure 3.3 Empirical moment function K(q) describing the scaling of the moment of daily runoff time series over different scales for sub-watershed W-TB of the Little River watershed in Tifton, Georgia. r^2 for the straight line fitted to the linear portion of the curve was 0.99.

lower than the straight line portion was taken as the non-linear portion of the curve. Assuming the existence of a distinct break between the non-linear and linear portions of the curve, then the derivative K'(q) [i.e., the slope of the of the K(q) curve] is discontinuous at the point where the linear and nonlinear portion of K(q) join. Such discontinuity of the first derivative of the K(q) function has been called first-order multifractal phase transition (Schertzer and Lovejoy, 1987). The moment q at which the discontinuity of K′(q) occurs also determines the critical moment q_D, which was about 2.1 in Figure 3.3. This value was smaller than the q_D estimated from the exceedance probability distribution plot (Figure 3.2 and Table 3.1), although it was close to the averaged q_D value of Little Mill Creek watershed. For moment $q \geq q_D$, the divergence of moments would be expected.

Since all possible values of runoff are not included in a finite number of samples (or observations) in a single realization, a maximum order of singularity γ_{max} can exist. The slope of the linear portion of K(q) curve represents an estimate of this maximum order of singularity and gives $\gamma_{max} = 0.36$. A value of γ_{max} can also be estimated from the first derivative of the theoretical K(q) function [$K'(q_D)$] with $q_D = 2.1$. This estimate was about 0.13, which was smaller than the previous value and indicated a first-order multifractal phase transition.

Multifractal Parameters α and C_1

In the foregoing discussion, values of the multifractal moment function K(q) were obtained empirically using the trace moment method. As discussed in the materials and methods section, the DTM technique can be applied to analyze the daily runoff records to estimate the multifractal parameters α and C_1 of the theoretical UMM that would produce the best fit to the empirical K(q) values obtained by the trace moment method. In the DTM analyses, 33 values of η ranging from 0.1 to 4.0 with a constant logarithmic increase were used to define $K(q, \eta)$. The average trace moments (q = 2) of the daily runoff rate $\langle R_\lambda(q, \eta) \rangle$ were plotted versus log λ in a log-log plot for various η values. As an example, Figure 3.4 shows plots obtained for sub-watershed W-TB of the Little River watershed for $\eta = 0.5, 1.0, 1.5, 2.0$, and 2.5. According to the results obtained in the

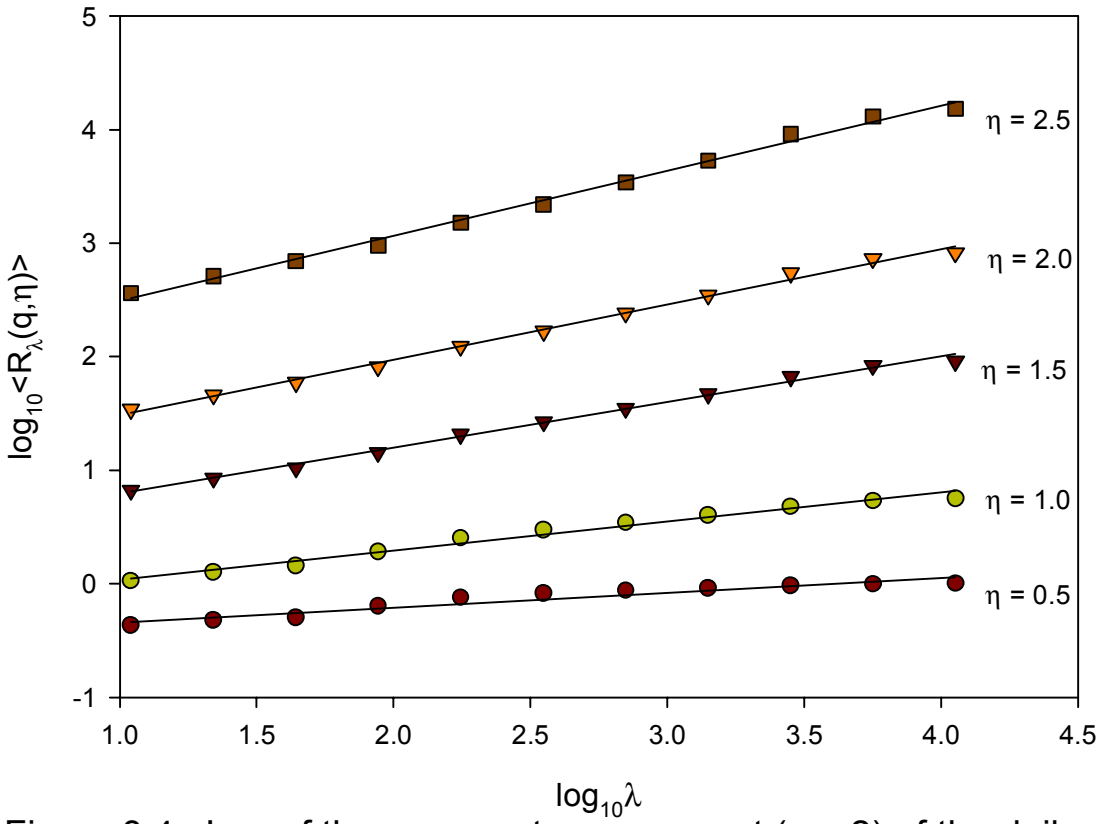

Figure 3.4. Log of the average trace moment (q = 2) of the daily runoff rate $<R_\lambda(q,\eta)>$ versus log λ (scale ratio) for sub-watershed W-TB of the Little River watershed in Tifton, Georgia for η = 0.5, 1.0, 1.5, 2.0, 2.5, 3.0, 3.5. In all cases, r^2 for linear regression lines fitted for time scales from 1 day (λ = 11242) to 1024 days (λ = 11) were > 0.99.

trace moment method, the time regime displaying multifractal pattern ranged from 1 day to 1024 days, therefore only time scales within this range were used in applying DTM method and shown in Figure 3.4. Well-defined straight lines were fitted for each η (Figure 3.4).

The slope of the best fitted line in plot of log ($<R_\lambda(q, \eta)>$) versus log λ gave the value of $K(q, \eta)$ for a given η (Figure 3.4). The values of $K(q, \eta)$ obtained using the DTM technique were then plotted versus η in a log-log plot as shown in Figure 3.5 using sub-watershed W-TB as an example. The plots showed that the linear relation between log $K(q, \eta)$ and log η was only valid if the moment η was too small or too large. The slope of the best fitted straight line for the linear portion of the plot in Figure 3.5 determined the parameter α of the function K(q) for the theoretical UMM as given in Eq. (3.6). The linear portion of the log $K(q,\eta)$ versus log η plot was defined by progressively removing points from the beginning or end of the data until the r^2 for the linear regression was maximized. The parameter C_1 of the theoretical function K(q) was then calculated using Eq. (3.10). The theoretical function K(q) was then expressed using α and C_1 in terms of Eq. (3.5) or Eq. (3.6). Figure 3.6 shows the theoretical K(q) function using the parameters $\alpha = 0.93$ and $C_1 = 0.19$ (the solid line) as well as the empirical K(q) values (the dots) from the trace moment analysis. The values obtained using the theoretical function for sub-watershed W-TB of the Little Creek watershed at each point matched the empirical values very well (Figure 3.6). These results indicated that the scaling function K(q) obtained using DTM technique can be used to characterize the multiscaling pattern of the daily runoff for this sub-watershed.

Similar analyses were performed for all 32 sub-watersheds and the α and C_1 values are included in Table 3.1. In some cases the theoretical K(q) functions gave values that were greater than the empirical values at high moments ($q > 3$) as shown in the plot for sub-watershed W-2 in the Sleepers River watershed (Figure 3.7). The goodness of the matching of theoretical function values to empirical values were found to be related to the fit of linear regression of log $K(q, \eta)$ versus log η. The closer the fit was to a straight line, more closely the theoretical function matched the empirical values.

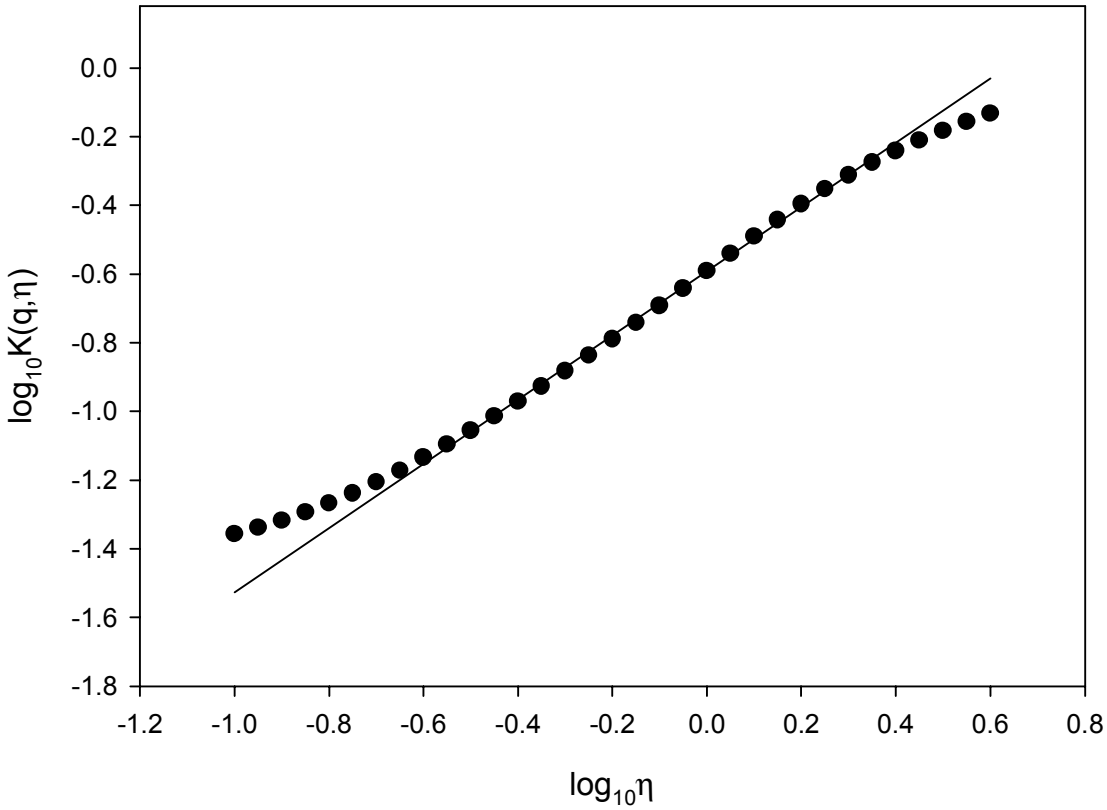

Figure 3.5. Double trace moment log-log plot of the moment scaling function $K(q,\eta)$ versus moment order η with $q = 2$ for daily runoff rate in sub-watershed W-TB of Little River watershed in Tifton, Georgia. r^2 for the straight line fitted to the linear part of the plot was 0.99.

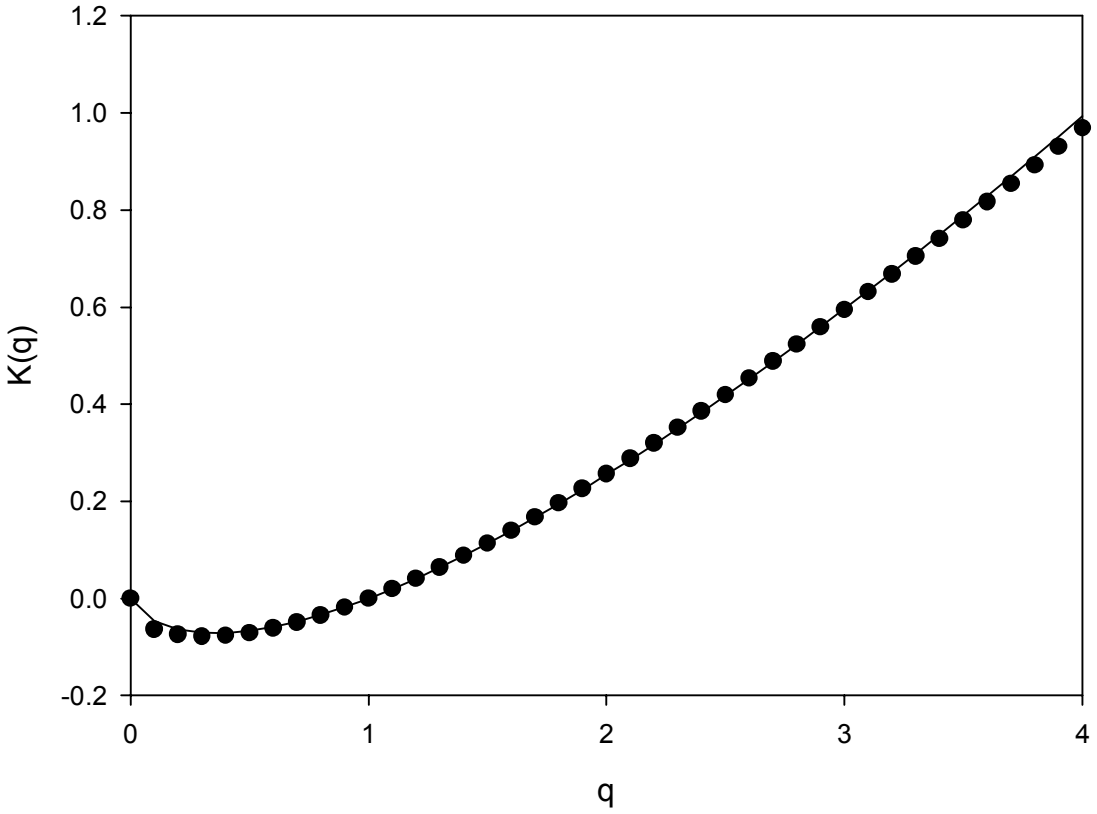

Figure 3.6. Moment scaling functions K(q) for sub-watershed W-TB of the Little River watershed in Tifton, Georgia. Dots are the empirical values and the solid line is the universal multifractal function using α = 0.93 and C_1 = 0.19.

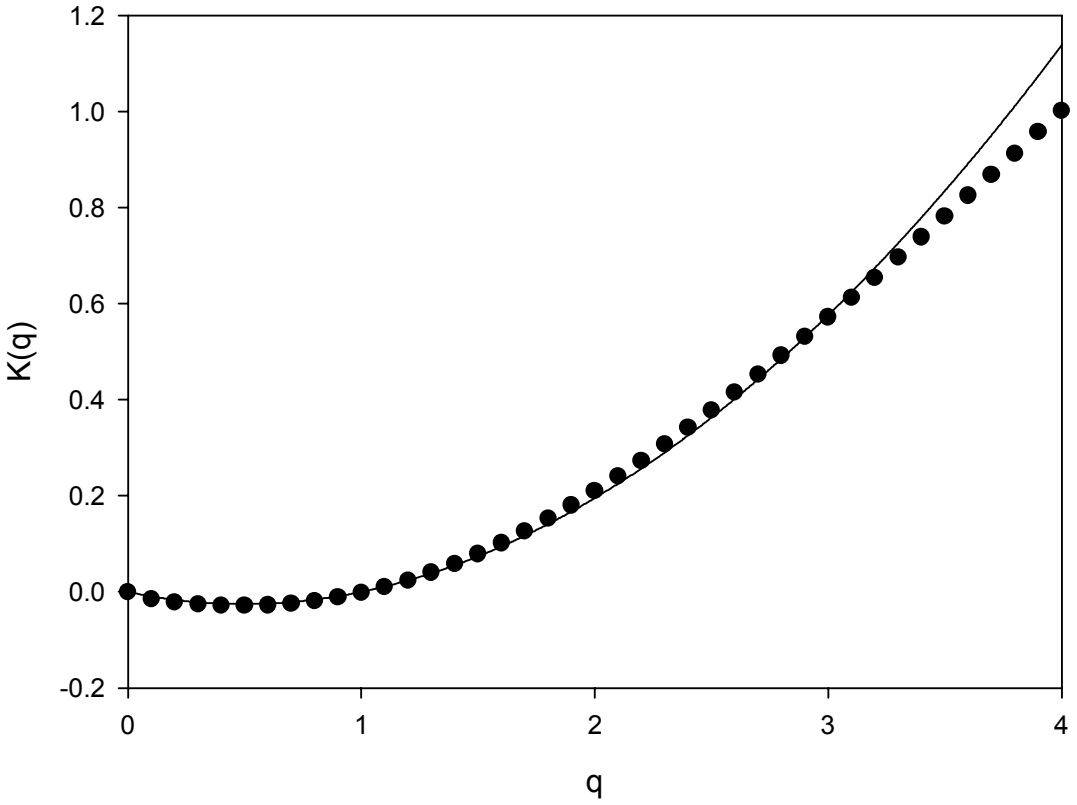

Figure 3.7. Moment scaling functions K(q) for sub-watershed W-2 of the Sleepers River watershed in Danville, Vermont. Dots are the empirical values and the solid line is the universal multifractal function using α = 1.94 and C_1 = 0.10.

For all 32 sub-watersheds the plots for the empirical K(q) values showed linear and nonlinear portions. The values obtained using the theoretical K(q) function of the UMM closely matched the empirical values in the nonlinear portion for all sub-watersheds. Divergences were obtained in the linear portion for some sub-watersheds, probably because Eq. (3.7) is a nonlinear equation and may not be appropriate to describe the linear characteristics.

The multifractal parameters α and C_1 estimated by the DTM technique for the runoff time series of the sub-watersheds of a given watershed were also averaged to obtain the mean value for that watershed (Table 3.1). The α and C_1 values for sub-watersheds W-14 and W-23 were not included in calculating the average α and C_1 values for the Reynolds Creek watershed. As already discussed in Chapter 2, these sub-watersheds were much smaller than the others and the runoff series did not exhibit similar scale invariance. The values of parameter α and C_1 for all the other sub-watersheds fall within the reasonable range of the previous studies on river flow and runoff time series. In their study of low-frequency runoff series for 30 French catchments, Tessier et al., (1996) reported $\alpha = 1.45 \pm 0.2$ and $C_1 = 0.20 \pm 0.1$. In another study, average values of $\alpha = 1.70 \pm 0.11$ and $C_1 = 0.12 \pm 0.03$ were found for 19 daily river flows with watershed size ranging from 5 to 1.8×10^6 km^2 (Pandey et al., 1998).

The parameter α is called the multifractal index and quantifies how far the process is from monofractality. A value of $\alpha = 0$ indicates a monofractal process. The results in Table 3.1 show the α values were all close to or greater than 1, suggesting that the runoff processes were far from being a monofractal process, and can be better modeled via the multifractal approach. The results also showed that $\alpha < 2$ in all cases which indicated that the runoff series were non-Gaussian. Indeed, most of the α values ranged between 1 and 2 which indicated that the logarithm of these daily runoff time series followed a distribution somewhere between an asymmetrical Cauchy ($\alpha = 1$) and a normal ($\alpha = 2$) (Pandey et al., 1998). The Little River watershed had a much smaller α value (1.10 ± 0.13) than the other three watersheds (1.61 ± 0.06, 1.61 ± 0.24 and 1.63 ± 0.19), which

indicated that the runoff processes of the latter three watersheds were even further from the single scaling than the Little River watershed.

Parameter C_1 is called as the co-dimension and characterizes the sparseness or inhomogeneity of a process. A low C_1 value (close to 0) indicates that the values of the time series vary around the mean value with a very small variance (i.e., a smoother hydrograph for a runoff time series). On the other hand, a large C_1 value (> 0.5) indicates that the process has very low values almost everywhere except for some very specific locations that have values much higher than the mean. The C_1 value for W-23 sub-watershed in the Reynolds Creek watershed was 0.67 which was much higher than that of all other sub-watersheds because most (> 90%) of the records in the runoff time series for W-23 sub-watershed were zero (Table 3.1). The Sleepers River watershed had smaller C_1 values (0.11 ± 0.02) than the other three watersheds (0.19 ± 0.01, 0.17 ± 0.01 and 0.17 ± 0.04), which indicated that the Sleepers River watershed generated a smoother hydrograph than the other three watersheds.

Both the α and C_1 values of runoff time series within a watershed were close to each other although the sizes of these sub-watersheds were very different. Exceptions were the runoff series for W-14 and W-23 sub-watersheds of the Reynolds Creek watershed probably due to their extremely small sizes as already discussed in Chapter II. The results also showed that C_1 had less variation than α (Table 3.1). As indicated by the q_D values (Table 3.1) obtained in the analysis of the exceedance probability distribution, the variations of α and C_1 for runoff time series for the sub-watersheds within the Little Mill Creek watershed were particularly small in comparison with the other runoff time series. This indicated that the Little Mill Creek watershed might have small spatial variation on some factors influencing runoff generation, such as topography, soil type, etc.

The multifractal scaling function K(q) is determined by α and C_1. Therefore similar α and C_1 parameters for sub-watersheds indicated that the runoff processes of these sub-watersheds may have similar multifractal scaling properties. Labat et al. (2002) found that three karstic basins of different internal structures (one of them was an intermittent

spring) were characterized by similar multifractal parameters (α and C_1) and they concluded that the multifractal parameters appeared as the only invariant for these basins. Other previous studies also indicated the multifractal parameters α and C_1 were universal for all runoff time series (Tessier et al., 1996; Pandey et al., 1998). Moreover, α and C_1 for runoff time series were found to be roughly the same as for rainfall and therefore only a linear transfer function would be needed to relate the river runoff series to observed rainfall series (Tessier et al., 1996; Pandey et al., 1998; Labat et al., 2002).

FINDINGS AND CONCLUSIONS

Multifractal analysis techniques were used to study the scaling properties of daily runoff in 32 sub-watersheds in four agricultural watersheds. Empirical moment scaling K(q) curves using the trace moment method were nonlinear and concave, indicating that the runoff time series studied exhibited a multifractal behavior. The multifractal scaling was valid over a time scale range from 1 day to 1024 days. The critical moment q_D was estimated from the exceedance probability distribution plot and varied from watershed to watershed.

The Universal Multifractal Model (UMM) successfully reproduced the multiscaling behavior of the runoff time series. Theoretical K(q) functions were defined using UMM in terms of multifractal parameters α and C_1, and these matched the empirical K(q) values very well. The α and C_1 parameters were reasonably close to each other for sub-watersheds within a watershed and were generally similar among the four watersheds. The similar multifractal parameters among the sub-watersheds (watersheds) indicated the existence of invariance from one sub-watershed (watershed) to another despite differences in their size and other topological and geological patterns. The multifractal techniques provided a useful theoretical framework for runoff time series analysis, especially for occurrence and distribution of extreme events. High-resolution synthetic runoff data could be produced by using multifractal models and applied in the hydrological analysis, such as water resources planning, flood forecasting, sediment and pollutant transport, and other aspects of watershed management.

REFERENCES

Barnsley, M. F. 1993. Fractals Everywhere. 2nd edition. Academic Press, Boston.

De Lima, M. I. P., and J. Grasman. 1999. Multifractal analysis of 15-min and daily rainfall from a semi-arid region in Portugal. Journal of Hydrology 220: 1-11.

Deidda, R., R. Benzi, and F. Siccardi. 1999. Multifractal modeling of anomalous scaling laws in rainfall. Water Resources Research 35: 1853-1867.

Gupta, V. K., and Waymire, E. 1990. Multiscaling properties of spatial rainfall and river flow distributions. Journal of Geophysical Research (D.) 95: 1999–2009.

Gupta, V. K., O. J. Mesa, and D. R. Dawdy. 1994. Multiscaling theory of flood peaks: Regional quantile analysis. Water Resources Research 30: 3405-3421.

Gupta, V. K., and D.R. Dawdy. 1995. Physical interpretations of regional variations in the scaling exponents of flood quantiles. Hydrological Processes 9: 347-361.

Harris, D., M. Menabde, A. Seed, and G. Austin. 1996. Multifractal characterization of rain fields with a strong orographic influence. Journal of Geographic Research 101: 26405-26414.

Hubert, P., Y. Tessier, S. Lovejoy, D. Schertzer, F. Schmitt, P. Ladoy, J. P. Carbonnel, S. Violette, and I. Desurosne. 1993. Multifractals and extreme rainfall events. Geophysical Research Letters 20: 931-934.

Ijjasz-Vasquez, E. J., I. Rodriguez-Iturbe, and R. L. Bras. 1992. On the multifractal characterization of river basins. Geomorphology 5: 297-310.

Kumar, P., P. Guttarp, and E. Foufoula-Georgiou. 1994. A probability-weighted moment test to assess simple scaling. Stochastic Hydrology and Hydraulic 8: 173-183.

Labat, D., A. Mangin, and R. Ababou. 2002. Rainfall-runoff relations for karstic springs: multifractal analysis. Journal of Hydrology 256: 176-195.

Lavallee, D., S. Lovejoy, D. Schertzer, and P. Ladoy. 1993. Nonlinear variability of landscape topography: Multifractal analysis and simulation. In Fractals in Geography, N. S. Lam and L.De Cola, editors. Prentice-Hall, New Jersey.

Lovejoy, S. and D. Schertzer. 1985. Generalized scale invariance and fractal models of rain. Water Resources Research 21: 1233-1250.

Lovejoy, S., D. Schertzer, and A. A. Tsonis. 1987. Functional box-counting and multiple elliptical dimensions in rain. Science 235: 1036-1038.

Lovejoy, S., and D. Schertzer. 1990. Multifractal, universality classes and satellite and radar measurements of cloud and rain fields. Journal of Geophysical Research 95: 2021-2034.

Mandelbrot, B. B. 1983. The fractal geometry of nature. W.H. Freeman, New York.

Olsson, J., J. Niemczynowicz, R. Berndtsson, and M. Larson. 1992. An analysis of the rainfall time structure by box-counting—some practical implications. Journal of Hydrology 137: 261-277.

Olsson, J., and J. Niemczynowicz. 1996. Multifractal analysis of daily spatial rainfall distributions. Journal of Hydrology 187: 29-43.

Olsson, J., V. P. Singh, and K. Jinno. 1999. Effect of spatial averaging on temporal statistical and scaling properties of rainfall. Journal of Geophysical Research 27: 19117-19126.

Over, T. M., and V. K. Gupta. 1996. A space-time theory of mesoscale rainfall using random cascades. Journal of Geophysical Research 101: 26319-26331.

Pandey, G., S. Lovejoy, and D. Schertzer. 1998. Multifractal analysis of daily river flows including extremes for basins of five to two million square kilometers, one day to 75 years. Journal of Hydrology 208: 62-81.

Prokoph, A. 1999. Fractal, multifractal and sliding window correlation dimension analysis of sedimentary time series. Computers & Geosciences 25: 1009-1021.

Rodriguez-Iturbe, I., and A. Rinaldo. 1997. Fractal river basins: chance and self-organization. Cambridge University Press, New York.

Schertzer, D. and S. Lovejoy. 1987. Physical modeling and analysis of rain and clouds by anisotropic scaling multiplicative processes. Journal of Geophysical Research 92: 9693-9714.

Schmitt, F., S. Vannitsem, and A. Barbosa. 1998. Modeling of rainfall time series using two-state renewal processes and multifractals. Journal of Geophysical Research 103: 23181-23193.

Sivakumar, B. 2001. Is a chaotic multifractal approach for rainfall possible? Hydrological Processes 15: 943-955.

Svensson, C., J. Olsson, and R. Berntsson. 1996. Multifractal properties of daily rainfall in two different climates. Water Resources Research 32: 2463-2472.

Tessier, Y., S. Lovejoy, P. Hubert, D. Schertzer, and S. Pecknold. 1996. Multifractal analysis and modeling of rainfall and river flows and scaling, casual transfer function. Journal of Geographic Research 101: 26427-26440.

CHAPTER IV
FRACTAL CHARACTERISTICS OF STREAM NETWORKS EXTRACTED WITH THE DIGITAL ELEVATION MODEL

INTRODUCTION

Mathematically defined fractal objects, such as the Cantor set and Koch curve, are strictly self-similar objects. That is, a piece of the object is identical to a reduced copy of the object itself. This means that the object scales isotropically so that distances between points are scaled by the same factor in all directions under a dilation (or contraction) transformation. However, strict self-similarity is rarely observed for natural objects such as stream networks. In such natural objects patterns in each portion of the object may be reflected in a larger portion, but not exactly like the larger portion. When statistical measures of these patterns are similar over different resolutions of scale, such natural objects are said to be statistically self-similar. A statistically self-similar object and its parts have identical statistical distributions (Mandelbrot, 1983).

A common feature of stream networks is that the geometrical characteristics and features of the whole are embedded in smaller portions of the network. Even a visual observation of stream networks will show that they exhibit some degree of self-similarity, at least over limited areas or within a certain applicable range of scales. Thus, without a scale on a map, it would be impossible to distinguish whether the map represents an entire stream network or a smaller sub-network of the system. Therefore, stream networks can be regarded as self-similar objects. This implies that within a given area, a sub-area when enlarged would resemble the original network.

Many studies have shown that the geometry of stream networks is self-similar and exhibit scale invariant properties over some ranges of scales (Mandelbrot, 1983; Hjelmfelt,

1988). A model called the self-similar tree was used to explore the fractal patterns of different stream networks. The same fractal dimensions were obtained for all the natural networks investigated (Claps and Oliveto, 1996). On the other hand, studies have shown that individual river channels should be considered as self-affine objects. Scale invariance is maintained in self-affine objects by assuming different scaling factors according to the various spatial coordinate directions (Nikora et al., 1996). This implies that for two-dimensional objects (such as a stream network map), the scaling factors in the longitudinal and transverse directions are not equal. Self-affinity (anisotropic scaling) is generally more common in stream networks than self-similar behavior (Nikora and Sapozhnikov, 1993; Ijjasz-Vasquez et al., 1992). Especially in the case of non-compact basins with relatively sparse stream density, a more correct quantitative description of stream networks can be obtained by introducing more than one scaling parameter (Nikora, 1994). The parameter used to characterize scaling behavior of fractional Brownian motion (fBm) models has been accepted as a useful parameter to express the degree of self-affinity. Physically, this parameter (obtained by the area-scaling method) for stream networks has been interpreted as an expression of the "relief texture" of landform surface (Ouchi and Matsushita, 1992). The fractal dimension of stream networks for which this parameter > 1 (implying far from being ideally self-similar), vary widely between estimation procedures (Puente and Castillo, 1996). Recently, some studies indicated that the stream networks displayed multifractal behavior (Ijjasz-Vasquez et al., 1992; De Bartolo et al., 2000; Tchiguirinskaia et al., 2000; Cheng et al., 2001)

Estimating the Fractal Dimension of Stream Networks

Since the introduction of applications of fractal concepts to natural objects by Mandelbrot (1983), a number of studies have been published on the characterization of the scaling properties of stream networks using fractal theory (Claps and Oliveto, 1996; Puente and Castillo, 1996; Tarboton, 1996). For fractal stream networks, the fractal dimension (D) is used to characterize the irregularity and complexity of the network.

The fractal dimension of stream networks can be determined by many conventionally applied techniques such as the main stream-area relationships, ruler method, and the box-counting method, and a computational method making use of Horton ratios. Power-law relationships have been observed between the stream length or perimeter of drainage basins and the basin area. Hack (1957) empirically showed that the main stream (i.e., the longest flow path of the network) length (L) and basin area (A) are related by a power law with an exponent α as follows:

$$L \propto A^{\alpha} \qquad (4.1)$$

Where α remained close to 0.60 for stream networks of many basins in the United States and the world. Other values of α were reported (Gray, 1961), and reviewed by Robert and Roy (1990). Generally, α is greater than 0.5. It is believed that $\alpha = 0.5$ corresponds to an isometric basin where shape is independent of size or length (Cheng et al., 2001). In light of the self-similarity concept, this power-law relationship actually indicated the possibility that the main stream length in a network could be a fractal characteristic. Mandelbrot (1983) later claimed that the fractal dimension of the main stream is equal to 2α. Since then, the fractal properties of streams have been widely investigated. Hjelmfelt (1988) confirmed this result using data on eight rivers in Missouri. According to Montgomery and Dietrich (1992), the relationship between stream length and drainage area tended to also hold for unchanneled valleys, source areas, and low-order channels. Hence, they concluded that there is a basic geometrical similarity between drainage basins and the smallest basins they contain, that holds down to the finest scale to which the landscape is dissected (Montgomery and Dietrich, 1992). However, Robert and Roy (1990) concluded that the fractal dimension could not be inferred from the exponent of the length/area relationship. In addition, the main stream length/area fractal dimension may be unreliable for a system of small order (Beer and Borgas, 1993).

Mandelbrot (1983) described the so-called ruler technique developed by Richardson (1961) to measure the coastline length (L) by stepping along it with dividers or a ruler of size (l). The total length L is approximately as $L = Nl$, where N is the number of divider steps. By taking $l \rightarrow 0$, a relationship between the steps N and the l was established as:

$$N(l) \propto l^{-D} \qquad (4.2)$$

In Eq. (4.2), D is the fractal dimension of the coastline and it is determined by computing the slope of a log-log plot of the number of steps versus ruler size. Typically, the number of steps needed to traverse a stream path is not an integer, thus a fractional length of ruler size *l* often remains at the end of the path. This is one source of error in the estimation of D in the Richardson method (Richardson, 1961). The fractional steps can be added into the measured total length (Breyer and Snow, 1992). Other sources of error include the problem of the starting point of a ruler walk, and of nonlinearity in the relationships between measured length (or number of steps) and step length (Andrle, 1992). Based on their results, multiple starting points should be used to get the mean value of total length. In addition, the same number of steps is commonly obtained from more than one ruler size, especially for large ruler sizes, and it was therefore advisable to use the smallest size (Breyer and Snow, 1992).

Another extensively used approach to estimate the fractal dimension of stream networks is the box-counting method (Tarboton et al., 1988; Rosso et al., 1991; Puente and Castillo, 1996). In this method, 2-dimensional grids of size r are superimposed to cover the network. If N(r) is the number of grids containing at least a piece of the network, then

$$N(r) \propto r^{-D} \qquad (4.3)$$

The existence of this relationship is indicated when a plot of log [N(r)] versus log r gives a straight line. The slope of this line gives D. For stream networks, two distinct straight lines of different slopes were obtained in a plot of log [N(r)] versus log r by Tarboton et al. (1988), who found that the slope of the regression line was close to –1 for small box size, and close to –2 for large box size.

The fractal dimensions of stream and stream networks have been related to Horton's classical laws of stream morphometry (Horton, 1932, 1945). Several formulas were

proposed to estimate the fractal dimension of the stream networks using Horton ratios (La Barbera and Rosso, 1989, 1990; Beer and Borgas, 1993; Tarboton, 1990, 1996; Schuller et al., 2001). In the Horton ratios method of fractal dimension computation, the fractal dimension is expressed as a function of two or more of the stream morphometric ratios namely R_B, R_L, and R_A, which represent the bifurcation, length, and area ratios, respectively.

Horton's laws (Horton, 1932, 1945) may be valid only in a limited range of scale. Crave and Davy (1997) presented a statistical analysis on two watersheds. They found that the variables drainage area, main stream length, and upstream length follow power-law distributions over a limited range of scales. The drainage density and main stream length present no simple scaling with area. With increasing scale, drainage density approaches a constant value, and main stream length approaches the square root of the area. These asymptotic limits were reached for drainage areas larger than 100 km^2. For smaller areas, the asymptotic limit represents either a lower bound (drainage density) or an upper bound (main stream length) of the distributions. Horton ratios also vary with the size of the source areas used to define the stream networks, but not in any systematic manner (Helmlinger et al., 1993).

In contrast to previous approaches using some morphometric parameters or their ratios, the fractal nature of stream networks can also be described by their statistical distributions. Assuming that stream networks are self-similar, Mandelbrot (1983) stated that the exceedance probability of a specified stream length can be given as:

$$\Pr(length > l) \propto l^{-D} \qquad (4.4)$$

where D is the fractal dimension, and l is a arbitrary value of the random variable of stream length. This probability distribution is hyperbolic, which has the desired property of being self-similar, regardless of size, soil, geology, and climate of the basin. Except for stream length, other morphometric patterns of stream networks, such as stream number, contributing area, and drainage density, etc., also possess such hyperbolic distributions (Rodriguez-Iturbe and Rinaldo, 1997).

Relationship between Network Fractal Dimension and Geomorphology

Fractal models make possible a much more complete and realistic description of geomorphology than does Euclidean geometry. Xu et al. (1993) stated that, "it (fractal model)…becomes the most successful mathematical model for describing real landscapes because the fractal dimension appears to capture the essence of the surface topography of the earth in a way that other geomorphological attributes do not".

Mathematically, the fractal dimension of a stream channel network (considered as a set of lines partially filling the plane), is limited to the range $1 < D < 2$. If a stream network were truly space-filling, as is the case with a topologically random network, one would expect to compute a fractal dimension of 2.0 for the stream network. This corresponds to the modal value of Horton's order ratios for randomly generated topological networks. By comparing the channel network pattern with Peano's space-filling, self-similar curve, Mandelbrot (1983) concluded that channel networks are space-filling and so have a fractal dimension of 2.0.

It is recognized that not all areas within a watershed contribute runoff to the stream system (Lam and Cola, 1993). This implies the fractal dimension should be smaller than 2 for natural networks (Veltri et al., 1996). A channel network with fractal dimension near 2 should be interpreted as an indication of a directionally unconstrained surface drainage pattern, rather than a space-filling one (Lam and Cola, 1993). Drainage basins with fewer geological constraints were found to be predominantly associated with younger sediments, while drainage basins developed within older lithologies had a higher degree of geological constraints and hence a lower fractal dimension (Cheng et al., 2001). In the same study, the fractal dimensions of drainage basins were also related to the amount of basin flow.

The fractal dimension of the stream network can be closely correlated to the local topographical pattern of the basin. The self-similarity dimensions (one form of fractal dimension) were computed using the three-dimensional box-counting method in a landscape study based on the Digital Terrain Model (DTM) data of Taiwan Island (Cheng et al., 1999). The self-similarity dimension ranged from 2.6 to 2.8 for regions where the

elevation was over 1000 m, and was interpreted as characterizing the uniform erosion factors governing these regions. In contrast, the self-similarity dimension of the regions under 1000 m elevation has a negative exponential relationship with its elevation, which indicated greater spatial variations of the erosion factors (Cheng et al., 1999). In another study on landscape roughness characteristics, Lifton and Chase (1992) found that tectonics strongly influenced fractal dimension at larger scales, while rock-type variation apparently influenced fractal dimension at smaller scales.

The correlation between the fractal dimension and geomorphometric measures may be very weak. After examining 24 traditional geomorphometric parameters, Klinkenberg (1992) found that the fractal dimension only captured some aspect of the surface roughness. Chase (1992) pointed out that the fractal dimension of landscape topography was much more responsive to climate parameters than to tectonic uplift. Even though basins may have significant differences in physiography, the fractal dimension values may fall within narrow ranges (Breyer and Snow, 1992). This was interpreted by the similarity of smaller scale boundary irregularity although the basins differed greatly in overall shape (Breyer and Snow, 1992).

Extraction Stream Network Using DEM

Stream networks are generally extracted either manually from images or topological maps, or automatically from digitized data such as DEM or DTM. In comparison with the digital approach, manual methods are generally time-consuming, error-prone, and subjective. Several researchers have pointed out a number of inadequacies associated with the manual extraction of stream networks (Tarboton et al., 1988; Helmlinger et al., 1993). In recent years, attention has been directed to automated network extraction techniques in view of their inherent advantages and continuously increasing data quality (Ichoku et al., 1996; Moussa and Bocquillon, 1996; da Ros and Borga, 1997). Automated techniques provide the ability to create new, more meaningful characteristics of stream networks, such as contours, slope, aspect, visibility. The recent availability and accessibility of digitized data for watersheds, and the continuously updated GIS

programs, permits a more careful study of the fractal nature and dimension of stream networks.

Various methods were proposed for delineating the stream networks with DEMs (Tarboton et al., 1988; Tarboton et al., 1989; Ijjasz-Vasquez and Bras, 1995; Ichoku et al., 1996). The most common procedure for the extraction of stream networks from raster formatted data for a drainage area is to use a minimum drainage area as a criterion for classifying a pixel as part of the stream network (Jenson and Domingue, 1988; Tarboton et al., 1988). This critical support area is called the threshold area. Several attempts have been made to predict the most appropriate threshold area so that the extracted stream network will closely resemble the one observed in the field (Tarboton et al., 1989; Montgomery and Dietrich, 1992). However, the problem of defining the channel initiation scale has not been adequately resolved. Therefore, arbitrary threshold areas will continue to be used for stream network extraction using DEM, even though it is recognized that different threshold areas will result in substantially different stream networks for the same basin (Tarboton et al., 1989).

Tarboton et al. (1989) proposed a method of predicting the initiation scale based on the stability threshold, which defined the transition from stable diffusive processes to unstable channel-forming processes. The area at which a break of slope in a slope-area plot occurred was interpreted as the scale at which stability changes and was used as the threshold area to define a stream network. In other words, the support area of contribution was determined by the location of a break in the scaling response of link slopes versus contributing areas, instead of local slopes. The slope-area-threshold criteria were further discussed by Ijjasz-Vasquez and Bras (1995). The variance of the physical process, and the low accuracy achievable in the estimation of the local slope value from available digitized elevation data are the limiting factors in the practical application of such concepts for extraction of the drainage network (Roth et al., 1996).

Another method for selection of the threshold area value makes use of scaling invariance of the probability distribution of some variables of natural stream networks under wide

ranges of spatial scales. The cumulative probability distribution of a link-contributing area A was defined by Rodriguez-Iturbe et al. (1992) in real networks as:

$$\Pr(A \geq a) = a^{-\gamma} \qquad (4.11)$$

where a is the arbitrary value for the contribution area. Rigon (1993) showed that this equation could be used for predicting the threshold area value. Other techniques to extract stream networks using DEM were discussed by Meisel et al. (1995) and Ichoku et al. (1996).

The threshold area is often assumed to be constant over the entire basin (Jenson and Domingue, 1988). On the other hand, some studies have emphasized that the threshold area should be regarded as a function of the local valley slope, and therefore may vary within the basin (Montgomery and Dietrich, 1989; Montgomery and Foufoula-Georgiou, 1993). These studies discussed different aspects of the application of thresholds in the DEM, which depend on local topographic slope rather than use a constant threshold over an entire basin. Based on extensive field studies, an empirical power law relationship ($A \propto S^{-\theta}$) between contribution area (A) and local slope (S) was identified (Montgomery and Dietrich, 1989; Montgomery and Foufoula-Georgiou, 1993). A stream network is then defined if $AS^{\theta} > C$, where C is a constant. This relationship indicates that the greater the local valley slope, the smaller the threshold area defining the initiation of a channel, which is as generally observed. However, the parameter θ of this relationship is determined based on field studies, and a threshold value still needs to be subjectively assigned. In the Montgomery and Dietrich (1994) investigation, θ was found equal to 2.0.

The threshold problem in DEM extracted networks remains unresolved. There is no universal approach to determine threshold area. However, since there is a general consensus that different threshold areas will result in substantially different DEM stream networks for the same basin, it is better to extract a stream network using several arbitrary threshold areas and choosing the one that best corresponds with observation.

The objective of this chapter was to investigate the scale invariance of DEM-extracted stream networks for the four watersheds studied in the previous chapters. Stream networks were extracted from recently updated DEM of high resolution using several threshold values of contribution area. The fractal dimension of stream networks was estimated using the box-counting method and Horton ratios. The scaling behavior of the DEM-extracted stream networks was also investigated using the multifractal approach.

MATERIALS AND METHODS

DEM Data and Stream Network Extraction

The most recent (July 2004) digital elevation data for the four main watersheds (Table 2.1) were downloaded from the U.S. Geological Survey (USGS) National Elevation Dataset (NED), which is a new raster product assembled by USGS. It has been developed by using the highest-resolution, best quality elevation data available across the U.S., and is updated bimonthly to incorporate the best available DEM data. The dataset provides seamless coverage with a consistent datum, elevation unit, and projection, and it particularly benefits the analysis of large areas because there is no need to merge separate DEMs to obtain a study area as required for traditional DEM. In addition, some error-reduction processing steps were taken to improve the data quality during NED preparation.

NED provides elevation data of 1 arc second (30 m) resolution for the continental U.S. Higher resolution data of 1/3 arc second (10 m) are available for some regions. Since the watershed delineation and other spatial analysis are based on the values of each grid, higher resolution data are more useful. NED of 10 m resolution was used for the watersheds except for the Little Mill Creek watershed where NED of 30m resolution was used. Table 4.1 provides the general description of elevation data for the four agricultural watersheds. The elevations of the Little River watershed ranged from 82.1 m to 148.0 m and indicated that it is a very flat area although it had the largest size (333.8 km^2).

Table 4.1 Description of elevation data

Watershed	Area (km^2)	Resolution (m)	Elevation Range (m)
Little River watershed	333.8	10	82.1 — 148.0
Little Mill Creek watershed	48.5	30	248.2 — 392.9
Reynolds Creek watershed	233.5	10	1084.6 — 2245.1
Sleepers River watershed	111.2	10	205.6 — 784.1

Generally, extracting stream network with DEM involved several routine steps that were implemented in the Spatial Analyst extension of ArcGIS 8.3. Flow direction was defined based on the steepest gradient of flow paths. A stream network was constituted by including the pixels of flow accumulation values greater than a chosen threshold area. According to Hoover et al. (1991), a threshold of 60 or 70 for DEM at 30m resolution (i.e., thresholds of 0.05 ~ 0.06 km^2) will depict a network comparable to one derived from topographic maps. Therefore, various threshold areas around 0.05 km^2 were used to extract stream networks. The hierarchical ordering of stream network and some geomorphological watershed parameters were obtained using GIS analysis.

Modified Box-Counting Method

In the classical box-counting method, grids of various sizes are superimposed onto a stream network. The number of cells covering at least a piece of the network is then counted. To take advantage of the raster format of DEM input and output data, a modified box-counting method was developed. Grids of 10 m ×10 m were aggregated to generate a series of new grids of successively coarser resolution increasing by a factor of 2 (20 m ×20 m, 40 m ×40 m, …., 20480 m ×20480 m). If a cell in the grid crossed by a stream takes a value of 1 and 0 otherwise, then the value of a generated lower resolution cell was assigned as the maximum value (1 or 0) of higher resolution cells contained in that cell. In this procedure, the upper left cell of the grid was used for starting the aggregation. All the procedures were performed in ArcGIS 8.3. The slope of the plot of $\log_2 N(r)$ against $\log_2 r$ gave the fractal dimension of the DEM-extracted stream network. N(r) represents the number of cells with value of 1 at resolution (cell size) r.

Estimation of Horton Ratios of DEM Extracted Stream Network

The structure of stream networks can be described as a system of streams with a hierarchical relationship among the different branches. The quantitative study of stream networks began with Horton (1945) and subsequently modified by Strahler (1952, 1957). Streams are defined as segments of the stream network that are composed of continuous links of the same order. A link is a section of the stream network between two successive

junctions between a source and the first junction downstream, or between the outlet and the first junction upstream. The Horton-Strahler ordering system is constructed by defining the order of streams. The first order streams are defined as those streams with no tributaries. When two streams of the same order join, a stream of one order higher is formed, and when two streams of different order join, the continuing stream retains the order of the higher-order of two streams. Figure 4.1 shows a scheme of the Horton-Strahler stream network ordering system.

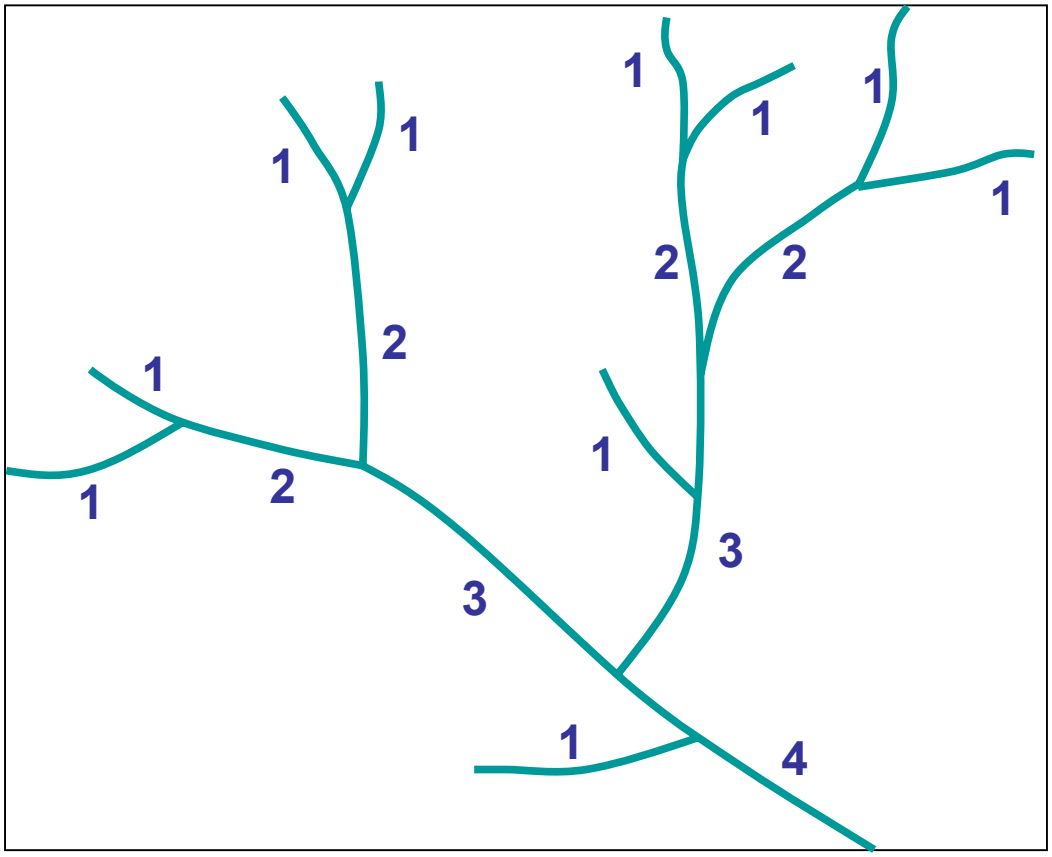

Figure 4.1. Scheme of a Horton-Strahler stream network ordering system of order 4.

After the streams of a network extracted from DEM were hierarchically ordered in terms of the Horton-Strahler stream ordering system, the following ratios were established for streams of order ω:

$$R_B = N_{\omega-1}/N_{\omega} \qquad (4.12)$$

$$R_L = L_\omega / L_{\omega-1} \quad (4.13)$$

$$R_A = A_\omega / A_{\omega-1} \quad (4.14)$$

R_B, R_L, and R_A represent bifurcation, length, and area ratios, respectively, where N_ω, L_ω, and A_ω, respectively, denote the number, average length, and average contribution area of order ω. Values of N_ω, L_ω, and A_ω were plotted against order ω and straight lines fitted by the least square regression. The Horton ratios R_B, R_L, and R_A were estimated from the slopes of the fitted lines.

Multifractal Analysis of DEM-Extracted Stream Networks

For raster data with cell of size δ, the probability [$Pr(\delta_i)$] of a measure of interest on the stream network contained in the i^{th} cell with resolution δ was defined as:

$$\Pr(\delta_i) = N(\delta_i) / N \quad (4.15)$$

where $N(\delta_i)$ = number of cells at the finest resolution of the raster data with value of 1 (meaning the cell covered the flow path) within the i^{th} cell at resolution δ, and N = total number of cells over the entire raster set with value of 1 at the finest resolution .

As described above under the modified box-counting method, extracted stream networks of different resolutions were obtained in raster format. A so-called partition function $Z_q(\delta)$ was defined as follows (Ijjasz-Vasquez et al., 1992; De Bartolo et al., 2000):

$$Z_q(\delta) = \sum_{i=1}^{N(\delta)} [\Pr(\delta_i)]^q \quad (4.16)$$

where N(δ) = number of cells at resolution δ.

The fractal dimension corresponding to the q^{th} moment was calculated as:

$$D(q) = \frac{1}{q-1} \lim_{\delta \to 0} \frac{\log Z_q(\delta)}{\log \delta} \quad for\ q \neq 1 \qquad (4.17)$$

The slope of a plot of log $Z_q(\delta)$ / (q-1) versus log δ would give an estimate of the fractal dimension corresponding to the q^{th} moment. For q = 0, the fractal dimension is identical to the one defined above under the box-counting method, as the slope of the plot of log $N(\delta)$ against log δ.

Since many of the sub-watersheds were small in size and the order of these stream network (the highest order of the stream) was low, the estimates of Horton ratios as well as the fractal dimensions were unreliable from regression. Therefore, the scaling of stream networks was investigated only for the four main watersheds.

RESULTS AND DISCUSSION

The morphometric characteristics (order of network, magnitude of streams, mean length of the first order streams, length of the highest order stream, main stream length, total stream length, drainage density, and stream frequency) of the DEM-extracted stream networks (Figures 4.2 to 4.5) of four agricultural watersheds using various threshold values of contribution area are presented in Table 4.2. Because of the relatively small size of the Little Mill Creek watershed, the threshold areas used to extract stream network were smaller than the other three watersheds in order to obtain enough streams to estimate Horton ratios. The shape of the Sleepers River watershed was less-elongated than the other three (Figures 4.2 to 4.5).

The lengths of watershed boundary were 118.28, 22.42, 91.90, and 53.22 km for the Little River, Little Mill, Reynolds Creek, and Sleepers River watershed, respectively. As expected, the order of the network, the total stream number and length, the main stream length as well as the drainage density and stream frequency decreased as the threshold area increased. This is because for higher threshold areas, some grids with smaller contribution areas were excluded from the network and a relatively less detailed stream network was generated. In contrast, the mean length of first-order streams ($<L_1>$) was smaller when a small threshold value was used. However, the dependence of the length of the highest order of network (L_Ω) on threshold area was somewhat more complicated than for the other morphometric characteristics. For example, L_Ω of the Reynolds Creek watershed were 4.37, 2.19, 4.37, and 2.20 km, respectively, corresponding to the threshold areas of 0.05, 0.1, 0.2, 0.5 km^2 (Table 4.2). The reason was that when the order of the network changed, the starting point of the highest order stream might also change. At the threshold area of 0.05 km^2, the Sleepers River watershed had higher drainage density and stream frequency than the other three watersheds.

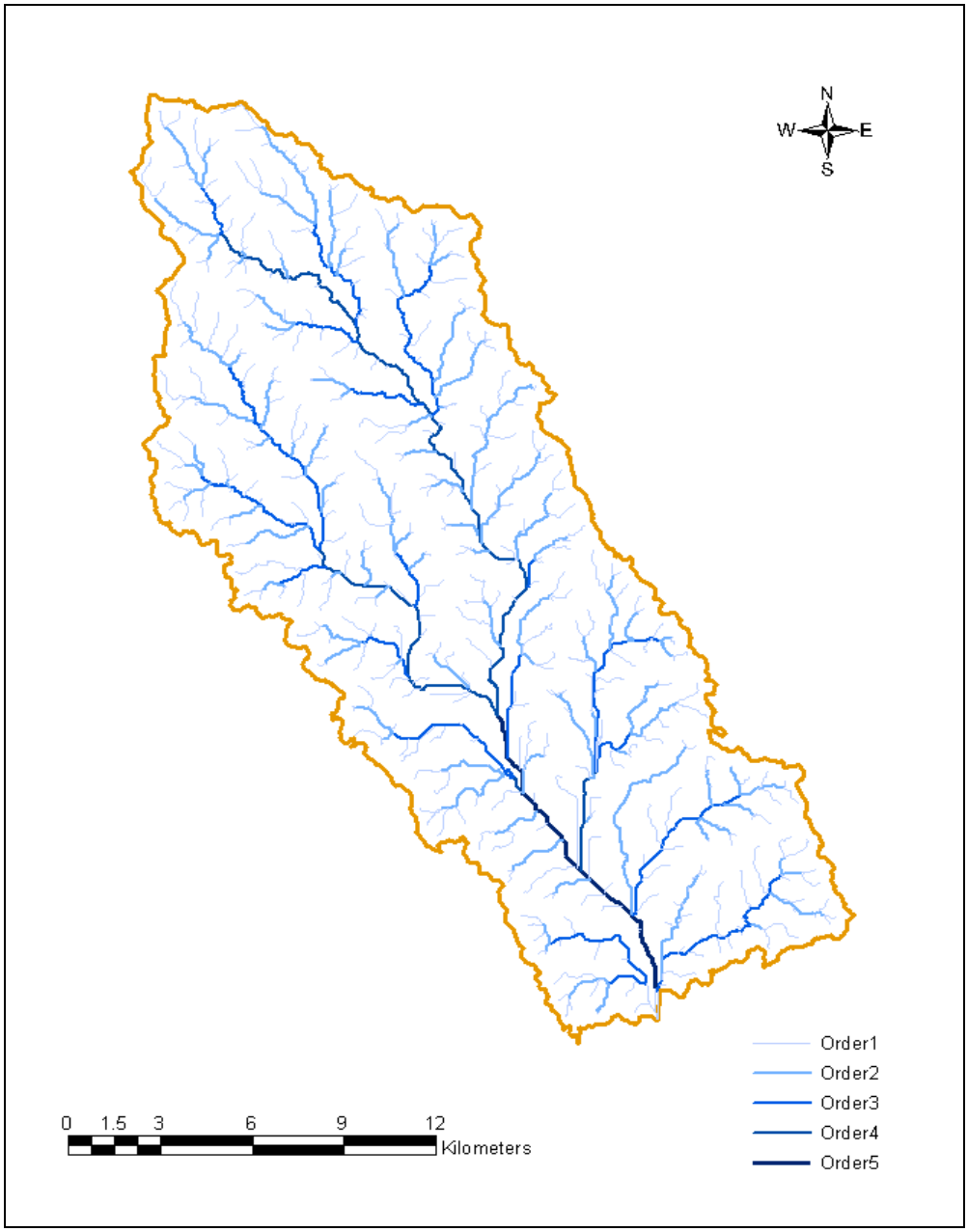

Figure 4.2. The stream network of the Little River watershed extracted using DEM.

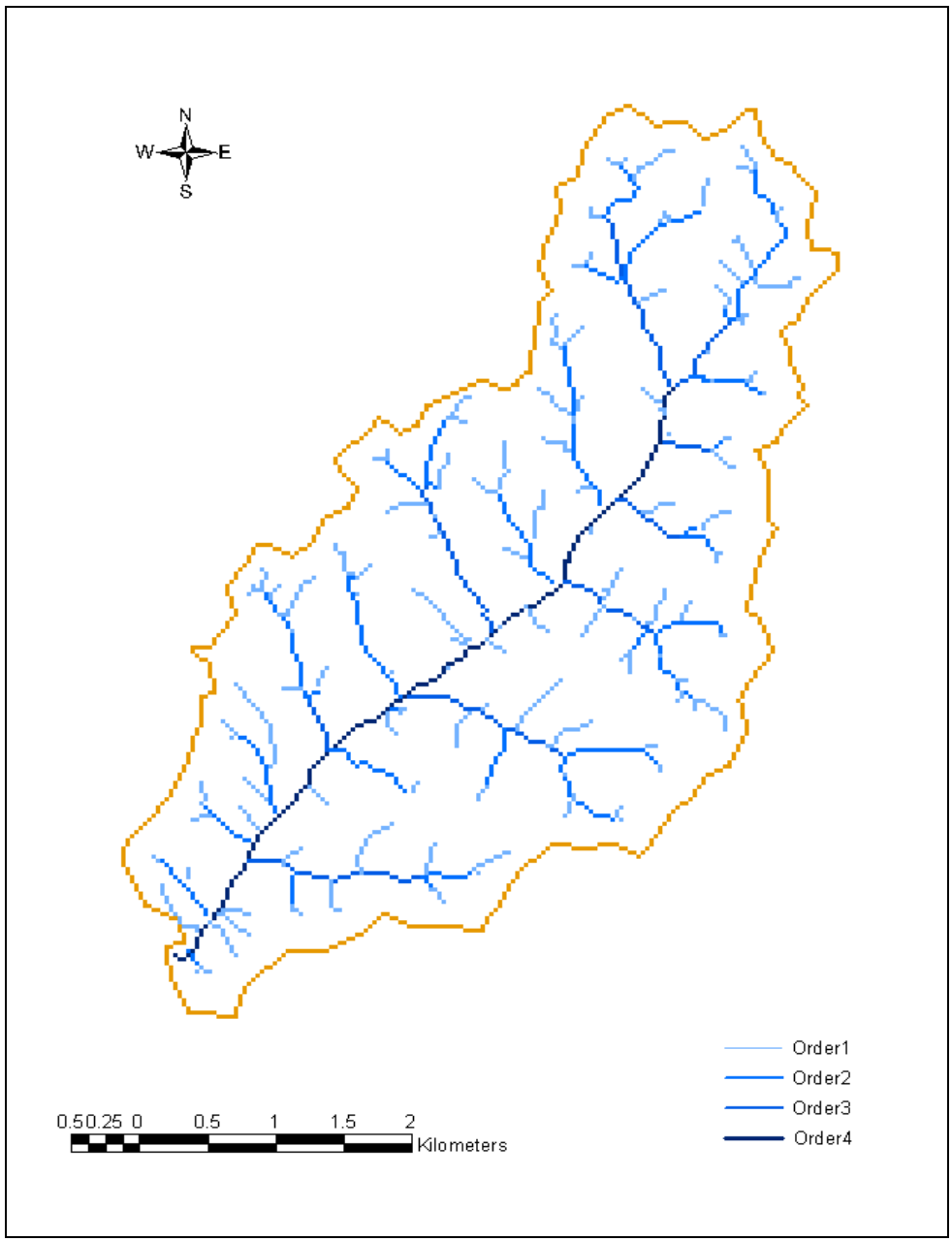

Figure 4.3. The stream network of the Little Mill Creek watershed extracted using DEM.

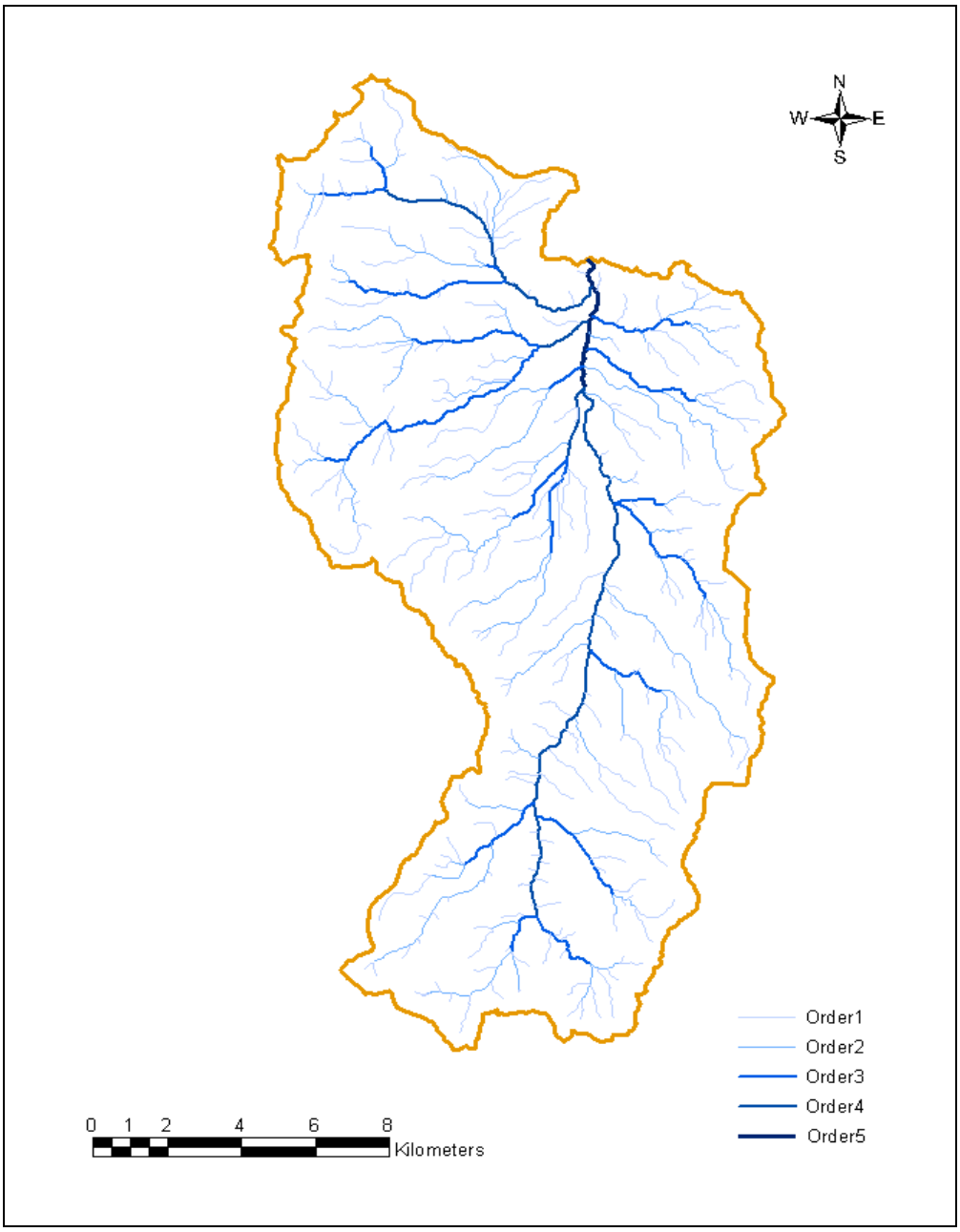

Figure 4.4. The stream network of the Reynolds Creek watershed extracted using DEM.

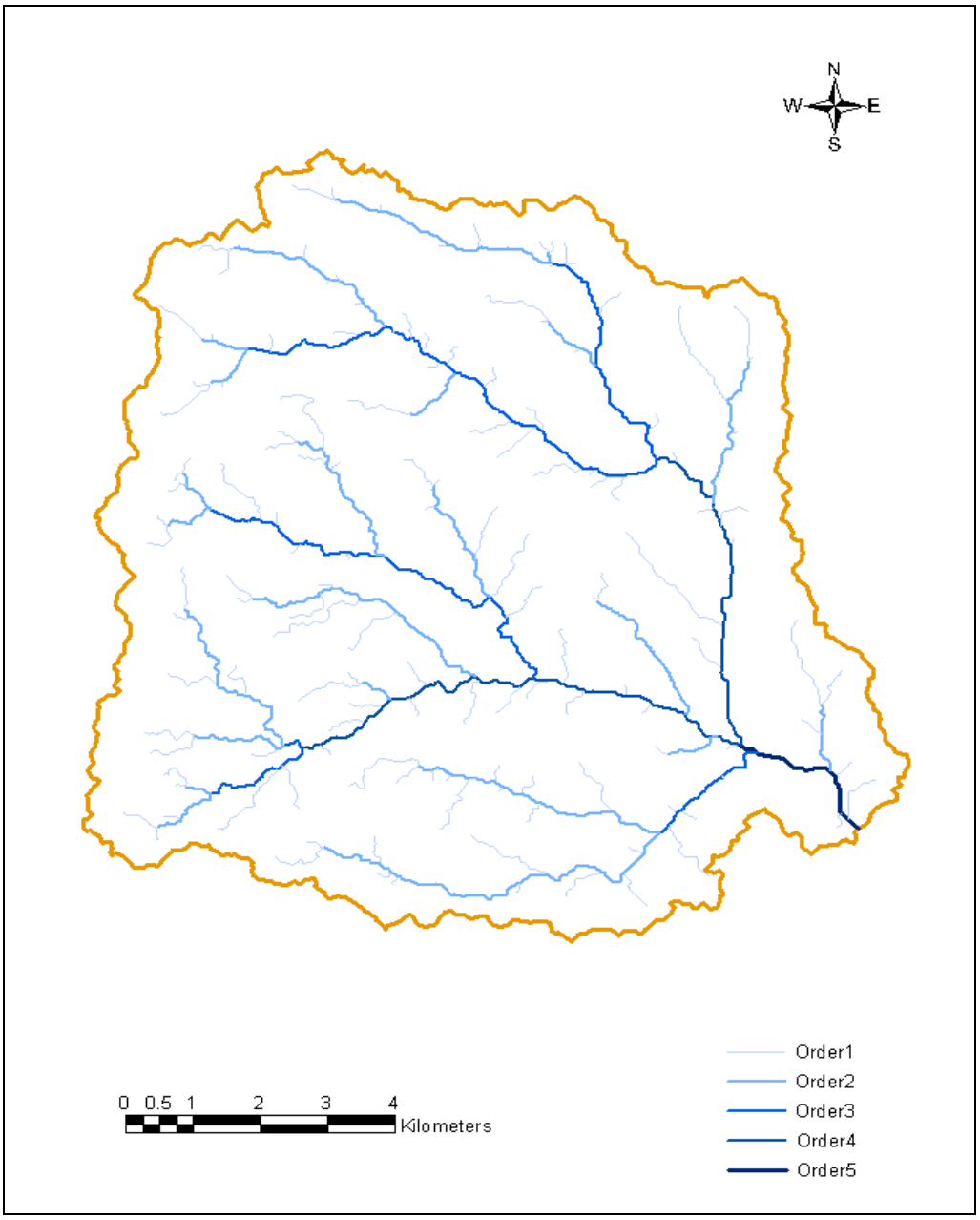

Figure 4.5. The stream network of the Sleepers river watershed extracted using DEM.

Table 4.2 Morphometric characteristics of DEM-extracted stream networks using different contributing threshold areas for four agricultural watersheds.

Watershed	Threshold (km^2)	Network Order	Magnitude	$<L_1>$ (km)	L_Ω (km)	Lm (km)	L_T (km)	Drainage Density (km / km^2)	Stream Frequency (1 / km^2)
Little River	0.05	6	2060	0.21	11.78	42.97	782.09	2.34	6.17
Watershed	0.10	6	1118	0.37	11.99	42.74	722.11	2.16	3.35
	0.20	5	568	0.62	11.99	42.61	565.19	1.69	1.70
	0.50	5	250	0.95	12.93	42.08	376.15	1.63	0.75
Little Mill Creek	0.0125	5	481	0.11	6.37	8.93	87.02	4.70	26.00
Watershed	0.025	4	213	0.17	6.37	8.84	62.83	2.76	11.51
	0.05	4	115	0.27	6.37	8.79	48.37	2.61	6.22
Reynolds Creek	0.05	6	1400	0.31	4.37	27.67	690.75	2.96	6.00
Watershed	0.10	6	704	0.49	2.19	27.60	515.13	2.21	3.01
	0.20	5	391	0.67	4.37	27.43	394.03	1.69	1.67
	0.50	5	171	1.10	2.20	27.04	262.32	1.12	0.73
Sleepers River	0.025	6	1638	0.22	6.23	18.80	516.03	4.64	14.73
Watershed	0.05	6	881	0.28	2.68	18.70	362.38	3.26	7.92
	0.10	5	407	0.39	6.23	18.55	245.19	2.26	3.66
	0.20	5	191	0.50	2.68	18.24	167.34	1.50	1.72

$<L_1>$ = mean length of the first order stream, L_Ω = length of the highest order stream, Lm = main stream length, and L_T = total stream length

Table 4.3 Fractal dimensions of stream network estimated as the absolute value of slope of linear fit to plots of N(r) versus r as shown in Figure 4.6 using the box-counting method for various threshold values.

Watershed	Threshold (km^2)	D_b	r^2	D_{b1}	r^2	D_{b2}	r^2
Little River	0.05	1.37	0.987	0.99	0.995	1.58	0.997
Watershed	0.1	1.32	0.987	0.97	0.996	1.55	0.998
	0.2	1.28	0.988	0.96	0.996	1.50	0.998
	0.5	1.21	0.990	0.95	0.997	1.42	0.999
Little Mill	0.0125	1.38	0.990	1.03	0.994	1.57	0.998
Watershed	0.025	1.30	0.988	0.95	0.995	1.51	0.999
	0.05	1.23	0.987	0.92	0.995	1.45	0.998
Reynolds Creek	0.05	1.36	0.984	1.00	0.993	1.64	0.997
Watershed	0.1	1.31	0.984	0.97	0.995	1.60	0.998
	0.2	1.25	0.984	0.95	0.998	1.54	0.998
	0.5	1.19	0.987	0.94	0.996	1.44	0.998
Sleepers River	0.025	1.42	0.987	0.98	0.993	1.62	0.997
Watershed	0.05	1.36	0.986	0.95	0.995	1.58	0.996
	0.1	1.29	0.987	0.93	0.995	1.50	0.997
	0.2	1.21	0.985	0.92	0.996	1.41	0.997

D_b is the slope of linear fit to all points; D_{b1} and D_{b2} are slopes of fits to points on either side of the break point (see Figure 4.6), r2 is the coefficient of determination of the linear fits.

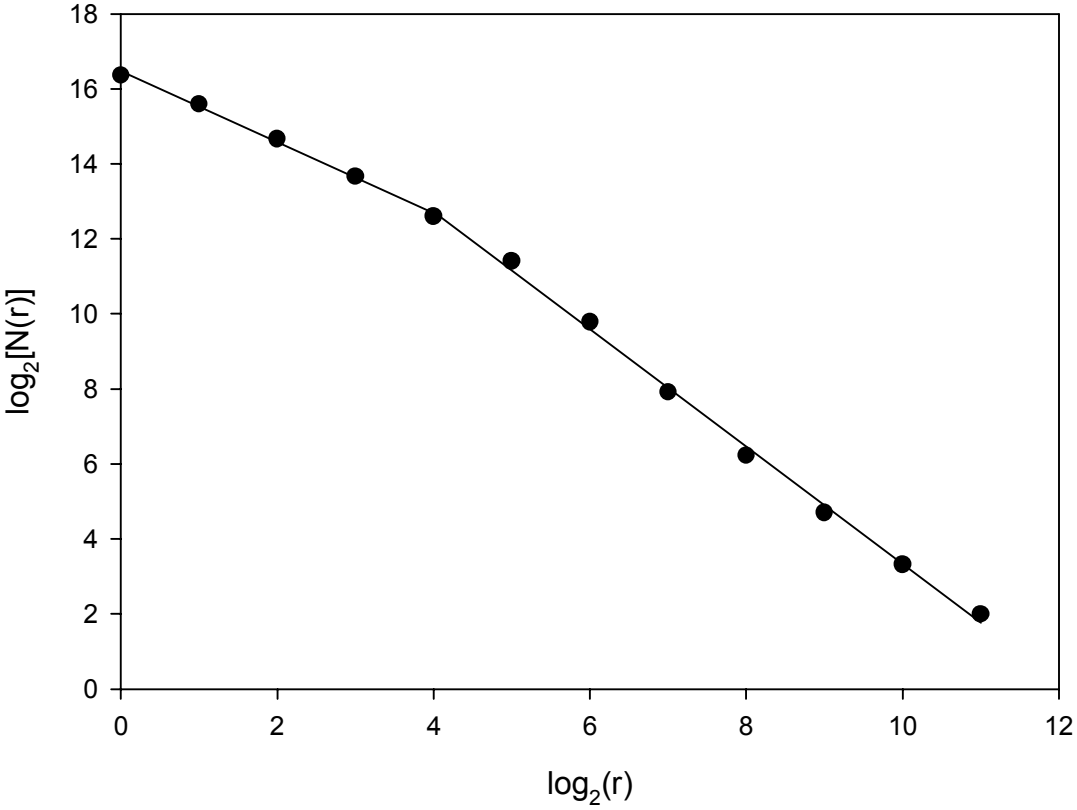

Figure 4.6. Log-log box counting plot of number of covering boxes N(r) at box size (r) for stream network using threshold = 0.05 km^2 for the Little River watershed in Tifton, Georgia. Separate straight lines were fitted to the points on either side of the break point. r^2 for fits were > 0.99.

Fractal Dimension Estimated by Box-Counting Method

The fractal dimensions of the stream network estimated using the box-counting method are presented in Table 4.3. In this table, the slope of the fitted line of $\log_2 N(r)$ versus $\log_2 r$ over the entire range of box sizes gave the fractal dimension (D_b), where N(r) was the number of boxes of size $r \times r$ covering the network. However, as shown in the example for the Little River watershed (Figure 4.6), the relationship between $\log_2 N(r)$ and $\log_2 r$ was better characterized by two distinct slopes, one corresponding to the small box sizes and the other corresponding to the large box sizes. The slope of the former range was denoted as D_{b1}, and the latter was denoted as D_{b2}. The scaling range for D_{b1} was much smaller than that for D_{b2}. For example, the box sizes ranged from 1 pixel to 32 pixels in scaling range for D_{b1} and from 32 to 1024 pixels for D_{b2}. Since some trivial streams extracted from DEM might not really exist, the fractal dimension of the network might be more appropriately represented by D_{b2}. The values of D_{b1} were close to 1.0, which confirmed the results of previous studies reported by Tarboton et al. (1988). However, D_{b2} ranged from 1.42 to 1.64 depending on the threshold values, and these values were much smaller than those reported by Tarboton et al. (1988). In their study, D_{b2} was found to be equal to 2.0 and was interpreted as the plane-filling pattern.

The fractal dimensions decreased as threshold values increased because at a higher threshold value a relative sparser network would be generated and occupy less space. The stream network of the Little Mill Creek watershed extracted at the threshold area of 0.05 km^2 had a smaller D_{b2} value than the other three watersheds at the same threshold area. This may indicate that this estimate of the fractal dimension of a DEM-extracted stream network of low order might not give satisfactory results. As stated above, the coarser resolution of the DEM for the Little Mill Creek watershed might also affect the estimation of the fractal dimension from box-counting method. The fractal dimensions of the other three watersheds were almost the same, although the drainage density of the Sleepers River watershed at the 0.05 km^2 threshold area was higher than other watersheds (Table 4.2). A watershed of higher drainage density was more "space filling" and was expected to have higher fractal dimension. It was reported that the fractal dimension of an arid climate site was higher than that of a humid climate site (Lifton and Chase, 1992).

The four watersheds were far separated and were in different climates. However, the results showed that the fractal dimensions were not markedly influenced by the different climates.

Fractal Dimension Estimated by Horton Ratios

The bifurcation (R_B), length (R_L), and area (R_A) ratios (the Horton ratios) calculated for the stream network extracted at various threshold areas are listed in Table 4.4. Since the outlet of the Reynolds Creek watershed was close to the start point of its highest order stream, the stream of highest order was very short. Such watersheds are called "immature" watersheds. Therefore the highest order was not used in determination of R_L and R_A. For the same reason, the streams with the highest order at threshold areas of 0.05 and 0.20 km^2 for Sleepers River watershed were excluded in estimation of these characteristics. Generally, the values of Horton ratios tended to decrease as the threshold value increased. The fractal dimensions of the stream length and stream network were also estimated using Horton ratios. The fractal dimension (d) of stream length was determined as $d = \max (1, 2 * \log R_L/\log R_A)$, and the d-values ranged from 1.00 to 1.28 (Table 4.4). An average d-value of 1.14 has been reported (Tarboton et al., 1989). The fractal dimension of stream length measures the extent of the streams' meandering (i.e., the change of stream length as the catchment area changes). A fractal stream will have a greater length when measured at a finer scale.

The branching pattern of a stream network can be characterized by the fractal dimension (D) of the network. Two equations in terms of Horton ratios were used to calculate D values that were denoted as D_1 ($D_1 = \log R_B/\log R_L$) and D_2 ($D_2 = 2 * \log R_B/\log R_A$). The values of D_1 tended to increase with increasing extraction threshold. D_1 values were close to even greater than 2.0 at various threshold values (Table 4.4). D_1 values of Little Mill Creek watershed were much smaller than for the other three watersheds. This might be caused by the uncertainty of determination of Horton ratios for watersheds of low order. Another possible cause was the coarser resolution (30 m) of DEM data of the Little Mill Creek watershed in comparison with 10 m DEM of the other three watersheds (Table 4.1). In fact, the r^2 of regression lines in the plots for the Little Mill Creek

Table 4.4 Estimated fractal dimension of stream length (d) and stream network (D) using Horton's ratios for four agricultural watersheds, where d = max (1, 2 log R_L/log R_A), D_1 = log R_B/log R_L, and D_2 = 2*log R_B/log R_A.

Watershed	Threshold (km^2)	R_B	R_L	R_A	d	D_1	D_2
	0.05	3.98	2.23	4.22	1.11	1.72	1.92
Little River	0.1	3.77	2.05	3.93	1.05	1.85	1.94
Watershed	0.2	3.72	1.95	3.98	1.00	1.97	1.90
	0.5	3.35	1.77	3.52	1.00	2.12	1.92
	0.0125	3.69	2.2	3.79	1.18	1.66	1.96
Little Mill	0.025	3.47	2.35	3.79	1.28	1.46	1.87
Watershed	0.05	3.19	1.95	3.33	1.11	1.74	1.93
	0.05	3.81	1.95	4.11	1.00	2.00	1.89
Reynolds Creek	0.1	3.58	1.83	3.81	1.00	2.11	1.91
Watershed	0.2	3.45	1.66	3.75	1.00	2.44	1.87
	0.5	3.08	1.39	3.33	1.00	3.42	1.87
	0.025	3.95	1.92	4.23	1.00	2.11	1.91
Sleepers River	0.05	3.77	2.02	3.99	1.02	1.89	1.92
Watershed	0.1	3.53	1.81	3.85	1.00	2.13	1.87
	0.2	3.18	1.88	3.48	1.01	1.83	1.86

watershed were lowest in comparison with other watersheds. In contrast, the results showed that the values of D_2 were not sensitive to the threshold value, ranging from 1.87 to 1.96, and were identical for the four watersheds (Table 4.4). This indicated that the fractal dimension of stream network might be more appropriately represented by D_2, although Beer and Borgas (1993) had reported that D_2 may not be an appropriate measure for a real stream network. Fractal dimension quantifies the complexity or irregularity of a fractal object. The similar estimated fractal dimension for four watersheds indicated that these stream networks had the same complexity or irregularity.

The D values can be used to characterize the plane filling pattern of the stream network. Theoretically 2.0 is the maximum value for a two-dimensional network, although dimensions greater than 2.0 had been obtained in other studies (Tarboton et al., 1988; Helmlinger et al., 1993; Puente and Castillo, 1996; da Ros and Borgas, 1997). By assuming that a watershed collects water from every pixel to the outlet, the stream network within that watershed should display the fractal dimension of 2.0 (Tarboton et al., 1988; La Barbera and Rosso, 1989). However, Claps and Oliverto (1996) argued that the stream network structures were definitely non-plane filling. The fractal dimensions of stream networks estimated by the box-counting method were lower than the dimensions estimated by Horton ratios method (Table 4.3 and 4.4).

Cumulative Probability Distribution of Contribution Area

The cumulative probability distribution of contribution area was also examined for the four watersheds. The cumulative probability of finding a pixel within a watershed having the contribution area (A) larger than certain value (a) is given by:

$$\Pr(A \geq a) = a^{-\alpha} \qquad (4.18)$$

where the scaling exponent α is a constant and was estimated from the slope of the log $\Pr(A \geq a)$ versus log a for $a << A_\Omega$, where A_Ω was the watershed size. Figure 4.7 shows the cumulative probability distribution (dotted points) of contribution area of the Little

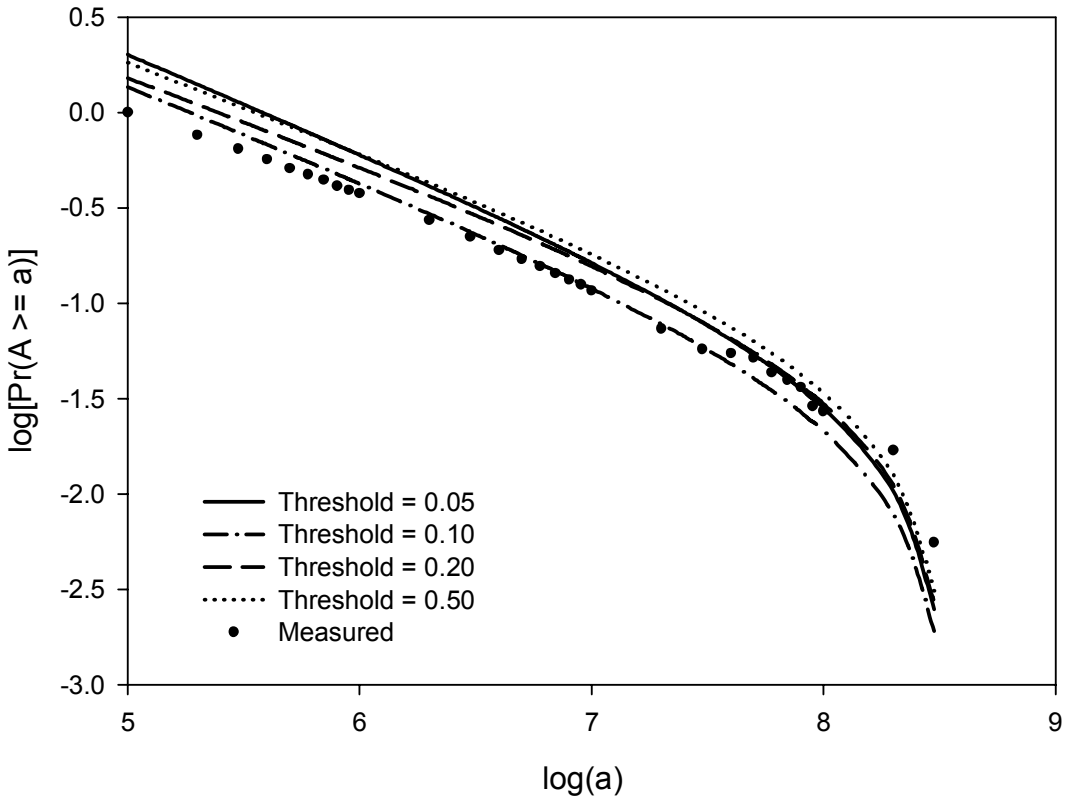

Figure 4.7 Cumulative probability distribution for contribution area (a, m^2) of the Little River watershed in Tifton, Georgia. The theoretical distributions were calculated from Eq.(4.13) for various threshold values.

River watershed as an example. Deviation from the linear trend occurred at large values of contribution area. The scaling exponents of four watersheds were 0.53 (the Little River watershed), 0.50 (the Little Mill Creek watershed), 0.55 (the Reynolds Creek watershed), and 0.52 (the Sleepers River watershed), respectively. These exponents were slightly greater than the theoretical value of 0.43 for a completely plane-filling watershed (La Barbera and Roth, 1994).

More importantly, the cumulative probability distribution can be related to Horton ratios by (La Barbera and Roth, 1994; Roth et al., 1996):

$$\Pr(A \geq a) = \frac{\left(\frac{R_L}{R_B}\right)^{\Omega}}{1-\left(\frac{R_L}{R_B}\right)^{\Omega}} \left[\left(\frac{a}{A_\Omega} \right)^{-\frac{d}{2}(D-1)} - 1 \right] \qquad (4.13)$$

where d = fractal dimension of the stream length, D = fractal dimension of the stream network, and Ω = order of the stream network. These theoretical cumulative probability distributions of the contribution area were calculated using the R_B, R_L, d, and D values determined as in Table 4.4. Since R_B, R_L, d, and D were all dependent on the threshold area used in the DEM extraction process, cumulative distributions were calculated corresponding to each threshold value.

The observed and theoretical cumulative probability distributions of contribution area were plotted in the same figure for the various thresholds. As an example, Figure 4.7 shows the cumulative probability distribution obtained from the DEM (dotted points) and the theoretical distributions (solid lines) calculated using Eq. (4.13) for the Little River watershed.

The results showed that the theoretical probability distribution exceeded the probability limit of 1.0 at small distribution areas, which might be caused by the errors in R_B, R_L, d, and D estimation. In most cases, the slopes of the linear portion of the cumulative

probability distributions of a watershed were the same. These results indicated that the estimates of Horton ratios and fractal dimensions were valid. Figure 4.7 also showed that the cumulative probability distribution using the R_B, R_L, d, and D values of threshold area of 0.1 km^2 displayed a better match with the measured distribution. Based on the cumulative probability distribution plots, the appropriate threshold area in DEM extraction process were found to be 0.1 km^2. It should be noted that since only a few threshold values were used, the threshold of 0.1 km^2 was by no means the most appropriate area to extract stream networks. The theoretical probability distributions of the Little Mill Creek watershed had a poor match with empirical distribution. Since the order of the Little Mill Creek watershed was low, the estimation of Horton ratios as well as the fractal dimensions based on the Horton ratios might not be reliable. The cumulative probability distribution plots might provide a useful approach to determine an appropriate threshold value to delineate the stream network from DEM data.

Multifractal Analysis of Stream Networks

As an example of the multifractal approach to analyze the DEM-extracted stream networks, Figure 4.8 shows the scaling of the partition function [$Z_q(\delta)$] for the Little River watershed. In Figure 4.8, [$\log Z_q / (q-1)$] versus $\log \delta$ were plotted together for various q (q = 2 to 15). The results showed that [$\log Z_q / (q-1)$] versus $\log \delta$ displayed good linear relationships for each moment of order q (Figure 4.8). The slope of the fitted line represented the fractal dimension corresponding to the moment of order q. These fractal dimensions were very close regardless of q. The fractal dimensions ranged from 1.44 to 1.38 for the Little River watershed, 1.42 to 1.35 for the Little Mill Creek watershed, 1.39 to 1.35 for the Reynolds Creek watershed, and 1.41 to 1.36 for the Sleepers River watershed. This indicated that the fractal dimensions of these stream networks were not dependent on the q, which indicated that the geometry of the stream network should be regarded as a fractal rather than a multifractal object. The multifractal analysis of the other three watersheds also showed similar single scaling patterns regardless of q.

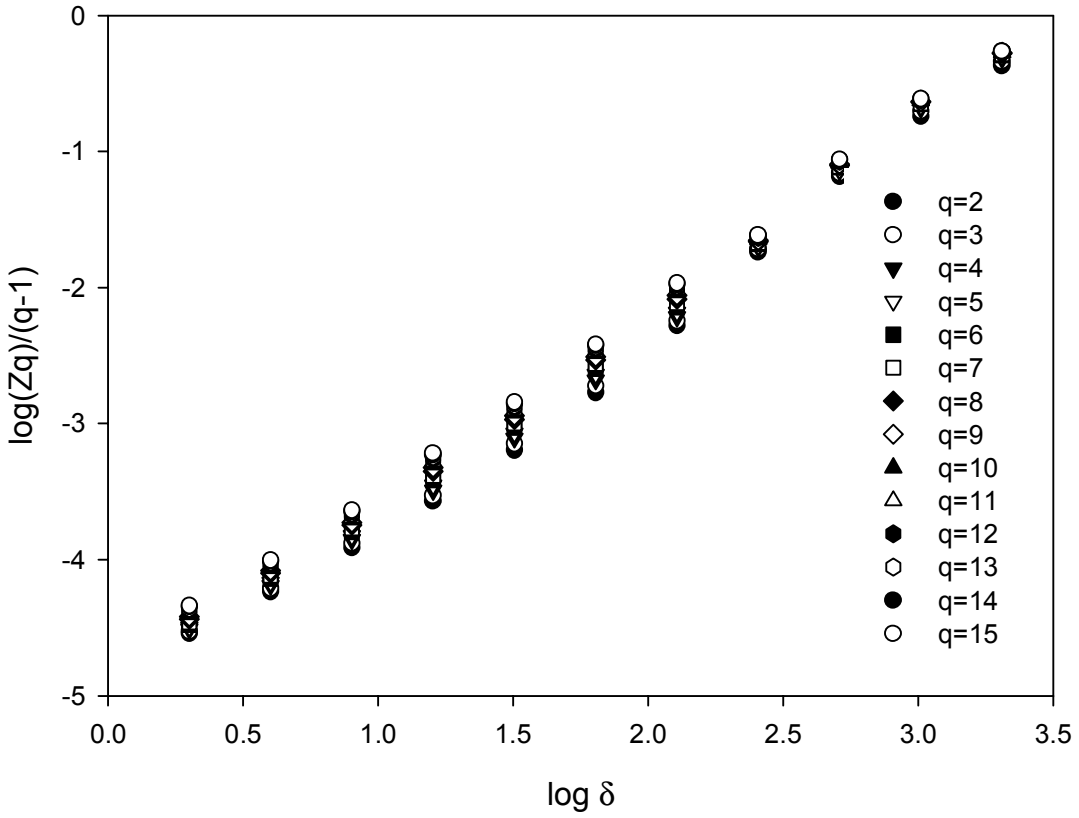

Figure 4.8. Scaling of the partition function Zq for moment order q = 2 to 15 versus box size (δ) for the Little River watershed, in Tifton, Georgia.

FINDINGS AND CONCLUSIONS

The stream networks of four agricultural watersheds were extracted using the most recently updated (July 2004) NED DEMs with high resolution. The geomorphological attributes and Horton ratios as well as fractal dimensions were dependent on the threshold values of contribution area used in the extraction process. The completeness of the extracted networks was apparently not always guaranteed for different threshold area selections and supported the findings of Da Ros et al. (1997). The threshold area also affected the estimation of morphometric properties as reported by Helmlinger et al. (1993) and Ichoku et al. (1996). The cumulative probability distribution of contribution area might provide an approach to identify the appropriate threshold area for extracting stream network from DEM.

The scaling characteristics of the stream networks using the box-counting method, Horton ratios method, cumulative probability distribution method, and a multifractal approach, showed that the stream networks displayed scale-invariance over scales and the fractal dimensions were almost the same for four watersheds. These results indicated that these watersheds might possess similar morphometric scaling properties. The DEM extracted stream network exhibited a single scaling pattern, rather than multifractal behavior.

Fractal dimension of the stream length and networks based on Horton ratios showed that the values of $2 * \log R_B / \log R_A$ provided a more stable estimate of the fractal dimension than those calculated using $\log R_B / \log R_L$. Although self-similarity of stream networks are assumed for Hortonian streams, in reality stream networks are not strictly self-similar.

REFERENCES

Andrle, R. 1992. Estimating fractal dimension with the divider method in geomorphology. Geomorphology 5: 131-141.

Beer, T. and M. Borgas. 1993. Horton's laws and the fractal nature of streams. Water Resources Research 29: 1475-1487.

Breyer, S. P. and R. S. Snow. 1992. Drainage basin perimeters: a fractal significance. Geomorphology 5: 143-157.

Chase, C. G. 1992. Fluvial landsculpting and the fractal dimension of topography. Geomorphology 5: 39-57.

Cheng, Q., H. Russell, D. Sharpe, F. Kenny, and P. Qin. 2001. GIS-based statistical and fractal/multifractal analysis of surface stream patterns in the Oak Ridges Moraine. Computers & Geosciences 27: 513-526.

Cheng, Y.C., P. J. Lee, and T. Y. Lee. 1999. Self-similarity dimensions of the Taiwan Island landscape. Computers & Geosciences 25: 1043-1050.

Claps, P. and G. Oliveto. 1996. Reexamining the determination of the fractal dimension of river networks. Water Resources Research 32: 3123-3135.

Crave, A. and P. Davy. 1997. Scaling relationships of channel networks at large scales: examples from two large-magnitude watersheds in Brittany, France. Tectonophysics 269: 91-111.

Da Ros, D. and M. Borga. 1997. Use of digital elevation model data for the derivation of the geomorphological instantaneous unit hydrograph. Hydrological Processes 11: 13-33.

De Bartolo S.G., S. Gabriele, and R. Gaudio. 2000. Multifractal behavior of river networks. Hydrology and Earth System Sciences 4: 105-112.

Gray, D. M. 1961. Interrelationships of watershed characteristics. Journal of Geophysical Research 66: 1215-1223.

Hack, J. T. 1957. Studies of longitudinal stream profiles in Virginia and Maryland. U.S. Geological Survey Professional Paper 294B.

Helmlinger, K. R., P. Kumar, and E. Foufoula-Georgio. 1993. On the use of digital elevation model data for Hortonian and fractal analyses of channel networks. Water Resources Research 29: 2599-2613.

Hjelmfelt, A. T. 1988. Fractals and the river-length catchment-area ratio. Water Resources Bulletin 24: 456-459.

Horton, R. E. 1932. Drainage basin characteristics. Transactions American Geophysical Union 13: 350-361.

Horton, R. E. 1945. Erosional development of streams and their basins – hydrophysical approach to quantitative geomorphology. Geological Society of America Bulletin 56:275-370.

Hoover K. A., M. G. Foley, and P. G. Heasler. 1991. Sub-grid-scale characterization of channel lengths for use in catchment modeling. Water Resources Research 27: 2865-2873.

Ichoku, C., A. Karnieli, and I. Verchovsky. 1996. Application of fractal techniques to the comparative evaluation of two methods of extracting channel networks from digital elevation models. Water Resources Research 32: 389-399.

Ijjasz-Vasquez, E. J., I. Rodriguez-Iturbe, and R. L. Bras. 1992. On the multifractal characterization of river basins. Geomorphology 5: 297-310.

Ijjasz-Vasquez, E. J. and R. L. Bras. 1995. Scaling regimes of local slope versus contributing area in digital elevation models. Geomorphology 12: 299-311.

Jenson, S. K. and J. O. Domingue. 1988. Extracting topographic structure from digital elevation data for geographic information system analysis. Photogrammetric Engineering and Remote Sensing 54: 1593-1600.

Klinkenberg B. 1992. Fractals and morphometric measures: is there a relationships? Geomorphology 5: 5-20.

La Barbera, P. and R. Rosso. 1989. On the fractal dimension of stream networks. Water Resources Research 25: 735-741.

La Barbera, P., and G. Roth. 1994. Invariance and scale properties in the distribution of contribution area and energy in drainage basins. Hydrological Processes 8: 125-135.

Lam, N. S. and L. De Cola. 1993. Fractals in geography. Prentice-Hall, New Jersey.

Lifton N. A. and C. G. Chase. 1992. Teconic, climatic and lithologic influences on landscape fractal dimension and hypsometry: implications for landscape evolution in San Gabriel Mountains, California. Geomorphology 5: 77-114.

Mandelbrot, B. B. 1983. The fractal geometry of nature. W.H. Freeman, New York.

Meisel, A., S. Raizman, and A. Karnieli. 1995. Skeletonizing a DEM into a drainage network. Computers & Geosciences 21: 187-196.

Montgomery, D. R. and W. E. Dietrich. 1989. Sources areas, drainage density, and channel initiation. Water Resources Research 25: 1907-1918.

Montgomery, D. R. and W. E. Dietrich. 1992. Channel initiation and the problem of landscape scale. Science 255: 826–830.

Montgomery, D. R. and E. Foufoula-Georgiou. 1993. Channel network source representation using digital elevation models. Water Resources Research 29: 3925-3934.

Montgomery, D. R. and W. E. Dietrich. 1994. In Processes, model, and theoretical geomorphology, Kirkby M.J. (ed.). Wiley: chichester: 221- 246.

Moussa, R. and C. Bocquillon. 1996. Fractal analyses of tree-like channel networks from digital elevation model data. Journal of Hydrology 187: 157-172.

Nikora, V. I. and V. B. Sapozhnikov. 1993. River network fractal geometry and its computer simulation. Water Resources Research 29: 3569-3575.

Nikora, V. I. 1994. On self-similarity and self-affinity of drainage basins. Water Resourses Research 30: 133-137.

Nikora, V., R. Ibbitt, and U. Shankar. 1996. On channel network fractal properties: a case of study of the Hutt river basin, New Zealand. Water Resources Research 32: 3375-3384.

Ouchi, S. and M. Matsushita. 1992. Measurement of self-affinity on surface as a trial application of fractal geometry to landform analysis. Geomorphology 5: 115-130.

Puente, C. E. and P. A. Castillo. 1996. On the fractal structure of networks and dividers within a watershed. Journal of Hydrology 187: 173-181.

Richardson, L. F. 1961. The problem of contiguity: an appendix of statistics of deadly quarrels. General Systems Yearbook 6: 139-187.

Robert, A. and Roy, A. 1990. On the fractal interpretation of the mainstream length drainage area relationship. Water Resources Research 26: 839-842.

Rodriguez-Iturbe, I. and A. Rinaldo. 1997. Fractal river basins: chance and self-organization. Cambridge University Press, New York.

Rosso, R., B. Bacchi, and P. La Barbera. 1991. Fractal relation of mainstream length to catchment area in river networks. Water Resources Research 27: 381-387.

Roth, G., P. La Barbera, and M. Greco. 1996. On the description of the basin effective drainage structure. Journal of Hydrology 187: 119-135.

Schuller, D. J., A. R. Rao, and G. D. Jeong. 2001. Fractal characteristics of dense stream networks. Journal of Hydrology 243: 1-16.

Strahler, A. N. 1952. Hypsometric (area-altitude) analysis of erosional topography. Geological Society of America Bulletin, 63: 1117-1142.

Strahler, A. N. 1957. Quantitative geomorphology of drainage basins and channel networks. McGraw-Hill, New York.

Tarboton, D. G., R. L. Bras, and I. Rodriguez-Iturbe. 1988. The fractal nature of river networks. Water Resources Research 24:1317–1322.

Tarboton, D. G., R. L. Bras, and I. Rodriguez-Iturbe. 1989. The analysis of river basins and channel networks using digital terrain data. Report 326, Ralph M. Parsons Laboratory, Department of Civil Engineering, MIT, Cambridge, Massachusetts.

Tarboton, D. G., R. L. Bras, and I. Rodriguez-Iturbe. 1990. Comment on the fractal dimension of stream networks, by La Barbera and Rosso. Water Resources Research 26: 2243-2244.

Tarboton, D. G. 1996. Fractal river networks, Horton's law and Tokunaga cyclicity. Journal of Hydrology 18: 105-117.

Tchiguirinskaia, I., S. Lu, F.J. Molz, T.M.Williams, and D. Lavallee. 2000. Multifractal versus monofractal analysis of wetland topography. Stochastic Environmental Research and Risk Assessment 14: 8-32.

Veltri, M., P. Veltri, and M. Maiolo. 1996. On the fractal description of natural channel networks. Journal of Hydrology 187: 137-144.

Xu, T., I. D. Moore, and J. C. Gallant. 1993. Fractals, fractal dimensions and landscapes — a review. Geomorphology 8: 245-262.

CHAPTER V
SUMMARY

Information transfer across spatial and temporal scales is common to many hydrological investigations. To quote Sposito (1998): "Whether processes in the natural world are dependent or independent of the scale at which they operate is one of the major issues in hydrologic sciences". During the last twenty years, research in diverse fields has firmly established that a wide variety of natural objects and processes exhibit spatial or temporal scale invariant geometrical or statistical patterns. Included in this category are hydrologic variables such as rainfall rates, soil moisture patterns, and hydrologic conductivity. Popularized by Mandelbrot (1983), fractal concepts have been applied for the past two decades to investigate fractal scale invariance in natural objects and phenomena. More recently, application of these concepts in hydrology have currently become a major subject of research in this field.

In this study, fractal scaling concepts and approaches were used to investigate the scale invariance of daily runoff time series in four ARS experimental agricultural watersheds and their 32 sub-watersheds. Fractal scaling of the patterns of DEM-extracted stream network morphometry in the four watersheds was also examined.

Runoff rate time series were obtained from the database for small agricultural watersheds across the U.S. developed by the Hydrological and Remote Sensing Laboratory of the Agricultural Research Service of the US Department of Agriculture (USDA/ARS/HRSL). Currently, about 16,600 station years of rainfall and runoff are available in the database. This database included metadata and auxiliary information such as map and land-use information that can be accessed either by downloading from the ARS website or on the CD-ROM distributed by ARS. This database provided the hydrological data for analysis in this study.

DEM-extracted stream network morphometry for the four watersheds were based on GIS manipulation of digital elevation data downloaded from the most recent (July 2004) U.S. Geological Survey (USGS) National Elevation Dataset (NED). NED of 10 m resolution was used for the three watersheds and 30 m resolution for the fourth. Several threshold area values for stream initiation were used to extract stream networks for each of the four watersheds.

The principal measures of fractal scaling determined for the runoff series were the Hurst exponent obtained by rescaled range (R/S) analysis, the fractal dimension estimated by the shifted box-counting method, and the multifractal scaling function parameters (α and C_1) of the Universal Multifractal Model (UMM). Corresponding measures for the DEM-extracted stream networks at each threshold value were the fractal dimension estimated using the box-counting technique and the Horton ratios of the network. In addition, the multifractal scaling behavior of the extracted stream network for each watershed was examined.

The major findings of this study can be summarized as follows:

1. Long-term records of daily runoff rate showed scale invariance over certain time scales. The same fractal dimensions and Hurst exponents were obtained for the sub-watersheds within each watershed, suggesting that the runoff of these sub-watersheds have similar distribution of occurrence and similar long-term memory.

2. Two scaling ranges in the runoff rate series were identified in the shifted box-counting plots with break points at about 12 months. The Hurst R/S analysis showed that the runoff time series also displayed a rather strong long-term persistence which dissipated after 15 to 18 months.

3. The runoff time series exhibited a multifractal behavior over a time scale range from 1 day to approximately 3 years, but displayed a single scaling pattern over larger time scales.

4. The multifractal parameters α (quantifies how far the process is from monofractality) and C_1 (characterizes the sparseness or inhomogeneity of the mean of the process) were reasonably close to each other for sub-watersheds within a watershed and were generally similar among four watersheds. Theoretical UMM multifractal scaling function K(q) functions matched the empirical K(q) counterparts very well.

5. For the DEM-extracted networks, the morphometric attributes and Horton ratios as well as their fractal dimensions were dependent on the threshold values of contribution area used in the extraction process. The fractal dimensions were almost identical for DEM-extracted stream networks of the four watersheds. The DEM extracted stream network displayed a single scaling pattern, rather than multifractal behavior.

6. The cumulative probability distribution of contribution area might provide an approach to identify the appropriate threshold area for extracting stream network from DEM. The values of 2 * log R_B/log R_A provided a more stable estimate of the fractal dimension than those calculated using log R_B/log R_L.

The findings of the fractal and multifractal analysis indicated that the runoff time series of the watersheds (and sub-watersheds) studied displayed scaling-breakpoints over certain ranges of scale. A purely natural phenomenon or process is usually complex enough to possess some known or unknown mechanisms without characteristic scale (Machlup, 1981). However, human activity is more likely to bring some external interventions into the natural process, and hence the scale-invariant property is only exhibited over certain scales. The watersheds investigated were all agricultural watersheds, thus the influences of agricultural activities are expected. How, and to what extent agricultural activities might affect the validity of scale invariance was not investigated in this study. One previous report indicated that the break point of scaling for river flow corresponded to the regular dam operation (Pandey et al., 1998). Another possible cause for the existence of scaling breakpoints or change in dimensions might be the variation of dominant process or structures over the different scaling ranges.

Runoff is the result of the interaction of climate, topography, soil properties, and vegetation as well as other conditions. These conditions differed widely for the four watersheds investigated. However, similar scaling characteristics were exhibited among these watersheds. Pandey et al. (1998) concluded that the variation of scaling parameters among basins was random rather than systematic. The findings in this study indicated that the fractal dimension might be used as a universal parameter to characterize runoff time series. However, the usefulness of this finding should not be exaggerated. The similarity in the fractal dimensions only tells that the runoff series display similar statistical patterns across scales. Therefore it is unrealistic to use a fractal model with a single fractal dimensionality to represent this complex process for predictive purposes. As the results indicated, watersheds with different climatic and topographic characteristics may have the same fractal dimensions. Therefore, such differences need to be captured using other parameters.

In this study, the Horton ratios and box-counting method were used to estimate the fractal dimension of DEM-extracted stream networks. Many methods have been developed to estimate fractal dimension. Usually the dimensions computed from different methods are not the same. This might be because the mathematical or physical bases of these methods are generally different. The fractal dimension estimated by the box-counting method best quantifies how the complexity of stream networks changes across scales, while the dimension calculated from Horton ratios may characterize the plane-filling pattern or the constraints for stream initiation. Thus caution should be taken when one interprets the estimated fractal dimension or compares the fractal dimensions of different studies.

In the last few decades, DEM data have been extensively used in stream network extraction and hydrological modeling because of its inherent advantage. The extracted stream network and its morphometric attributes greatly depend on the quality of the DEM. The availability and accessibility of high resolution data in the near future [e.g., LIght Detection And Ranging (LIDAR) data], and the improvement of GIS algorithms

may make the stream network extraction more precise and comparable to real networks to a greater extent than was possible in this study.

Although both the runoff time series and the DEM-extracted watershed stream morphometry exhibited scale invariant property, the runoff series displayed multifractal behavior while the stream network displayed monofractal behavior. It would appear that runoff being a more complex and dynamic process; its scaling cannot be directly inferred from the relatively static morphometric patterns. However, it should be noted that since elevation data used to generate the DEM-extracted network is relatively fixed, the resulting network is also assumed to be fixed. But in reality, the network is dynamic and can change over time with changes in climate and human activities. This represents a fundamental difficulty in trying to determine some possible relationships between the scaling in runoff time series and the watershed morphology extracted with DEM. In fact, the physical significance of fractal characteristics of the stream network remains to be explained as Xu et al. (1993) stated "… one cannot verify whether or not surface fractals contain definite information about river networks".

Scale invariance is useful because it may permit relating the geometrical and statistical properties of patterns in observations taken on the part to the whole and vice versa. If it can help characterize, simulate, and interpolate hydrologic patterns across scale it would prove very useful in water resources planning, flood forecasting, sediment and pollutant transport, and other aspects of watershed management. As examples: it can enable fusion and integration of monitoring data sets produced at different scales or produced at the same scale from different sources. Or, the regional impact of local planning decisions and vice versa can be assessed if scale invariant relations exist between the macro-scale and local scale processes. This would help maximize the usefulness of environmental monitoring data often collected at considerable investments in cost and time. Also, it would be expected that outputs of watershed scale hydrological models ought to exhibit scale invariance. This may be used as a test of the appropriateness of such models.

The results of this research demonstrated the existence of scale invariant patterns in hydrological runoff rates and drainage patterns, not only in sub-watersheds within a given watershed, but between watersheds evolved under widely different geographical conditions. This implies the possibility that these hydrological patterns may be extrapolated from gauged to non-gauged watersheds. However, techniques for such extrapolation would require much further research to better understand and quantify how climate and land-use interact with geomorphology to impact these processes and the evolution of drainage patterns (Sivapalan and Kalma, 1995). The key question is why and how do natural cycles, such as seasonal weather patterns or land use activities, over the long term generate scale invariant patterns.

REFERENCES

Machlup, S. 1981. Earthquakes, thunderstones, and other 1/f noises. In: Sixth International Conference on Noise in Physical Systems, Ed. P.H.E. Meijer, R.D. Mountain, and R.J. Soulen, Jr., pp.157-160. Special publication 614. Washington, D.C: National Bureau of Standards.

Mandelbrot, B. B. 1983. The fractal geometry of nature. W.H. Freeman, New York.

Pandey, G., S. Lovejoy, and D. Schertzer. 1998. Multifractal analysis of daily river flows including extremes for basins of five to two million square kilometers, one day to 75 years. Journal of Hydrology 208: 62-81.

Sivapalan, M. and J. D. Kalma. 1995. Scale problems in hydrology: Contributions of the Robertson Workshop. Hydrological Processes 9(3/4):243-250.

Sposito, G. 1998. Scale dependence and scale invariance in hydrology. Cambridge, United Kingdom.

Xu, T., I. D. Moore, and J. C. Gallant. 1993. Fractals, fractal dimensions and landscapes — a review. Geomorphology 8: 245-262.

VITA

Xiaobo Zhou was born in Chongqin, P. R. China and spent his childhood in this mountainous city. Because of his excellent performance in high school, he was exempted from the national college entrance exam and entered Huazhong University of Science and Technology in 1992, and received his B.S. degree in Biomedical Engineering in 1996. He obtained his M.S. degree in Environmental & Resources in Zhejiang University in 1999. In the fall of that year, he started his Ph.D. program in Crop and Soil Environmental Sciences at Virginia Polytechnic Institute and State University. He received the M.S. degree in Civil Engineering from this institution in May, 2004. Xiaobo Zhou married his wife Bing Liu in 1999.